Regulation of Apoptosis and Differentiation by the Apoptosis Signal-Regulating Kinase Family

---

Dissertation

zur

Erlangung der naturwissenschaftlichen Doktorwürde
(Dr. sc. nat.)

vorgelegt der

Mathematisch-naturwissenschaftlichen Fakultät

der

Universität Zürich

von
Elisabeth ORTNER

aus Österreich

Promotionskomitee

Prof. Dr. Karin Moelling (Leitung der Dissertation)
Prof. Dr. Urs Greber

Zürich, 2007

Table of Contents

1. Summary

Apoptosis is a genetically encoded suicide program of cells, which is induced either by the death receptor-mediated extrinsic pathway or the mitochondrial intrinsic pathway. The extrinsic pathway is triggered by binding of death ligands such as Fas and TNF-α, whereas the intrinsic pathway is induced by cellular stress stimuli, including withdrawal of survival factors, UV-light, γ-irradiation, and cytotoxic drugs. Serum-starvation activates the intrinsic pathway by elevation of cellular ROS (reactive oxygen species). Both apoptotic pathways activate the executioner caspases-3, -6 and -7, which cleave numerous substrates including poly (ADP-ribose) polymerase (PARP), resulting in self-destruction of the cell.

ASK2 (apoptosis signal-regulating kinase 2) has been described as highly homologous interaction partner of ASK1. Both belong to the family of mitogen-activated protein kinase kinase kinases (MAPKKK) that is involved in multifunctional signaling networks, regulating cell survival, proliferation, differentiation, and apoptosis. ASK2 is a serine-threonine kinase that activates the stress signaling MAP kinases JNK (c-Jun N-terminal kinase) and p38 MAPK. A recent report demonstrated that ASK2 forms a heteromeric complex with ASK1 and thereby functions as a MAPKKK by activating JNK and p38 MAPK. Within this heteromeric complex, ASK2 and ASK1 positively regulate their kinase activity. In the present study, we investigated the function of ASK2 in apoptosis by modulating its expression level in HeLa cells, which were subjected to stress by serum-starvation. Overexpression as well as knockdown of ASK2 increased apoptosis in serum-starved cells. In non-stressed cells, overexpressed ASK2 formed homo-oligomers, whereas endogenous ASK2 and ASK1 hetero-oligomerized. Stress-induction by serum-starvation led to a decrease of this heteromeric complex formation of ASK2 and ASK1. Concomitant overexpression of ASK2 and ASK1 impaired starvation-induced apoptosis and stabilized both proteins. Although localization was observed in mitochondria, cytoplasm, and nucleus, ASK2 co-precipitated specifically with Trx2 (thioredoxin 2) containing the mitochondrial target sequence but not with a cytoplasmic-localized construct of Trx2 or cytoplasmic Trx1. Based on these findings, we propose a model in which ASK2 regulates apoptosis in a dose-dependent manner by forming homo- or heteromeric complexes with ASK1 possibly in the intrinsic apoptotic pathway.

The PI3K-AKT pathway regulates the c-Raf-MEK-ERK pathway by an inhibitory crosstalk mediated by AKT phosphorylation of c-Raf on Ser259, which occurs among others, stage-specifically during the skeletal muscle differentiation process of C2C12 myoblasts. In the present study, a peptide encoding a sequence around Ser916 of ASK2 was identified as an AKT substrate in a radioactive *in vitro* phosphorylation peptide screen. The ASK2-homologous kinase ASK1 is inhibited by AKT phosphorylation on Ser83 thereby preventing stress signaling and apoptosis. An *in vitro* phosphorylation assay with GST-fusion proteins of ASK2 determined AKT phosphorylation sites on Ser916 and also to a minor extent on Ser46, which would be analogous to the phosphorylation site on ASK1 on Ser83. Overexpression of ASK2 together with wild-type and also kinase-inactive AKT increased caspase-3 activation in serum-starved cells indicating a kinase-independent pro-apoptotic function of AKT. Subsequent *in vivo* analyses only identified a PI3K-dependent negative regulation of an ASK2-involving apoptotic pathway analyzed at the level of stress signaling and PARP cleavage. This was examined in serum-starved cells in which ASK2 expression was modulated either by overexpression or siRNA-mediated downregulation. A point mutation of Ser916 to alanine abolished cleavage of PARP after serum-starvation. Summarizing, an ASK2-comprising apoptotic pathway is regulated dependent on the kinase activity of PI3K but not AKT.

Apoptosis and skeletal muscle differentiation exhibit morphological similarities, including membrane blebbing during cell fusion and caspase-3 activation. Since ASK1 and ASK2 activate caspase-3 after stress-induction, we analyzed both for a regulatory function in C2C12 muscle differentiation. Using an shRNA-mediated RNA interference approach, ASK1 expression was downregulated, which slowed down C2C12 myogenesis. However, subsequent studies elucidated that the puromycin selection of the transduced C2C12 myoblasts was unspecifically responsible for the decrease of ASK1 transcription and consequently for the decelerating effect on the muscle differentiation process.

2. Zusammenfassung

Apoptose ist ein genetisch kodiertes Selbstmordprogramm von Zellen, welches entweder durch den Todesrezeptor-vermittelten extrinsischen oder den mitochondrialen intrinsischen Weg induziert wird. Der extrinsische Weg wird durch die Bindung von Todesliganden wie Fas oder TNF-α ausgelöst, während der intrinsische Weg durch zelluläre Stress-Stimuli induziert wird, wie den Entzug von Überlebensfaktoren, UV-Licht, γ-Strahlung und cytotoxischen Stress. Serumentzug aktiviert den intrinsischen Weg durch Erhöhung des zellulären ROS (reaktive Sauerstoff-Spezies) Gehaltes. Beide Apoptosewege aktivieren die Effektorcaspasen -3, -6 und -7, welche zahlreiche Substrate schneiden inklusive der Poly (ADP-Ribose) Polymerase (PARP), was in der Selbstzerstörung der Zelle resultiert.

ASK2 (Apoptose Signal-regulierende Kinase 2) ist als hoch homologer Interaktionspartner von ASK1 beschrieben worden. Beide gehören zur Familie der Mitogen-aktivierten Protein Kinasen Kinasen Kinasen (MAPKKK), welche in multifunktionalen Signalnetzwerken involviert ist und dabei das Überleben von Zellen reguliert, so wie Proliferation, Differenzierung und Apoptose. ASK2 ist eine Serin-Threonin Kinase, die die Stress-Signal MAP Kinase JNK (c-Jun N-terminale Kinase) und p38 MAPK aktiviert. Eine kürzlich erschienene Studie zeigte, dass ASK2 einen heteromeren Komplex mit ASK1 ausbildet und dadurch als MAPKKK in der Aktivierung von JNK und p38 MAPK fungiert. Innerhalb dieses heteromeren Komplexes regulieren ASK2 und ASK1 ihre Kinaseaktivität in positiver Weise. In der vorliegenden Studie untersuchten wir die Funktion von ASK2 in Apoptose, indem ihre Expressiosrate in HeLa Zellen, die Stress durch Serumentzug ausgesetzt wurden, moduliert wurde. Sowohl Überexpression als auch Knockdown von ASK2 erhöhten Apoptose in Serum-gehungerten Zellen. In nicht-gestressten Zellen bildete überexpremiertes ASK2 Homo-Oligomere aus, während endogene ASK2 und ASK1 hetero-oligomerisierten. Stressinduktion durch Serumentzug führte zu einer Verminderung der heteromeren Komplexbildung von ASK2 und ASK1. Gleichzeitige Überexpression von ASK2 und ASK1 verhinderte die durch Hungern induzierte Apoptose und stabilisierte beide Proteine. Obwohl eine Lokalisation in Mitochondrien, Cytoplasma und Kernen beobachtet wurde, co-präzipitierte ASK2 spezifisch mit Trx 2 (Thioredoxin 2), welches die mitochondrialen Zielsequenz enthielt, aber nicht mit einem cytoplasmatisch-lokalisierten Trx2-Konstrukt oder cytoplasmatischen Trx1. Basierend auf diesen Befunden schlagen wir ein Modell vor, in

welchem ASK2 Apoptose dosis-abhängig reguliert durch Bildung von Homo- oder Hetero-Oligomere mit ASK1 möglicherweise im intrinsischen Apoptoseweg.

Der PI3K-AKT Signalweg reguliert den c-Raf-MEK-ERK Signalweg durch AKT-Phosphorylierung von c-Raf an Ser259, was unter anderem phasen-abhängig während des Skelettmuskel-Differenzierungsprozesses von C2C12 Myoblasten stattfindet. Ein Peptid, das eine Sequenz um Ser916 von ASK2 kodierte, wurde als ein AKT-Substrat in einem radioaktiven *in vitro* Phosphorylierungs Peptid-Screen identifiziert. Die ASK2-homologe Kinase ASK1 wird durch AKT-Phosphorylierung an Ser83 inhibiert, wodurch Stress-Signaltransduktion und Apoptose verhindert werden. Ein *in vitro* Phosphorylierungs-Assay mit GST-Fusionsproteinen von ASK2 bestimmte eine AKT-Phosphorylierungsstelle an Ser916 und zu einem schwächeren Ausmass auch an Ser46, welches analog zur Ser83 Phosphorylierungsstelle von ASK1 wäre. Überexpressison von ASK2 zusammen mit AKT Wildtyp und auch Kinase-inaktivem AKT erhöhten die Caspase-3 Aktivierung in Serum-gehungerten Zellen, was auf eine Kinase-unabhängige, pro-apoptotische Funktion von AKT hinweist. Nachfolgende *in vivo* Analysen identifizierten nur eine PI3K-abhängige, negative Regulation eines ASK2-inkludierenden Apoptosewegs, was auf Ebene der Stress-Signaltransduktion und der Spaltung von PARP anlysiert wurde. Dies wurde in Serum-gehungerten Zellen untersucht, in welchen die ASK2 Expression entweder durch Überexpression oder siRNA-vermittelte Reduktion moduliert wurde. Eine Punktmutation von Ser916 zu Alanin hob eine Spaltung von PARP nach Serumentzug auf. Zusammenfassend, ein ASK2 einbeziehender Apoptoseweg wird abhängig von der Kinase-Aktivität von PI3K aber nicht von AKT reguliert.

Apoptose und Skelettmuskeldifferenzierung weisen morphologische Ähnlichkeiten auf wie Membranausstülpung während der Zellfusion und Caspase-3 Aktivierung. Da ASK1 und ASK2 Caspase-3 nach Stressinduktion aktivieren, untersuchten wir beide auf eine regulatorische Funktion in der C2C12 Muskeldifferenzierung. Unter Verwendung eines shRNA-vermittelte RNA-Interferenz Ansatzes wurde die Expression von ASK1 herrunterreguliert, was die C2C12 Myogenese verlangsamte. Jedoch zeigten nachfolgende Studien, dass die Puromycin-Selektion der transduzierten C2C12 Myoblasten unspezifisch für die Reduktion der ASK1 Transkription und folglich für den verlangsamenden Effekt auf den Muskeldifferenzierungsprozess verantwortlich war.

3. Introduction

3.1. Apoptosis

3.1.1. Characterization of the apoptotic and necrotic cell death

Apoptosis is a highly regulated process, which is also called programmed cell death (PCD). It is responsible for the development of multicellular organisms, maintenance of tissue homeostasis, elimination of damaged cells (e.g. upon DNA damage) and host defence (1,2). The term apoptosis origins from the Greek, meaning "dropping off" of petals or leaves from plants and was coined by Currie and colleagues in 1972 (3). It describes the process when cells decide to commit suicide, which is in contrast to the injury-caused death by necrosis (4). Cells undergoing apoptosis share several morphological and biochemical characteristics (3). In contrast to necrosis, which is characterized by cell swelling, apoptosis induces membrane blebbing, cell body shrinkage with concurrent preservation of the organelles, chromatin condensation, DNA fragmentation, and formation of small membrane-bound cell fragments or apoptotic bodies. These apoptotic bodies are rapidly phagocytosed by macrophages or neighboring cells to prevent harmful inflammatory responses. Apoptosis can be induced by two kinds of signals first the withdrawal of anti-apoptotic signals such as growth factors or impairment of adhesion. Detachment-induced apoptosis of cells is termed anoikis (5,6). The second kind of pro-apoptotic signals include an increase of oxidants within the cell, DNA damage by UV-light, γ-irradiation or chemotherapeutic drugs, accumulation of misfolded proteins, or binding of death activators such as tumor necrosis factor-α (TNF-α) or Fas ligand (FasL) to their death receptor (2,7-10).

The necrotic cell death process is induced by mechanical damage or exposure to toxic chemicals. Necrosis is characterized by cell- and nuclear swelling, disruption of organelles, rupture of the cell leading to the release of the cellular content and, finally, to an inflammatory response (11).

3.1.2. The extrinsic versus intrinsic pathway of apoptosis

Two major pathways are described to lead to apoptosis, the "extrinsic" and the "intrinsic" apoptosis pathway. The extrinsic pathway is triggered by extracellular signals that activate a death receptor-dependent signaling cascade whereas the intrinsic pathway is mediated via mitochondria leading to the release of cytochrome c and the formation of apoptosomes (9,12-14). Both pathways converge at the activation of caspases, which are the executioners of apoptosis (Figure 1) (15). These proteases are responsible for a proteolytic cascade that promotes cell disassembly. Cell debris are removed by phagocytosis (9,16).

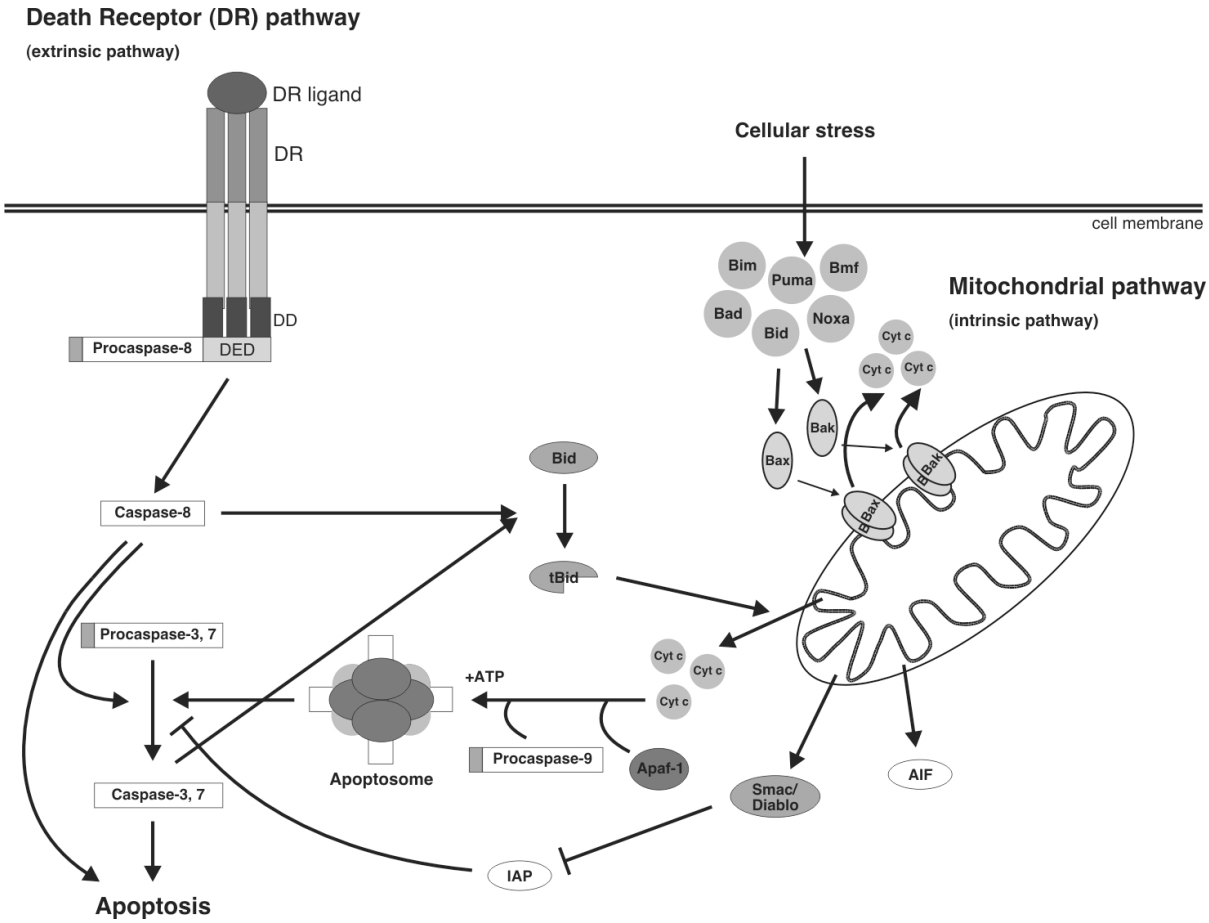

Fig. 1: Schematic overview of the extrinsic and intrinsic apoptosis pathways (see text for abbreviations)

Binding of a death ligand to its death receptor activates the receptor mediated extrinsic pathway. Eight death receptors (DR) are described (shown in Figure 2): tumor necrosis factor receptor 1 (TNFR1; also known as death receptor 1 (DR1)), Fas/DR2/CD95/APO-1, DR3/APO-3/LARD/TRAMP/WSL1), TNF-related apoptosis–inducing ligand receptor 1

(TRAIL1; also referred to as DR4 and APO-2), TRAIL2/DR5, KILLER/TRICK2, DR6, ectodysplasin A receptor (EDAR), and nerve growth factor receptor (NGFR) (7,17,18).

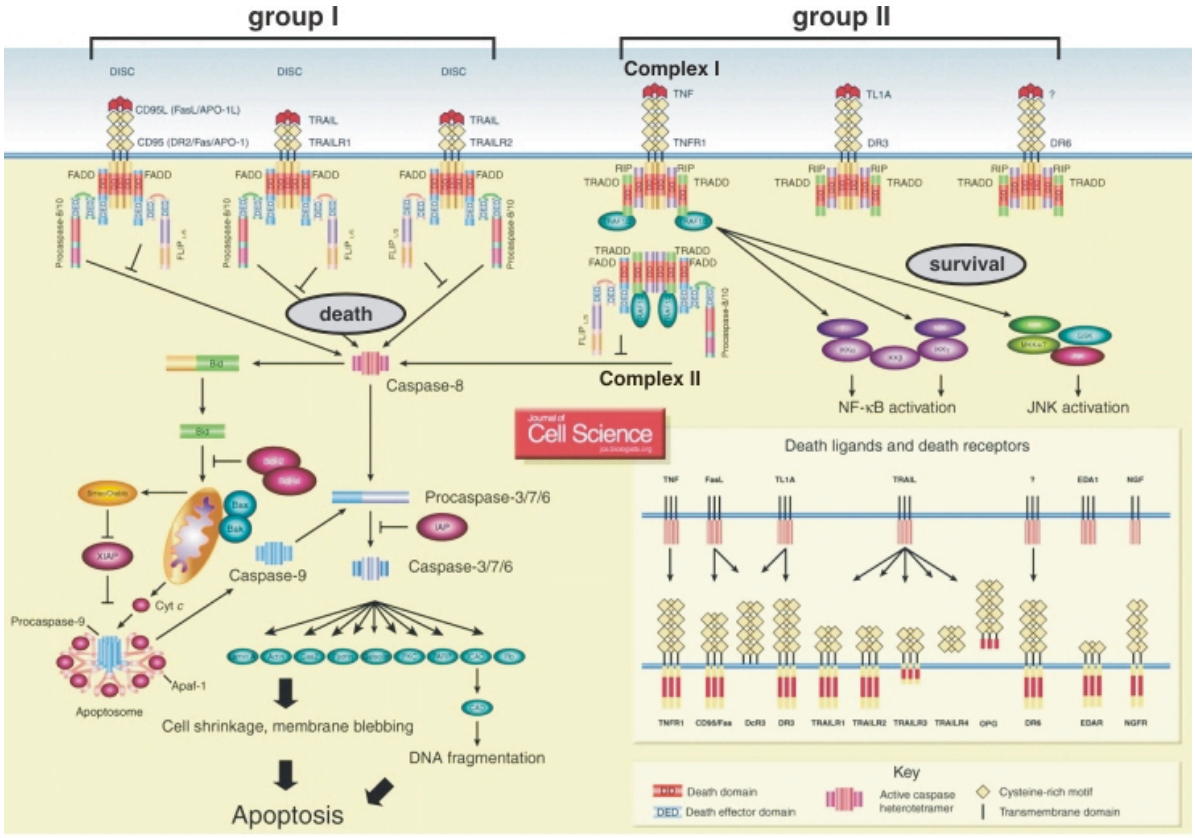

Fig. 2: Overview of the death receptor (DR) family (modified from (7))

DRs are further subdivided into two DR signaling groups. Group I comprises the death-inducing signaling complex (DISC) that is formed at the Fas receptor, TRAILR1 or TRAILR2 (19). In this complex the trimerized receptor binds with its cytoplasmic death domain (DD) to the DD-containing adaptor molecule Fas-Associated Death Domain (FADD), which itself interacts with procaspase-8 and procaspase-10 through their death effector domains (DED) and the cellular FLICE-inhibitory protein ($FLIP_{L/S}$). This DISC is then released into the cytoplasm where it propagates the apoptotic signal (19-21). An additional Fas-induced apoptotic pathway is mediated by the receptor-associated protein Daxx, which activates the JNK kinase cascade and leads to the activation of transcription factors such as c-Jun (22).

The DR signaling complex group II consists of TNFR1, DR3, DR6 and EDAR that transduce both apoptotic and survival signals in a hypothesized model by formation of two different complexes. Complex-I is built up by TNFR1, TNF, receptor-interacting protein (RIP),

TNFR-associated death domain protein (TRADD), TNFR-associated factor (TRAF-1/2), and other yet unidentified molecules and activates the NFκB signaling pathway and JNK through a TRAF-2 dependent mechanism. After translocation of complex-I to the cytoplasm FADD, procaspase-8/-10, and $FLIPS_{L/S}$ are recruited to form complex-II and induce death signaling. In this model, the efficiency of complex-II formation, caspase-8 activation and the amount of FLIP decide between death and survival signaling (7,23,24). For the less well characterized DR3 and DR6 signaling pathways it was shown, that RIP and TRADD are recruited to the receptor leading to nuclear factor-κB (NF-κB) activation and expression of survival genes (25,26).

Cellular stress induced by UV-light, γ-irradiation, treatment with cytotoxic drugs (e.g. Actinomycin D), accumulation of unfolded proteins or withdrawal of survival signals (e.g. growth factors) activate the intrinsic pathway of apoptosis (2,8,10,14). The intrinsic cell death pathway begins with an alteration of the mitochondrial membrane permeability mediated by member proteins of the pro- and anti-apoptotic Bcl-2 family. It is followed by cytochrome c release from the mitochondrial intermembrane/intercristae spaces into the cytoplasm. Subsequently, cytochrome c binds to apoptosis protease-activating factor-1 (Apaf-1), which itself aggregates to an oligomer in an ATP-dependent manner. After recruitment of procaspase-9 to this so-called apoptosome, caspase-9 is activated to cleave and thereby activate the executioner caspases-3, -6, and -7 (9,16,27,28).

The extrinsic pathway of apoptosis can also lead to mitochondria-mediated induction of apoptosis at the level of the Bcl-2 family member protein Bid. Caspase-8 activated by death receptor signaling can cleave Bid, which then translocates to mitochondria where it promotes cytochrome c relase (29,30).

3.1.3. The caspase protease family

Genetic studies in the nematode worm *Caenorhabditis elegans* led to the identification of caspases as important mediators of cell death (31). In *C. elegans* the four proteins cell death abnormal-3 (ced-3), -4, -9, and egg laying defective-1 (egl-1) are characterized to be involved in the apoptotic pathway, with ced-3 and ced-4 as apoptosis inducer, and ced-9 and egl-1 as their negative regulators (32-36). The first mammalian caspase identified, caspase-1, also known as interleukin-1β converting enzyme (ICE) was found to convert the precursor of interleukin-1β (IL-1β) to its mature form, a potent mediator of apoptosis (37).

Caspases are cysteine aspartate specific proteases that reside as inactive pro-enzymes, so-called zymogens, within the cell. They can be activated in three different ways either (i) by autocatalytic cleavage, or (ii) by transactivation via other caspases or (iii) by proteolysis by non-caspases such as granzyme B and cathepsin. All caspases have in common a conserved pentapeptide QACXG surrounding the cysteine residue of the active center. In a first activation step, an N-terminal prodomain of about 20 kDa is removed from the 30 to 50 kDa inactive pro-enzyme. Then, the truncated protein is further cleaved into a large and a small subunit of 20 kDa and 10 kDa, respectively. These two subunits form an active homo-dimer that subsequently to form a tetramer with two independent catalytic sites. Activated caspases are strictly dependent on an aspartate residue at the substrate site P1. The various caspase family members differ in their substrate specificity in the three amino acids P2 to P4 N-terminal to the P1 site (9,16).

There are at least 14 known mammalian caspases that can promote apoptosis with some members generating mature inflammatory cytokines and thereby regulating immune responses. There are three different methods to subdivide caspases. First, the family of caspases can be grouped into three subfamilies based on phylogenetic similarities and peptide substrate specificity with (i) the ICE-subfamily consisting of caspase-1, -4, -13, and -14 and murine caspase-11 and -12, (ii) the cell death defective-3 (CED-3) subfamily with caspase-3, -6, -7, -8, -9, and -10 and (iii) the caspase-2 subfamily (16). Second, caspases can be classified by their functional consequences and on differences in their prodomains. Initiator caspases contain long prodomains with a death-effector domain (DED) such as caspase-8 and -10 or a caspase activation and recruitment domain (CARD) as in the case of caspase-2 and -9. Effector caspases, including caspase-3, -6, and -7, are also called downstream caspases and only contain a short prodomain. The third group of caspases consists of caspase-1, -4, -5, and -11 and is involved in inflammatory responses. Caspase-1 and -4 also contain a CARD domain (9,16,38). Third, caspases are also divided into three groups regarding their substrate specificity with (i) caspase-1, -4, and -5 which have an hydrophobic amino acid at P4 and the optimal consensus sequence WEXD, (ii) caspase-2, -3, and -7 favour an aspartate at P4 and the optimal consensus sequence DEVD, and (iii) caspase-6, -8, and -9, which prefer the sequence L/VEXD (9,16,38,39). Figure 3 summarizes the family of caspases divided into three groups according their function (apoptosis initiators, apoptosis effectors, and cytokine maturation), which is the commonly used classification system, and depicts their structure and substrate specificity (39).

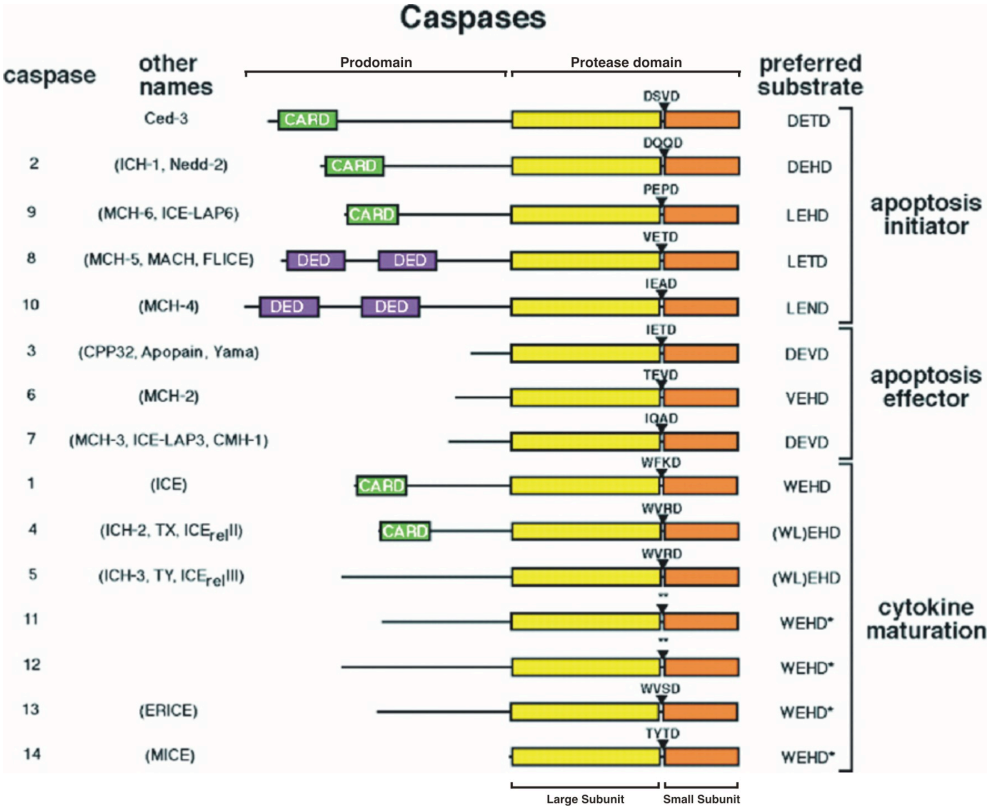

Fig. 3: Family of caspases (39)

Substrates of caspases are very divers and are divided into several classes as follows: i) cell death proteins, ii) structural proteins and associated molecules, iii) transcription factors and their regulators and cell cycle regulators, iv) receptors and signal transduction associated proteins, proteins involved in macromolecular synthesis, intracellular sorting, repair, and degradation, v) neurodegenerative disease proteins, and vi) cytokine precursors (16).

Caspases are negatively regulated by the cellular FLICE-inhibitory protein c-FLIP (also known as Casper, I-FLICE, FLAME, CASH, CLARP, MRIT and Ursupin), by members of the Bcl-2 family, and by members of the family of inhibitors of apoptosis (IAP; XIAP/MIHA, c-IAP-1/MIHB, cIAP-2/MIHC, and survivin), which prevent the formation of apoptosomes by binding to procaspase-9 and are antagonized by second mitochondria–derived activator of caspase (Smac)/Diablo, Arts and Omi/high temperature requirement protein-A2 (HTRA2) released from damaged mitochondria. Since caspases are part of the host defence against viral infections, viruses also encode caspase inhibitors to prevent apoptosis such as cowpox virus protein cytokine response modifier A (CrmA), baculovirus proteins p35 and IAPs, v-FLIP, and HBx protein from Hepatitis B virus (16,40,41).

In addition to their apoptotic function, caspases are involved and essential in several differentiation processes, including differentiation of muscle cells (42), and terminal differentiation of keratinocytes (43) and erythrocytes (44).

3.1.4. The pro- and anti-apoptotic functions of the Bcl-2 family

The B-cell leukemia 2 (Bcl-2) protein was initially identified as a human proto-oncogene located on chromosome 18, which is involved in human B-cell lymphomas. Since its identification, several other proteins sharing up to four Bcl-2 homology-domains designated BH1 to BH4 were grouped into the Bcl-2 family (45).

This family is divided into pro- and anti-apoptotic Bcl-2 proteins, which differ by the presence of the BH4 domain (see Figure 4A). BH3 only proteins are pro-apoptotic and initiate mitochondrial outer membrane permeabilization (MOMP) after induction of apoptosis. This leads to loss of membrane potential by formation of pores in the lipid bilayer consisting of oligomerized pro-apoptotic multidomain Bcl-2 proteins Bax (Bcl-2 associated X-protein (Bax) and Bcl-2 antagonist killer (Bak). The mitochondrial membrane is involved in the formation of MOMP via the mitochondrial permeability transition pore (mPT). mPT is responsible for the influx of ions and other small molecules, at least during endoplasmatic reticulum (ER) stress or stress induced by reactive oxygen species (ROS) (46). The mPT consists of a complex of voltage-dependent anion channels at the outer membrane, cyclophilin D at the inner membrane and adenine nucleotide transporters, which span the inner and outer membranes (47). The two pro-apoptotic membrane pore-forming proteins Bax and Bak are activated either directly by BH3 interacting death domain (Bid) and Bim, which are members of the BH3-only subgroups, or indirectly by inhibition of their negative regulators, including Bcl-2, Bcl-2 related protein long isoform (Bcl-XL), and Mcl-1. These negative regulators of Bax and Bak belong to the BH4-containing Bcl-2 subfamily and are themselves negatively regulated by binding to the BH3 only “de-repressor” proteins Bcl-2-antagonist of cell death (Bad), Bik, Bmf, Puma, Noxa or Hrk (see Figure 4B). Apoptosis is regulated not only by homo- or hetero-dimerization of pro- and anti-apoptotic Bcl-2 family member but also by cleavage of the N-terminal domain of Bid and Bax. Truncation of Bid is mediated by caspase-8, granzyme B and more weakly by caspase-2 and -3 and is negatively regulated by Bcl-2. After the N-terminal truncation, Bid and Bax translocate to and integrate into the mitochondrial membrane (27,28,45,47).

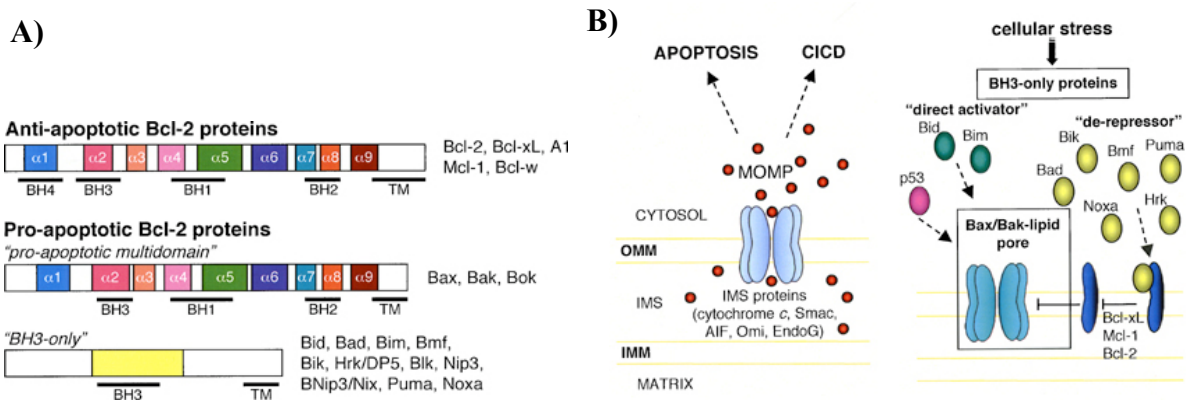

Fig. 4: A) Family of Bcl-2 proteins, B) Illustration for mitochondrial outer membrane permeabilization and overview of "direct activator" and "de-repressor" Bcl-2 family members which regulate lipid pore formation by Bax and Bak (47)

Another pro-apoptotic Bcl2 family member, Bad, is negatively regulated by phosphorylation by the anti-apoptotic kinase AKT and by binding of the scaffold protein 14-3-3 (48-50). Bad can also be phosphorylated and thus inactivated by the mitochondrial membrane-localized cAMP-dependent protein kinase A (PKA) (51). In contrast, Puma and Noxa are transcriptionally upregulated by the tumor suppressor p53 and other pro-apoptotic stimuli (52).

3.1.5. MAPK stress signaling pathways in apoptosis

Mitogen-activated protein (MAP) kinase signaling cascades are evolutionary well-conserved in all eukaryotic cells and are involved in multi-functional signaling networks that regulate cell growth, differentiation, and apopotosis (53,54). These signaling pathways are hierarchically ordered in a three kinase architecture in which MAP kinase kinase kinases (MAPKKK) activate MAPKK (also MEKK) by Ser/Thr phosphorylation, which in turn activate MAPKs (also MEK) by dual phosphorylation of a Thr-X-Tyr motif in the activation loop (53-56). Three MAPK cascades converge on extracellular signal-regulating kinases (ERKs), c-Jun N-terminal kinases (JNKs, also referred to as stress-activated protein kinases SAPKs), and p38 MAP kinases, with the latter two MAP kinases preferentially activated by cytotoxic stress (UV-light/γ-irradiation, heat/osmotic shock, and nitrosative/oxidative stress) and by proinflammatory cytokines such as TNF-α and interleukin-1 (IL-1) (55,57,58).

For the JNK subgroup three genes (jnk1, jnk2, and jnk3) with ten different splice variants have been described, which are activated by two distinct MAPKKs, MAPKK4/SEK1 and MAPKK7 (54,59). Non-phosphorylated JNK is complexed to p53 and thereby ubiquitinated, which consequently leads to proteasomal degradation. After being phosphorylated by MAPKK4/7, JNK dissociates from p53 and is subsequently stabilized (60,61). Activated JNK and p38 MAPK phosphorylate the transcription factor c-Jun and ATF-2. Homo- and hetero-dimerized Jun-Jun and Jun-ATF2, respectively, form the complex activator protein-1 (AP-1) (62-64), which associates with the released p53 leading to the cleavage of Bid. Truncated Bid subsequently causes translocation of Bax to mitochondria causing lipid pore formation and finally cytochrome c release (60,61,63-65). JNK also translocates to mitochondria after genotoxic stress induced by ionizing radiation. There, JNK binds to and phosphorylates the anti-apoptotic Bcl-XL and thereby positively increases cytochrome c release (66).

Signaling specificity of JNK is mediated by the formation of protein complexes, which consist of other kinases such as MAPKK4 or MAPKK7 and scaffold proteins of the JNK interacting protein (JIP) group with three members (53,67). The closely related JIP1 and 2 selectively bind to JNK, MAPKK7, and the MAPKK7 activators mixed lineage kinase 3 (MLK3) and dual-leucine zipper-bearing kinase (DLK) (68,69). The JIP3 protein also associates with JNK, MAPKK7, and members of the MLK kinase group (70).

Strength and duration of JNK activation as wells as cellular context and JNK isoform specificity determine the outcome of JNK activation such as apoptosis, cell survival or differentiation. A strong and persistent activation of JNK is necessary for PC12 neuronal cell death (71,72). In human B cells, JNK is selectively activated by CD40, which rescues cells from apoptosis (73). Homozygous disruption of *jnk1* in ES cell lines inhibits neurogenesis, which is isoform 1 specific since knockout of the two other jnk isoforms does not influence neuronal differentiation (74).

The p38 MAPK subgroup contains four genes, *p38α*, *p38β*, *p38γ*, and *p38δ*. Two upstream kinases are described for this subgroup similar to the JNK subgroup, namely MAPKK3 and MAPKK6. MAPKK4 was also shown to be a weak activator of p38 MAPKs at least *in vitro* (53,57).

Several studies identified p38 MAPK to be involved in divers cellular processes similar to JNK-dependent processes. Concurrent activation of p38 MAPK and JNK is observed in pancreatic β-cells, which are treated with human amylin, leading to apoptosis. Inhibition of p38 MAPK activity by the specific inhibitor SB203580 strongly suppressed apoptosis (75).

Both, p38 MAPK and JNK, are activated and necessary in anandamide-induced PC12 cell death (76). On the other hand, p38 MAPK activity is needed for neuronal outgrowth of differentiating PC12 cells (77).

To date, fifteen different MAPKKKs have been identified as upstream activators of the JNK pathway and fourteen of the p38 MAPK pathway with four kinases, which are only predicted to be activators based on sequence analyses (see Table 1).

MAPKKK	Swiss Prot	Entrez Gene			Stress signaling	References
MAPKKK1	MEKK1	MAP3K1			JNK, p38 MAPK(?)	(78-81)
MAPKKK2	MEKK2	MAP3K2			JNK, p38 MAPK	(82,83)
MAPKKK3	MEKK3	MAP3K3			JNK, p38 MAPK	(83,84)
MAPKKK4	MEKK4	MAP3K4	MTK1	MAP Three Kinase 1	JNK, p38 MAPK	(85-88)
MAPKKK5	MEKK5	MAP3K5	ASK1	Apoptosis signal-regulating kinase 1	JNK, p38 MAPK	(89,90)
ASK2	MEKK6	MAP3K6	ASK2	Apoptosis signal-regulating kinase 2	JNK	(91)
MAPKKK7A-D		MAP3K7A-D	TAK1	TGF-beta-activated kinase	JNK, p38 MAPK	(92-94)
MAPKKK8		MAP3K8	COT	Cancer Osaka thyroid oncogene	JNK, p38 MAPK	(95-99)
			TPL2	Tumor progression locus-2		
			ESTF	Ewing sarcoma transformant		
MAPKKK9		MAP3K9	MLK1	Mixed lineage kinase 1	JNK, p38 MAPK(?)	(100)
			PRKE1			
MAPKKK10	M3KA	MAP3K10	MLK2	Mixed lineage kinase 2	JNK, p38 MAPK	(100-102)
			MST	MKN28-derived Ser/Thr kinase		
MAPKKK11		MAP3K11	MLK3	Mixed lineage kinase 3	JNK, p38 MAPK	(103-106)
			PTK1	Protein tyrosine kinase 1		
			SPRK	SH3 domain-containing Pro-rich kinase		
		MLK4	MLK4	Mixed lineage kinase 4	JNK(?), p38 MAPK(?)	
MAPKKK12	M3KC	MAP3K12	ZPK	Zipper protein kinase	JNK, p38 MAPK	(107-110)
			DLK	Dual leucine zipper bearing kinase		
			MUK	MAPK upstream kinase		
MAPKKK13		MAP3K13	LZK	Leucine zipper bearing kinase	JNK, p38 MAPK(?)	(111-113)
	ZAK	ZAKα	MRK	MLK-related kinase	JNK, p38 MAPK	(114-116)
		ZAKβ	MLTK	MLK-like MAPK triple kinase		
			MLK7	Mixed lineage kinase 7		
			ZAK	Zipper sterile-alpha –motif kinase		

(?)..predicted activation

Table 1: List of the MAPKKK that lead to the activation of the stress signaling kinases JNK and p38 MAPK. All names of each MAPKKK according to SwissProt and Entrez Gene (NCBI) are listed.

3.1.6. Negative regulation of apoptosis by thioredoxins

Thioredoxins (Trx) are cellular redox–sensing enzymes that are present in many prokaryotes and eukaryotes where they are expressed ubiquitously. These small enzymes play multiple functions in the regulation of cell growth, apoptosis, differentiation, and inflammation (117-121). Two isoforms of Trx have been identified in mammalian cells, the cytosolic and nuclear localized Trx1 and the mitochondrial Trx2 (122,123). They contain two redox-active cysteine residues within the consensus sequence - Cys-Gly-Pro-Cys - in their catalytic center and exist either in a reduced thiol form or an oxidized form with an intramolecular disulfide

bridge between the two cysteine residues (123,124). Together with the glutathione and superoxide dismutase systems, the endogenous antioxidant Trx system participates in redox reactions by reversible oxidation of its active center dithiol to disulfide and catalyzes dithio-disulfide exchange reactions involving many thiol-dependent processes (118,123,124). Oxidized Trx-S_2 is reduced to Trx-$(SH)_2$ by the flavoenzyme thioredoxin reductase and Nicotinamide adenine dinucleotide phosphate hydrogen (NADPH) (123).

One of the earliest events in the mitochondrial pathway of apoptosis is the drastic alteration of the mitochondrial redox environment, which includes the rapid oxidation of NADPH and glutathione (125-127). Thus, the mitochondrial transmembrane potential ($\Delta\Psi_M$) is reduced and reactive oxygen species (ROS) are generated (128). The mitochondrial antioxidant system consisting of Trx2, Trx2 reductase (Trx2R), mitochondrial Trx peroxidase, and manganese superoxide dismutase (MnSOD) is the key regulator of mitochondrial ROS-induced cytotoxicity (121,129). Trx not only plays an important role in mitochondria dependent apoptosis but is also involved in a wide variety of biochemical functions. It acts as hydrogen donor for ribonucleotide reductase and methionine sulfoxide reductase, it facilitates refolding of disulfide-containing proteins and modulates the DNA binding activity of some transcription factors e.g TFIIIC, BZLF1 (123,130-133).

An essential anti-apoptotic function of Trx is the inhibition of the MAPKKK ASK1 (apoptosis signal-regulating kinase 1), which is an important mediator of apoptosis. Trx1 and Trx2 bind to the N-terminal inhibitory domain of ASK1 in a redox activity-dependent manner, whereby Trx1 promotes ASK1 ubiquitination and degradation. Mitochondria-located Trx2 negatively regulates ASK1 in a pathway that leads to cytochrome c release from mitochondria (134-136). These two regulation steps of ASK1 converge at the level of mitochondrial cytochrome c release and activation of caspase-3 (134).

3.2. MAPKK kinases

3.2.1. Classification of the MAPKKK family

To date, twenty members of the mammalian MAPKKK family have been identified. Their evolutionary relationship is summarized in a phylogenetic tree in Figure 5 and their structures are compared in Figure 6 (see also Table 1 for nomenclature).

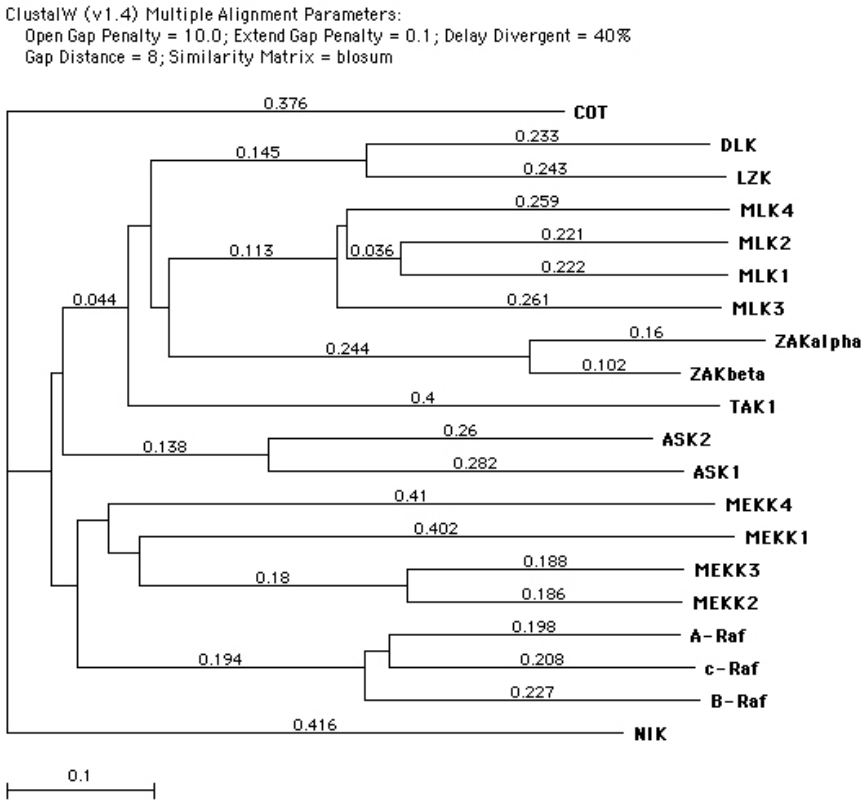

Fig. 5: Phylogenetic tree of the mammalian MAPKKK family generated with MacVector ™7.2.3.

MAPKKKs are part of a three-tiered kinase cascade composed of MAPKKKs, which phosphorylate and thereby activate MAPKKs, which in turn phosphorylate MAPKs (137). The MAPKKK signal transduction pathways are involved in extra-, intra-, and intercellular communication processes that regulate divers cellular outcomes, including cell growth, apoptosis, differentiation, cell motility and inflammation (138). This diversity is achieved by different activation mechanisms of MAPKKKs and a branching of the transduced signal to several MAPKs, which is specified by the interaction of scaffold and adapter proteins (137,139). MAPKKKs are activated by phosphorylation by an upstream kinase, by membrane recruitment through interaction with upstream activating proteins, and by oligomerization, mainly homo-oligomerization within a multiprotein complex consisting of additional regulatory components (137). Several upstream kinases of MAPKKKs belong to the family of STE20-related kinases, which is divided into two subgroups, the p21-activated kinase (PAK) and the germinal center kinase (GCK)/hematopoietic progenitor kinase 1 (HPK1) subgroups. Another group of activators of MAPKKKs contains Ras and the Rho family of small GTP-binding proteins (55,137,138,140).

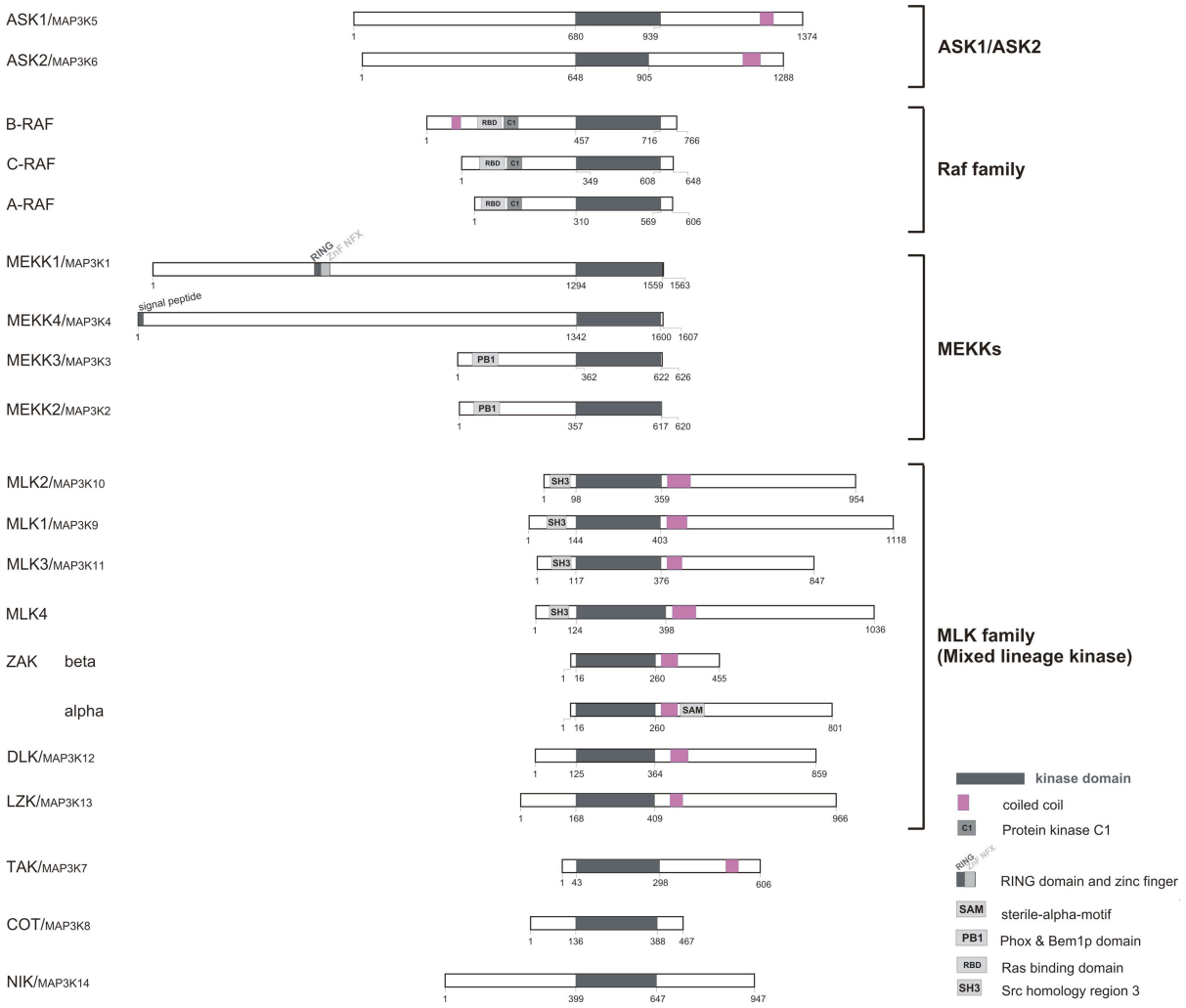

Fig. 6: Structural comparison of MAPKKK family members

3.2.2. The AKT kinase family and its regulation of MAPKKKs

The AKT kinase family consists of three isoforms (see Figure 7), AKT1 or protein kinase B α (PKBα), which was the first isolated AKT isoform, and AKT2/PKBβ and AKT3/PKBγ. AKT1 was identified as homologous kinase of protein kinase A (PKA) and PKC, which belong to the PK*A*-, PK*G*,- and PK*C*-related (AGC) kinase family. All three isoforms share a common architecture, with an amino-terminal pleckstrin homology (PH) domain, a central kinase domain, and a carboxy-terminal regulatory domain but they differ in their tissue distribution. While AKT1 is expressed ubiquitously, AKT2 is mainly found in insulin responsive tissue such as liver and fat- and muscle tissues, and AKT3 in brain and testis. For full activation of AKT, two phosphorylation sites are essential, one located in the activation loop of the kinase domain (Thr308 for AKT1) and the second in the carboxy-terminal

regulatory domain (Ser473 for AKT1). The upstream kinases responsible for these phosphorylation events are (3-phosphoinositide-dependent protein kinase 1 (PDK1) in the case of Thr308 and the SIN1-rictor-mammalian target of rapamycin (mTOR) complex serving as PDK2 for the latter one. Phosphatidylinositol 3-kinase (PI3K) phosphorylates phosphoinositol-4,5-bisphosphate (PIP_2), which produces phosphoinositol-3,4,5-trisphosphate (PIP_3). AKT binds to PIP_3 via the PH domain and is thereby recruited to the membrane. After being phosphorylated, AKT translocates from the membrane to the cytoplasm and nucleus (141,142).

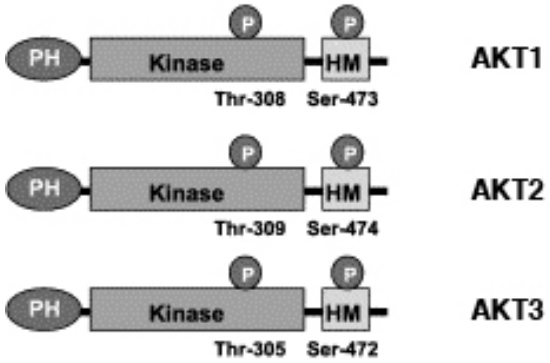

Fig. 7: Domain structure of AKT isoforms (141). The PH (pleckstrin homology) domain acts as phosphoinositide-binding site and the hydrophobic motif (HM) is located in the C-terminal region. Phosphorylation sites in the activation loop in the kinase domain and the hydrophobic motif are indicated.

AKT plays a fundamental role in the regulation of cell growth, proliferation, survival, and differentiation by phosphorylating a divers number of protein substrates at the minimal consensus sequence RxRxxS/T (141,143). Examples for this extensive group of AKT substrates are members of the Forkhead family of transcription factors (FOXOs), pro-apoptotic proteins such as Bad and caspase-9, and proteins that are implicated in metabolism, cell growth, and proliferation such as glycogen synthase kinase 3 (GSK3), mTOR, and tuberous sclerosis complex 2 (TSC2) (141,144). In addition, AKT is also an important regulatory kinase of several MAPKKKs. AKT phosphorylation of MLK3 on Ser674 (145), of ASK1 on Ser83 (146), and of MEKK3 at a not yet identified residue (147) negatively regulates apoptosis. AKT phosphorylation of c-Raf on Ser259 is involved in the regulation of muscle differentiation (148,149), phosphorylation of B-Raf on Ser364 is discussed to modulate the signal specificity of the Ras-Raf pathway (150), and phosphorylation of Cancer

Osaka thyroid oncogene (COT) on Ser400 regulates COT-induced NFκB-dependent transcription (151).

3.2.3. The apoptosis-inducing kinase ASK1

ASK1 (also known as MAPKKK5) is a ubiquitously expressed MAPKKK family member, which is an important mediator of apoptotic signaling induced by many stress signals including TNF-α, FasL, ROS, genotoxic stress, chemotherapeutic agents, and serum withdrawal. Stimulation of ASK1 leads to the activation of the stress signaling transduction pathway that finally induces phosphorylation and activation of JNK and p38 MAPK leading to stress responses or mitochondria-mediated apoptosis (89,152-154). Deletion of ASK1 in mice prevents sustained activation of JNK and p38 MAPK and thereby induction of apoptosis (155). ASK1 is localized in the cytoplasm (134,136), nucleus (156) and in mitochondria (134) where it activates mitochondria-mediated apoptosis in a JNK-independent manner by inducing cytochrome c release and caspase-3 activation (134). In addition, ASK1 also induces apoptosis in a kinase independent manner via the Fas death receptor pathway by interacting with Daxx. This apoptotic pathway does not lead to the activation of caspase-3 but to the phosphorylation and activation of transcription factors such as c-Jun (22,157).

3.2.3.1. Structure and regulation mechanisms of ASK1

Human ASK1 consists of 1,374 amino acids (aa) and has a molecular weight of 155 kDa. It contains an inhibitory N-terminal domain, a central serine-threonine kinase domain and a C-terminal regulatory domain with a coiled-coil domain for protein oligomerization (89,158). In non-stressed cells ASK1 resides in a high molecular weight signalosome (shown in Figure 8) as a preformed inactive homo-oligomer that is inhibited by Trx binding to its N-terminal domain and is associated with other not yet identified factors (152,158,159). Depending on its intracellular localization both cytoplasmic and nuclear Trx1 and mitochondrial Trx2 interact in a reduced form with ASK1 at Cys250 and Cys30, respectively (134,136). Binding of Trx1 negatively regulates ASK1, which is discussed in 2.1.6. After stimulation with TNF-α or ROS (e.g. superoxide, hydrogen peroxide, and hydroxyl radical) Trx is oxidized thereby forming an intramolecular disulfide bridge with its two redox-active cysteins and resulting in its dissociation from ASK1 (134-136). Association of TRAF2 and TRAF6 to ASK1 leads to

the formation of a higher molecular weight complex. Full activation of ASK1 is induced by trans-phosphorylation on Thr838 by an unknown kinase, a subsequent conformational change of the ASK1 homo-oligomer and a final trans-autophosphorylation step (158).

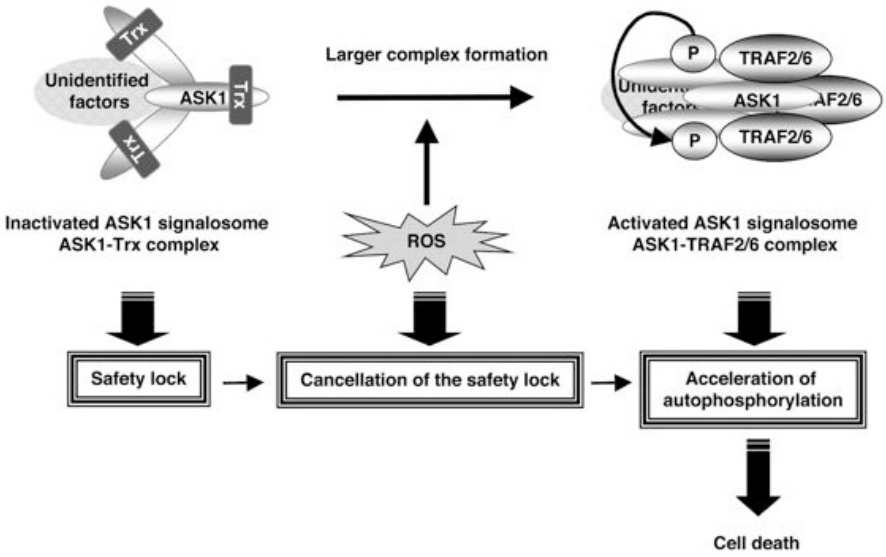

Fig. 8: A schematic model of ROS-induced active configuration of the ASK1 signalosome (adopted from Noguchi et al. (159))

ROS causes dephosphorylation of ASK1 on Ser967 by an ocadaic acid-sensitive phosphatase leading to the dissociation of the inhibitory scaffold protein 14-3-3 (160,161). Incubation of cells with TNF-α mediates interaction of ASK1-interacting protein (AIP) to the C-terminal domain of ASK1 around the 14-3-3 binding site, preferentially when Ser967 is dephosphorylated. Binding of AIP causes dissociation of 14-3-3 and consequently enhances ASK1 activity (171).

Oxidative stress-induced activation of ASK1 is negatively regulated in a feedback reaction by PP5 (protein phosphatase 5) but not via dephosphorylation of ASK1 on Thr845 (162). PP5 itself is negatively regulated by the mTOR, which is a sensor for mitogenic stimuli, nutrient conditions, and ATP, and lies downstream of PI3K (163).

Glutaredoxin (GRX) is an additional sensor to Trx for metabolic stress such as glucose deprivation, which increases intracellular levels of hydroperoxide and glutathione disulfide (GSSG) (164). Unlike Trx, GRX binds to the C-terminal domain of ASK1 in a redox-sensitive manner and reacts to metabolic oxidative stress through catalytic reactions with GSSG leading to its dissociation from ASK1 (165). GRX also reacts with glutathione-

containing disulfides but is a weaker sensor for hydrogenperoxide and oxidized proteins compared with Trx (165).

Several other negative regulators of ASK1 in addition to Trx, GRX, and PP5 carry out their inhibitory function by protein–protein interactions (summarized in Figure 9). Heat shock protein 72 (Hsp72) prevents apoptosis upon oxidative stress when cells are pre-exposed to mild heat shock (166). c-Raf, another MAPKKK family member, negatively regulates ASK1 in a catalytic-independent and not further characterized manner (167). Ectopically expressed Cdc25A phosphatase, which normally promotes cell cycle progression by activating G1 cyclin-dependent kinases, inhibits oxidant-induced activation of ASK1 by binding to the C-terminal region of ASK1 surrounding the 14-3-3 binding site (168). The retinoblastoma (Rb) suppressor protein is involved in the negative regulation of both cell proliferation and apoptosis by binding to ASK1. Upon apoptotic stimulation-induced association with Rb, ASK1 has to overcome the anti-apoptotic function of Rb for induction of apoptosis (156,169). ASK1 is not only localized in the cytoplasm but is also associated with the type 1 insulin growth factor-receptor (IGF-IR) at the cytoplasmic membrane in cells that are not simulated with IGF-I. The interaction of ASK1 and IGF-IR is mediated between the C-terminal domain of ASK1 and the intracellular domain of the IGF-IR β-chain. After stimulation and activation of IGF-IR by binding of IGF-I, ASK1 gets phosphorylated at tyrosine residues within its N-terminal domain and is thereby inactivated. The IGF-I-induced inhibition of ASK1 is independent from PI3K although the PI3K-AKT pathway is known to negatively regulate ASK1 (170). AKT, which is a downstream kinase of PI3K, phosphorylates ASK1 on Ser83 within the inhibitory N-terminal domain thereby decreasing ROS-stimulated ASK1 kinase activation (146).

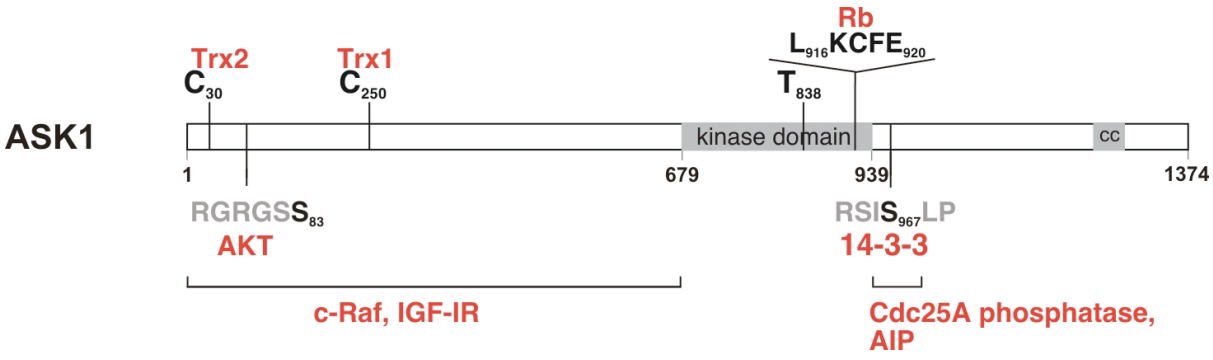

Fig. 9: Schematic overview of ASK1 regulatory proteins

3.2.3.2. The regulatorly function of ASK1 in cellular differentiation processes

In addition to its pro-apoptotic function, ASK1 also functions as an important regulatory kinase in several cellular differentiation processes. ASK1 is an intracellular inducer of keratinocyte differentiation, which is mediated by the ASK1-p38 MAPK cascade (120). The same signaling pathway is implicated in the regulation of neuronal differentiation in adult hippocampus-derived progenitor cells (172) and of neuronal differentiation and survival of the pheochromocytoma cell line PC12 (77). During erythroid differentiation, the ASK1-induced activation of JNK and p38 MAPK is necessary for a negative feedback loop and thereby for the downregulation of ERK activity (173).

3.2.4. The Raf kinase family

The MAPKKK subfamily of Raf proteins contains three members, A-Raf, B-Raf and c-Raf, which are encoded by three separate genes. c-Raf was the first characterized family member and identified as the cellular homologue of the v-raf or v-mil oncogene from the murine retrovirus 3611-MSV. Raf is part of the extensively investigated Raf-MEK-ERK signaling pathway that transduces extracellular signals to the nucleus and thereby regulates many cellular processes including proliferation, survival, and differentiation. The Raf-MEK-ERK signaling cascade is conserved from yeast to vertebrates and is activated by the small GTPase Ras, which in turn is induced by a large variety of mitogens at the cell membrane. Binding to Ras mediates the translocation of Raf from the cytoplasm to the cell membrane where additional activation steps occur involving dimerization or oligomerization, binding to other proteins, conformational changes and phosphorylation (174).

3.2.4.1. Isoforms and regulation mechanisms of Raf

Among the three Raf proteins, c-Raf is the best studied isoform, which is expressed ubiquitously in contrast to A- and B-Raf, which were originally thought to be restricted to urogenital tissues and to haematopoietic and neuronal cells, respectively (175). However, some recent data indicate a wider expression of the latter two Raf isoforms and B-Raf has gained much interest by the observation of its frequent mutation in melanoma and other cancers (174,176).

All three Raf isoforms share a similar protein structure with three highly conserved regions, CR1 and CR2 within the N-terminus and CR3 in the C-terminus encoding the kinase domain (Figure 10). CR1 consists of a Ras-binding domain (RBD) and cysteine-rich domain (CRD), which are both required for the cytoplasmic membrane recruitment of Raf.

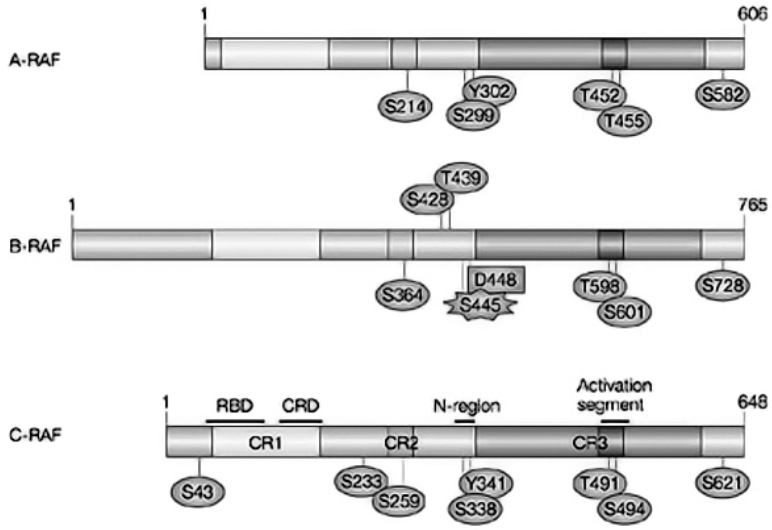

Fig. 10: Structure of Raf proteins including all known phosphorylation sites (174) CR1 to CR3 are conserved regions and CR1 contains the Ras-binding domain (RBD) and the cysteine-rich domain (CRD)

Binding of GTP-loaded Ras to the RBD in the regulatory is sufficient for B-Raf activation whereas additional activation steps are necessary to fully activate c-RAF. Inactive c-Raf is bound to a 14-3-3 dimer at the residues Ser259 and Ser621 flanking the kinase domain of Raf (177). A third 14-3-3 binding site is located in CR3 (174). After Ras-mediated translocation from the cytoplasm to the membrane, c-Raf undergoes a complex series of activation events starting with the dephosphorylation of Ser259 by PP2A followed by the dissociation of 14-3-3 (177,178). Raf is further phosphorylated in the activation loop and on Ser338 and Tyr341, which are both located within CR3. Src and Src-family kinases are proposed to mediate Tyr341 phosphorylation whereas the upstream kinase of Ser338 is not identified yet but suggested to be PAK1 and PAK2 (reviewed in (174,179)). These two phosphorylation sites on Ser338 and Tyr341 are also found in A-Raf suggesting a similar activation mechanism (180). B-Raf, which possesses a much higher kinase activity towards MEK than c-Raf, is constitutively phosphorylated on Ser338 and contains an aspartate at the position corresponding to Tyr341 which can mimick phosphorylation (181). B-Raf can be activated additionally by the Ras-related protein Rap1 (182). Raf is not only regulated by

phosphorylation but also by binding of several scaffold proteins, which is mainly investigated for c-Raf. These scaffold proteins mediate protein stabilization, which increases the efficiency of signaling and determines signal specificity by regulating the composition of the c-Raf-MEK-ERK complex and the subcellular localization of c-Raf. Examples for these scaffold proteins are the kinase suppressor of Ras (KSR), connector enhancer of KSR (CNK), and suppressor of Ras mutations-8 (SUR8). Binding of MP-1, which ties MEK and ERK together, recruits the Ras-c-Raf-MEK-ERK complex to endosomes through the interaction with the endosomal protein p14 (reviewed in (174,179)).

3.2.4.2. The regulatory role of Raf in divers cellular processes

Raf kinases participate in the control of cellular processes including proliferation, survival, and differentiation, which is mediated both in a kinase-dependent but also kinase-independent manner. The three Raf isoforms differ in their biological functions.

The intensity and duration of ERK activation by Raf determines whether proliferation or differentiation is induced. This is best studied in the PC12 model system for neuronal differentiation. Epidermal growth factor (EGF) activates the Ras-c-Raf-MEK-ERK pathway leading to a transient activation of ERK and thus to proliferation. In contrast, nerve growth factor (NGF) preferentially activates B-Raf via Rap1, which causes a sustained ERK activity that is required for neuronal differentiation. In addition, NGF also activates cAMP signaling that positively regulates B-Raf by activating Rap1 and on the other hand inhibits c-Raf by inducing PKA mediated phosphorylation of Ser259 (182-184). In contrast to the PC12 neuronal differentiation system, sustained ERK activity ensures proliferation of C2C12 myoblasts and inhibition of the c-Raf-MEK-ERK pathway induces differentiation into myotubes (148). In fibroblast, both the duration and the intensity of ERK activation are crucial for the biological outcome. Binding of platelet-derived growth factor (PDGF) induces a sustained activation of ERK, which is required for proliferation. In contrats, a stronger activation of ERK by a manipulated c-Raf causes cell-cycle arrest (reviewed in (174)).

Independent from the ERK pathway, Raf also exhibits an anti-apoptotic function by inhibiting the pro-apoptotic kinases mammalian sterile 20-like kinase (MST2) and ASK1 (167,185). Another kinase-independent regulatory role of Raf is implicated in cell migration by the regulation of the Rho kinase α (ROKα), which is explained by a scaffold or adaptor protein function of c-Raf (186).

3.2.4.3. Regulation of skeletal muscle differentiation by an AKT-Raf crosstalk

During vertebrate embryogenesis skeletal muscle is derived from mesodermal precusor cells in somites, which are committed to the skeletal muscle lineage. After induction of differentiation, the proliferative muscle precursor cells (myoblasts) start expressing determination-class MRFs (muscle regulatory factors), exit the cell cycle and undergo final differentiation steps to form muscle cells (myocytes). This differentiation process ends up in the generation of multinucleated myofibers (187,188).

During the myogenic lineage determination, the homeodomain transcription factor Pax3 leads to the activation of MyoD, which belongs to the family of basic helix-loop-helix (bHLH) transcription factors (189). MyoD and Myf5, another bHLH transcription factor, represent the primary MRFs, which are required for the determination of proliferating somitic cells to myoblasts. These myoblasts then differentiate into myocytes after activation of secondary MRFs such as myogenin and MRF4, which also belong to the family of bHLH transcription factors, and of the myocyte enhancer factor 2 (MEF2) group of MCM1 (also know as serum response factor (c-fos serum response element-binding transcription factor), Agamous, Deficiens, Serum response factor (MADS)-box transcription factors (190).

The murine C2C12 myoblast cell line is a widely used cell cultur model system for the investigation of the differentiation process of myoblasts into multinucleated myotubes (191). Differentiation of C2C12 myoblasts is induced by switching to low serum conditions, and can be enhanced by addition of insulin and insulin-like growth factors (IGF-I and IGF-II) (192,193). IGF-II is secreted by confluent C2C12 myoblasts leading to spontanous differentiation via an autocrine loop (193). These three growth factors, insulin, IGF-I and IGF-II, activate two main signaling pathways, the Ras-c-Raf-MEK-ERK pathway and the PI3K-AKT-p70S6-kinase pathway (194). The examination of a differentiation specific crosstalk between these two pathways elucidated a negative regulation of the Ras-c-Raf-MEK-ERK pathway by an AKT phosphorylation, which is carried out only in myotubes but not in myoblasts (148). A deeper analysis of this crosstalk determined Ser259 on c-Raf as the AKT phosphorylation site (149).

3.2.5. ASK2 is an interaction partner of ASK1

Human ASK2 (also referred to as MAPKKK6) is located on chromosome 1 at 1p36.11, consists of 1,288 aa, and has a calculated molecular weight of 143 kDa. ASK2 was originally found as an interaction partner of ASK1 in a yeast two hybrid screen (91). For this screen the ASK1 kinase domain together with the C-terminus was used as bait and a cDNA library constructed from HeLa cells was chosen as prey. One positive clone encoded a new serine-threonine MAPKKK, which was identified to share 45% aa homology with ASK1 and thus named MAPKKK6 (ASK2). The interaction between ectopically expressed ASK1 and ASK2 was confirmed by co-immunoprecipitation analysis. Furthermore, a tissue distribution analysis of ASK2 using a Northern blot of human tissues exhibited high mRNA levels in heart and skeletal muscle but only lower levels in lung, liver, kidney, testis, and spleen. A comparison of the ASK2 and ASK1 kinase activities demonstrated that ASK2 only leads to a weak activation of JNK but not of p38 MAPK and ERK. In contrast, a recent report (195) showed that mouse ASK2 only functions as MAPKKK when forming a heteromeric complex with ASK1. Overexpression of wild-type ASK2 together with a kinase-inactive ASK1 induces phosphorylation of JNK and also of p38 MAPK and activates caspase-3 in non-stressed HEK293 cells. Moreover, concomitant expression of kinase-inactive ASK1 increases the responsiveness of ASK2 to oxidative stress, which was detected by phosphorylation of ASK2 on Thr807 within the activation loop of the kinase domain indicating kinase activity. Additionally, ASK1 stabilizes ASK2 by inhibiting its proteasomal degradation. Within the heteromeric complex, ASK2 phosphorylates ASK1 on Thr838 whereas phosphorylation of ASK2 on Thr807 is supported only by binding to ASK1 but mediated by autophosphorylation. Due to their hetero-oligomerization and mutual activation, ASK2 is proposed to be one of the unidentified factors that build up the ASK1 signalosome (discussed in 2.2.3.1.).

3.3. Gene silencing by RNA-mediated interference (RNAi)

RNA-mediated interference (RNAi) or RNA silencing was first discovered in *C. elegans* (196) and describes the process of sequence specific post-transcriptional regulation of gene expression triggered by double-stranded RNA (dsRNA) (reviewed in (197,198)). The

regulation of gene expression by RNAi is conserved in most eukaryotic organisms and has evolved from the non-specific innate immune response against endogenous parasitic and exogenous pathogenic nucleic acids (199,200). RNAi plays a major role in regulating development and genome maintenance and is mediated by small non-coding dsRNA (196,200,201). These double-stranded small interfering RNAs (siRNAs) are generated by the RNaseIII endonuclease dicer and have a common length of 21 to 25 nucleotides. dsRNA can either be encoded in the genome by microRNA (miRNA) genes (201) or can derive from an artificial exogenouse source such as viral based vectors including retro-, lenti-, and adenoviral vectors (198), which are maturated into siRNA by the effector complex RISC (RNA-induced silencing complex). Third, siRNA can be chemically synthesized and directly transfected.

Generation of miRNAs starts with the transcription of large pri-miRNA precursors that form imperfect stem-loop structures. The pri-miRNA is cleaved into 70 to 90 bp fragments by a microprocessor complex consisting of the RNaseIII enzyme drosha and the dsRNA-binding protein pasha. This pre-miRNA is then transported from the nucleus to the cytoplasm by the Ran-GTP-dependent nucleo/cytoplasmic transporter exportin-5. In the cytoplasm, dicer cleaves the hairpin pre-miRNA into 21 to 25 bp long miRNA generating 2-nucleotide-long 3' overhangs. The endonuclease dicer not only contains two tandem RNaseIII domains but also a helicase domain, a dsRNA-binding domain (dsRBD) and a PAZ (Piwi-Argonaute-Zwille) domain. After unwinding of the miRNA duplex, only the guide strand is incorporated into the effector complex RISC. This complex contains members of the argonaute protein family, accessory factors, and the mRNA target (202) and carries out translational repression and mRNA cleavage, summarized in Figure 11 (reviewed in (197,201,203)).

Short hairpin RNAs (shRNAs) can be constructed in a plasmid backbone using the U6 or H1 RNA polymerase III promoter for their transcription (reviewed in (198,204)). RNAIII polymerase transcribes small, non-coding transcripts lacking a CAP-structure or a poly-A tail (205). These shRNAs are designed by two inverted repeats separated by a spacer sequence. Transcription of shRNAs is initiated at a defined nucleotide and terminated by a stretch of 4 thymidines. The transcription products are molecules of 50 to 70 nucleotides in length, which form a stem-loop structure *in vivo*. Dicer cleaves these hairpin dsRNAs into siRNAs, which are transferred into the RISC complex for gene silencing (204). Duplex siRNAs can be produced in a DNA vector-based manner by tandem placement of sense and anti-sense strands each containing an own RNA polymerase III promoter and ending with a stretch of 5

thymidines. Alternatively, sense and antisense strands for siRNA duplex formation can be subjected to cells seperately via two plasmids. After plasmid transfection and transcription, the two RNA strands form the siRNA duplex with 3' uridine-overhangs and are transported into the RISC complex where they mediate gene silencing. Chemically synthesized siRNA duplexes are 19 to 22 bp in length with 2 nucleotide overhangs at either end. They are transfected into cells and again carry out their gene silencing function within the RISC complex (reviewed in (198,204)).

miRNAs from plants differ from animal miRNAs by being completely complementary to the target sequence, which is degraded (200,201)). In contrast, miRNAs from animals exhibit multiple mismatches and function as small temporal RNAs (stRNA). These stRNAs regulate developmental transitions in *C. elegans* by inhibiting translation initiation *(reviewed in (206)*.

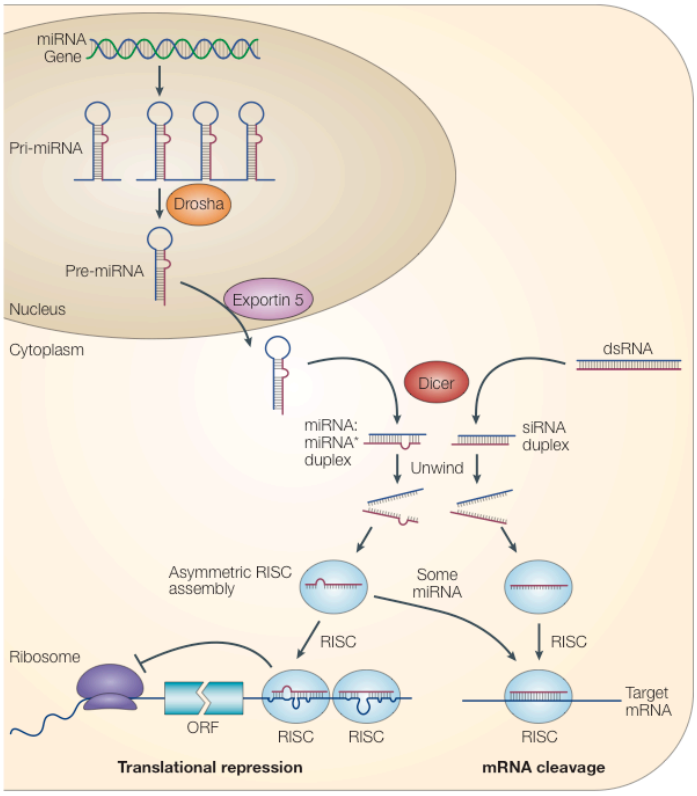

Fig. 11: Model for the biogenesis of miRNAs and siRNAs and for their post-transcriptional regulation of gene expression (adopted from He and Hannon (201))

mRNA decay and translational repression mediated by siRNA- and miRNA containing RISC complexes take place in P-bodies, which are discrete cytoplasmic compartements (207). In these foci, RNA and heteromeric protein complexes form a larger ribonucleoprotein structure that carries out the post-transcriptional regulation of eukaryotic gene expression.

4. Materials and Methods

4.1. Materials and antibodies

Insulin-like growth factor (IGF), LY294002, AKT inhibitor VIII, and digitonin were purchased from Calbiochem Signal Transduction (La Jolla, CA, USA). Protein-G-Sepharose, [γ-^{32}P]-ATP, Hybond^{TM}-ECL membrane, ECL Western blot detection kit and ECL films were purchased from Amersham Pharmacia Biotech (Uppsala, Sweden). Acrylamid (30%) and Bisacrylamid (2%) were from Roth (Karlsruhe, Germany). Dulbecco's modified eagle medium (DMEM), horse serum, newborn calf serum (NCS), TRIzol, BenchMark Pre-stained Protein Ladder and Tetramethylrhodamine, methyl ester, perchlorate (TMRM) were obtained from Invitrogen GIBCO (Basel, Switzerland). Fetal calf serum (FCS) came from Brunschwig (Basel, Switzerland). Trypsin-EDTA was from Biological Industries (Kibbutz Beit Haemek, Israel). Recombinant human tumor necrosis factor-alpha (TNF-α), cyclohexemide (CHX), and anisomycin were obtained from Sigma (St. Louis, MO, USA). Active AKT1 was from Upstate Biotechnology (Lake Placid, NY USA). Complete EDTA-free Protease Inhibitor Cocktail was from Roche Molecular Biochemicals (Basel, Switzerland). Bio-Rad protein detection kit and PrecisionPlus DualColor Standard were purchased from Bio-Rad Laboratories (Hercules, CA, USA).

A self-generated rabbit polyclonal antibody was used for detection of ASK2 (see chapter 4.5.5.) Anti-HA (12CA5) and anti-HA-HRP high affinity purified (3F10) antibodies were obtained from Roche Molecular Biochemicals (Basel, Switzerland). Anti-Flag (M2) and anti-Cytokeratin 18 were purchased from Sigma (St. Louis, MO, USA). Anti-Myc (9E10), anti-β-Actin (C4), anti-ERK2 (C-14), and anti-ASK1 (H-300), anti-Lamin A/C (N-18), anti-c-Raf (C-20), anti-Myogenin (M-225), anti-Troponin T-FS (C-18) and anti-Trx (FL-105) were obtained from Santa Cruz Biotechnology (Palo Alto, CA, USA). Anti-PARP, anti-Cleaved-Caspase-3 (Asp-175), anti-Phospho-AKT(S473), anti-Phospho-p38 MAPK(T180/Y182), anti-Phospho-JNK(T183/Y185), anti-Phospho-RxRxxS/T were obtained from Cell Signaling Technology (Beverly, MA, USA). Anti-Thioredoxin 2 was purchased from Abcam Ltd. (Cambridge, UK). Anti-Phosphoserine was from Chemicon (Temecula, CA, USA). Anti-MF20 was obtained from the Developmental Studies Hybridoma Bank (The University of Iowa, Department of Biological Sciences, Iowa City, USA). Anti-GST and HRP-conjugated

secondary antibodies were used from Amersham Pharmacia BioTech (Uppsala, Sweden). TRITC or FITC-labeled secondary antibodies were from Jacksons Immuno Research (West Grove, PA, USA).

4.2. Buffers and Media

TE buffer: 10 mM Tris HCl pH 7.5, 1 mM EDTA, pH adjusted to 8.0

TAE buffer: 4.84 g Tris base, 1.14 ml acetic acid, 2 ml 0.5 M EDTA pH 8.0 in 1 l ddH_2O

Loading buffer: 50 mM Na-Acetate, 1 mM EDTA, 40 mM Tris pH 7.9, 1% SDS, 2% bromphenolblue, 25% Ficoll, 5% glacial acetic acid

Bacteria media:

LB Agar according to Miller and LB Broth according to Miller were obtained from Scharlau Chemie S.A. (Barcelona, Spain) and prepared according to the manufacturer's protocol.

SOC: LB medium supplemented with 10 mM NaCl, 10 mM KCl, 10 mM $MgCl_2$, 10 mM $MgSO_4$, and 20 mM glucose

Sample buffer: 62.5 mM Tris pH 6.8, 2% SDS, 10% glycerol, 5% mercaptoethanol

Laemmli buffer: 1.44% glycine (w/v), 0.3% Tris base (w/v), 0.05% SDS (w/v)

Transfer buffer: 20% methanol (v/v), 0.72% glycine (w/v), 0.15% Tris base (w/v), 0.025% SDS (w/v)

Washing buffer: 50 mM Tris pH 7.5, 150 mM NaCl, 0.1% Tween20 (v/v)

Blocking buffer: 50 mM Tris pH 7.5, 150 mM NaCl, 0.1% Tween20 (v/v), 5% milk powder (w/v)

Antibody dilution buffer: 50 mM Tris pH 7.5, 150 mM NaCl, 0.1% Tween20 (v/v), 1% milk powder (w/v)

Stripping buffer: 62.5 mM Tris pH 6.8, 2% SDS (w/v), 0.7% β-mercaptoethanol (v/v)

4.3. Plasmids and DNA techniques

4.3.1. Restriction and isolation of DNA-fragments

Digestion of 0.2 to 50 µg plasmid DNA was performed using 0.5 to 50 U DNA restriction endonuclease in 1x restriction buffer (NEB, Allschwil, Switzerland or Fermentas,

Nunningen, Switzerland). DNA fragments were mixed with 0.3 vol loading buffer and separated on 0.8 to 1.2% agarose gel in TAE buffer supplemented with ethidium bromide (0.5 µg/ml). The desired DNA-fragment bands were excised from the gel under a 366 nm UV-lamp and isolated with the QIAquick® Gel Extraction Kit from QIAGEN (Basel, Switzerland) according to the manufacturer's protocol. DNA was eluted in 10 mM Tris pH 8.5.

4.3.2. Klenow DNA-polymerase treatment

DNA fragments were phosphorylated by Klenow treatment using 5 U Klenow Fragment (MBI Fermentas) and 33 µM dNTPs in 1x Klenow buffer for 60 min at 37 °C. DNA was purified using the QIAquick® PCR-Purification Kit (QIAGEN).

4.3.3. Alkaline phosphatase treatment of vector fragments

Vector DNA fragments were dephosphorylated using 1 U calf intestine alkaline phosphatase in 1x dephosphorylation buffer (Roche) for 45 min at 37 °C. DNA was purified using the QIAquick® PCR-Purification Kit (QIAGEN).

4.3.4. Ligation of DNA

For ligation, 0.5 µg vector DNA fragment were mixed with the threefold molar amount of insert DNA fragment and incubated with 1 U T4-DNA-ligase in 1x T4-DNA-ligase buffer (Invitrogen GIBCO) over night at 16 °C. The ligation reaction was transformed into transformation-competent DH5α bacteria cells.

4.3.5. Preparation of transformation-competent *E.coli* DH5α cells and transformation

To obtain a fresh culture, a single colony of DH5α cells was inoculated in 2 ml LB medium and cultivated over night at 37 °C. This culture was used for inoculation of a 50 ml culture, which was grown in a rotating incubator at 37 °C to an OD_{600nm} of 0.5 to 0.6. Cells were harvested by centrifugation for 5 min at 5,000 rpm (SS34 rotor) at 4 °C. The cell pellet was

resuspended in 10 ml ice-cold 50 mM $CaCl_2$ and incubated for 30 min on ice. After centrifugation for 5 min at 5,000 rpm (SS34 rotor) at 4 °C, cells were carefully resuspended in 2x 850 µl sterile 20% glycerol (ice-cold) supplemented with 50 mM $CaCl_2$, and aliquoted in ice-cold reaction tubes. Cells were either stored at –80 °C or immediately used for transformation. Transformation was performed by adding 5 µl of ligation reaction to 50 µl of competent DH5α cells. After a 1 h incubation on ice, cells were subjected to a heat-shock for 45 sec in a water bath with 42 °C and subsequently cooled on ice for 2min. Then, 500 µl SOC medium was added and cells were incubated for 45 min at 37 °C in a heating block. Finally, the transformation reaction was plated on selective agar plates, containing either 100 µg/ml ampicillin or kanamycin dependent on the transformed DNA plasmids.

4.3.6. Conservation of bacteria cells

For conservation, a fresh 10 ml LB over night culture was prepared. The next day, cells were pelleted by centrifugation for 5 min at 5,000 rpm. The cell pellet was resuspended in 0.8 ml LB medium together with 0.8 ml sterile 80% glycerol and stored at –80 °C.

4.3.7. Analytical DNA isolation (miniprep)

Generally, 2 ml LB bacteria medium was inoculated with a single colony of a bacteria culture and cultivated over night in a heated incubator at 37 °C. DH5α cells transformed with pMSCVpuroD3'LTR- or cFUGW constructs were grown at 30 °C. The next day, 1.5 ml of the over night culture were used for DNA preparation, the residual culture was used for preparation of glycerol cultures. DNA preparation was performed according to the EasyPrep method (208). Briefly, the cell suspension was sedimented for 3 min at 5,000 rpm and the pellet was resuspended in EasyPrep lysis buffer (10 mM Tris pH 8.0, 1 mM EDTA, 15% sucrose (w/v), 2 mg/ml lysozyme, 0.2 mg/ml RNase, 0.1 mg/ml BSA) and incubated for 5 min at room temperature. After boiling 1 min at 95 °C, the cell lysate was cooled on ice for 1 min and centrifuged for 15 min at 15,000 rpm to obtain the plasmid DNA in the supernatant.

4.3.8. Preparative DNA isolation (maxiprep)

For preparative DNA isolation, an over night culture with 250 ml LB medium was inoculated with a 2 ml culture freshly prepared from a frozen glycerol culture. This over night culture was pelleted by centrifugation for 10 min at 5,000 rpm in a GSA rotor and the plasmid DNA was isolated using the Genelute Plasmid Maxi-Prep Kit (Sigma) according to the manufacturer's instructions.

4.3.9. Plasmid constructions

Human ASK2 was cloned with an N-terminal HA-tag into the pcDNA3.1/Hygro(+) vector (Invitrogen GIBCO) as follows. First, annealed oligonucleotides encoding an HA-tag were inserted into the pcDNA3.1/Hygro(+) vector by using the AflII site, which generated an additional AscI site 3' to the HA-tag. The N-terminal region of the ASK2 coding sequence from the start codon to position 833 was cloned using two EST-clones (IMAGp998*B*166127 and IMAGp998*N*015354, RZPD, Germany). The ASK2 fragments were cut out at the EcoRI and NotI sites from these two EST-clones, ligated at the overlapping NotI site and cloned into the EcoRI site of the pBluescript KS(-) vector (Stratagene, La Jolla, CA, USA). This N-terminal ASK2 fragment was amplified by PCR using the following primers forward 5'-TTGGCGCGCCTCGCATGGCGGGGCCGTGTC-3' and reverse 5'-GGCATCATGAT GATGTCGGGGCTCAGCAG-3' and cloned into the EcoRV site of pcDNA3.1-Hygro(+)-HA. The residual ASK2 sequence from position 834 to 3864 was obtained by two PCR steps using the SuperScript human heart cDNA library (Invitrogen GIBCO) as template and the following primers: 1) forward 5'-TTGGCGCGCCTGGTATGAACTTGCTGCTCTCCTA CCGC-3' and reverse 5'-CTTGGAGGTGCCGAAGTCAGAAATC-3' and 2) forward 5'-CACCCGCCAGATCCTGCAGGGA-3' and reverse 5'-GCGCTCTAGACAGCTCTCAG GGTCCAGAGGTGA-3'. The two amplicons were ligated at the internal SbfI site and cloned into the pcDNA3.1-Hygro(+)-HA vector using the AscI and XbaI sites. This plasmid was then linearized using the AscI and RcaI sites and the N-terminal region was inserted. This N-terminal fragment was obtained by PCR using the previously generated pBKS-N-term-ASK2 as template and the following primers: forward 5'-TTGGCGCGCCCAGAATGGCG GGGCCGTGTCCC-3' and reverse 5'-GAATGACACCTACTCAGACAATGCGATGC-3'. The generated pcDNA3.1Hygro(+)-HA-ASK2 was used for further subcloning of ASK2 into the pcDNA3.1Hygro(+)-Myc vector using the AscI and XbaI sites. An untagged construct of

ASK2 was obtained by cutting ASK2 out of the pcDNA3.1Hygro(+)-HA-ASK2 plasmid with AscI and XbaI and by blunt end ligation into the EcoRV site of the pcDNA3.1Hygro(+) vector.

The expression plasmid pcDNA3-ASK1 was kindly provided by H. Gram (Novartis Pharma AG) and was used as template for PCR amplification of ASK1 for subcloning into the pcDNA3.1Hygro(+)-HA vector using the AscI and XbaI sites. The following primers were used: forward 5'-TTGGCGCGCCCAAAATGAGCACGGAGGCGGACGAGG-3' and reverse 5'-CACAATAGAATCATAGTCCTGGATATCTCTGTAGG-3'.

A Flag-tagged pCMV-Trx1 construct was kindly provided by W. Min (134). Flag-tagged Trx2 containing the mitochondria-target sequence (Flag-mtTrx2) and Flag-tagged Trx2 without the mitochondria-target sequence (Flag-Trx2) were generated by PCR amplification using a cDNA library made from Jurkat cells as template and the following primers: forward(mtTrx2) 5'-GTGAATTCAATGGCTCAGCGACTTCTTCTGAGGAG-3', forward(Trx2) 5'-GTGAATTCAAGGATCTCCTTGACAACCTTTAATATCCAGG-3', and reverse 5'-AAGGATCCTCAGCCAATCAGCTTCTTCAGGAAGGC-3'. The amplicon was cloned into the pCMV-Flag vector using the EcoRI and BamHI sites.

The pCMV5-HA-AKT and pCMV5-HA-AKT.KD constructs were kindly provided by B. Hemmings. GST-fusion constructs of human ASK2 were generated by PCR amplification using the following primers: forward 5'-CGCGGATCCATGGCGGGGCCGTGTC CCCGGT-3' and reverse 5'-CCGGAATTCTCACGTGTACTCATAATCAAACTCCAA CATC-3' for GST-R1 (BamHI/EcoRI), forward 5'-CGCGGATCCATGAACTTGCT GCTCTCCTACCGCGA-3' and reverse 5'-CCGGAATTCTCACGTGTACTCATAATCA AACTCCAACATC-3' for GST-R2 (BamHI/EcoRI), forward 5'-CGCGGATCCACGGA GACGGAGACGGGCGAGCGGC-3' and reverse 5'-CCGGAATTCTCACCCAGGCTGCA GGAAGGGGTCC-3' for GST-K (BamHI/EcoRI), forward 5'-CGCGGATCCACGGA GACGGAGACGGGCGAGCGGC-3' and reverse 5'-CCGGAATTCTCAGGGCCGTGG AGCATGTCGTGGGG-3' for GST-KA (BamHI/EcoRI), and forward 5'-GGAATTCCGG ATGCCCCTTCTGCCAGTCCCAC-3' and reverse 5'-ATAGTTAGCGGCCGCTCAGGGT CCAGAGGTGACTGGTG-3' for GST-ASK2-R3 (EcoRI/ NotI). The PCR amplicons were digested cloned into pGEX-6P-2 (Amersham Pharmacia Biotech) using the restriction enzymes indicated in the brackets.

All PCR reactions were performed using the Herculase Hotstart DNA Polymerase (Stratagene). Sequences of all constructed plasmids were verified by DNA sequencing (Microsynth, Balgach, Switzerland).

4.3.10. Site-directed mutagenesis of pcDNA3.1Hygro(+)-HA-ASK2

Point mutations were introduced into pcDNA3.1Hygro(+)-HA-ASK2 by oligo site-directed mutagenesis using the QuickChange® XL site-directed mutagenesis kit (Stratagene) according to the manufacturer's instructions. Ser46 and Ser916 of ASK2 were mutated to alanine, generating pcDNA3.1Hygro(+)-HA-ASK2^{Ser46Ala} and pcDNA3.1Hygro(+)-HA-ASK2^{Ser916Ala}, respectively. The following primers were used (mutation sites are underlined): forward 5'-CGGAGCCGGCCGCTCGCGGTGGTCTACGTGCTGAC-3' and reverse 5'-GTCAGCACGTAGACCACCGCGAGCGGCCGGCTCCG-3' for ASK2^{Ser46Ala} (HA-ASK2-S46A), and forward 5'-GGAGCCGCAGCCCCGCGTCCCCACGACATGCTC-3' and reverse 5'-GAGCATGTCGTGGGGACGCGGGGCTGCGGCTCC-3' for ASK2^{Ser916Ala} (HA-ASK2-S916A). The latter primer pair was also used to generate the GST-KA-S916A construct. The cycling conditions for PCR amplification were 95 °C for 1 min (1 cycle), 95 °C for 50 sec, 60 °C for 50 sec, and 68 °C for 10 min (18 cycles), 68 °C for 7 min (1 cycle).

After mutagenesis, one third of the reaction was transformed into DH5α competent cells as described above and mutagenesis was confirmed by DNA sequencing (Microsynth,).

4.3.11. Retro- and lentiviral plasmid constructions for shRNA expression

For RNAi-mediated gene knockdown, following DNA oligonucleotides were ligated into the pSUPER vector (OligoEngine, Seattle, USA): 5'-gatccccCGCTCATGCAGCCTAACT TCttcaagagaGAAGTTAGGCTGCATGAGCtttttggaaa-3' for mouse ASK1 shA4, 5'-gatcc ccCATACCTTCACGACAATCAGttcaagagaCTGATTGTCGTGAAGGTATtttttggaaa-3' for mouse ASK1 shA5, and 5'-gatccccCGTACGCGGAATACTTCGAttcaagagaTC GAAGTATTCCGCGTACGttttttggaaa-3 for luciferase shGLS used as control (209). Oligonucleotides were annealed at a concentration of 100 μM by incubating in 1x NEB2 buffer (NEB) for 5 min at 95 °C in a heating block. After turning off the heating block, the reaction tubes were left in the block until room temperature was reached and put on ice for 5

min. The annealed oligonucleotides were phosphorylated using 1 U T4 Polynucleotide Kinase (Invitrogen GIBCO) in reaction buffer (1.7 µl 1 M Tris ph 7.6, 1.5 µl 10 mM ATP, 0.4 µl $MgCl_2$) for 45 min at 37 °C and ligated into the pSUPER using the BglII and HindIII sites. From this plasmid oligonucleotides were excised either together with the H1 promoter using the EcoRI and XhoI sites for ligation into the retroviral vector pMSCVpuroD3'LTR, which was generated from the pMSCVpuro (BD Biosciences) by deletion of the 3'LTR using the NheI and XbaI, or were excised using the SmaI and HincII sites for blunt-end ligation into the PacI-digested lentiviral vector cFUGW (210). Sequences of all plasmids were verified by DNA sequencing (Microsynth).

4.4. Cell culture

4.4.1. Cell lines

HeLa (human cervix carcinoma) and HEK293 (human embryonic kidney) cells were obtained from ATCC (Rocville, MD, USA) and cultured in DMEM (Invitrogen GIBCO) supplemented with 10% FCS in a 5% CO_2 atmosphere at 37 °C. Cells were passaged with a ratio of 1:2 to 1:5. Mouse C2C12 myoblasts (ATCC) were grown in DMEM under high-serum conditions with 20% FCS. They were maintained at 37 °C in a humidified atmosphere of 8% CO_2 and were passaged every second day at a 1: 10 dilution to maintain 50% confluency.

4.4.2. Differentiation protocol for C2C12 cells

C2C12 myoblasts were grown subconfluently as described above to avoid spontaneous differentiation. To induce differentiation, cells were seeded to reach confluency the next day. Then, cells were switched to a low serum-containing growth medium supplemented with 2% horse serum (Invitrogen GIBCO) and incubated for 4 days without a further medium change.

4.4.3. Transfection

Transient transfection of plasmid DNA into HEK293 and HeLa cells was performed using jetPEI^{TM} (Polyplus Transfection, Biopac, France) according to the manufacturer's protocol. DNA and jetPEI were diluted separately in 150 mM NaCl, mixed thoroughly and incubated for 5 min at room temperature. After mixing together, the DNA-jetPEI solution was incubated for another 20 min at room temperature before adding to the cells. Medium was replaced with fresh growth medium 24 h after transfection.

4.4.4. RNA interference by siRNA transfection

Validated siRNAs specific for human ASK2 (Hs_MAP3K6_5- and Hs_MAP3K6_6 HP Validated siRNA), human ASK1 (Hs_MAP3K5_6 HP Validated siRNA), and negative control siRNA (AllStars Negative Control siRNA) were purchased from QIAGEN. HeLa and HEK293 cells were transfected with HiPerFect according to the manufacturer's protocol. Cell suspensions of HeLa and HEK293 cells were prepared in 6 well plates immediately before transfection using cell densities of $2.5x10^5$ or $7.5x10^5$ cells in 1.5ml growth medium, respectively. 5 nM siRNA was diluted in 100 µl DMEM containing 10% FCS before adding 12 µl HiPerFect. After mixing thoroughly, the siRNA-HiPerfect solution was incubated for 10 min at room temperature and added to the cell suspension. Medium was replaced with fresh growth medium 24 h after transfection.

4.4.5. Transduction

For retroviral transduction of pMSCVpuroΔ3'LTR, $1.8x10^7$ HEK293T cells were seeded in a 15 cm tissue culture plate and transfected with plasmid DNA the next day using the calcium chloride precipitation method. For this purpose, growth medium was exchanged with fresh growth medium 1 h prior to transfection. Then, 15 µg of pMSCVpuroΔ3'LTR construct and 15 µg of each packaging plasmid, pVPack-VSV-G and pVPack-GP (Stratagene), were diluted in ddH_2O in a total volume of 1.5 ml and mixed thoroughly. 150 µl 2.5 M $CaCl_2$ were mixed with 1.5 ml BBS buffer (50 mM BES, 280 mM NaCl, 1.5 mM Na_2HPO_4 adjusted to a pH of 6.94) and added dropwise to the diluted DNA solution under continuous soft-shaking. The transfection mixture was incubated for 20 min at room temperature before dropwise addition to the cell culture. After incubation over night, the transfection medium was

exchanged with 25 ml growth medium containing 20% FCS due to subsequent transduction of C2C12 cells. The next day, the virus-containing supernatant was sterile filtrated through a 0.45 μm filter (Nalgene, Rochester, NY, USA) and either used directly for transduction or stored at -80 °C. For transduction of C2C12 myoblasts, $4.5x10^5$ cells were seeded in a 10 cm tissue culture plate 1 day before transduction. The next day, cells have reached about 40% confluency and the growth medium was replaced with 5 ml of the virus-containing supernatant. After 6 h incubation, another 4 ml of fresh growth medium were added and cells were further incubated. The next day, transduced cells were selected by addition of 2 μg/ml puromycin to the growth medium.

For lentiviral transduction with pFUGW, $7x10^6$ HEK293T cells were seeded in a 10 cm tissue culture plate, cultivated over night and then transfected using the Lipofectamine™ 2000 (Invitrogen GIBCO) method according to the manufacturer's protocol. Briefly, 5 μg of pFUGW and 5 μg of each packaging plasmids, pHCMV-G and pCMV-ΔR8.2 (210,211), were diluted in OptiMEM® in a total volume of 1 ml and combined with 40 μl Lipofectamine™ 2000, which was diluted in 1 ml OptiMEM®. After 20 min incubation at room temperature, the transfection mixture was added dropwise to the cells. Medium was collected after 6 h to obtain the first virus-containing supernatant and cells were again incubated with 5 ml fresh growth medium for another 24 h. This second virus-containing supernatant was added to the first supernatant and the virus stock was concentrated as follows. The whole virus suspension was transferred into 2 ultracentrifugation tubes and centrifuged for 90 min at 27,800 rpm at 16 °C in a SW50.1 rotor (Ultra Clear centrifuge). The virus pellet was resuspended in 100 μl DMEM/F12 only (Invitrogen GIBCO) and incubated on ice for 30 min. After thoroughly pipetting up and down and a further incubation on ice for 60 min, both virus suspensions were mixed thoroughly and diluted in a total volume of 0.5 ml with DMEM containing 20% FCS. C2C12 cells at a density of $8x10^4$ in 250 μl growth medium were transduced with 250 μl of the concentrated virus stock for 1 h at 37 °C. Cells were gently mixed every 10 min and seeded in a 6 well plate.

4.4.6. Apoptosis assay by FACS analysis

Apoptotic cells were examined by FACS (fluorescence activated cell sorter) analysis using the Annexin V-FITC Apoptosis Detection Kit (Sigma) according to the manufacturer's protocol. Cells were washed twice with PBS, trypsinized, resuspended in growth medium and

collected by centrifugation for 3 min at 1,200 rpm at room temperature. After washing with PBS, cells were resuspended at a concentration of $1x10^6$ cells/ml in 500 µl 1x binding buffer. This cell suspension was incubated with 5 µl annexin V-FITC and 10 µl propidium iodide for 10 min at room temperature under protection from light. Fluorescence was determined immediately using the BD FACSCalibur Flow Cytometer (BD Biosciences, San Jose, CA, USA) with a laser excitation at 488 nm for FITC (fluorescein isothiocyanate) and at 536 nm for propidium iodide. Living cells show no staining, cells in early phase of apoptosis are only stained with annexin V-FITC, and necrotic cells additionally incorporate propidium iodide.
GFP-expressing C2C12 cells transduced with cFUGW were quantified by FACS analysis with a laser excitation at 488 nm.

4.4.7. Confocal immunofluorescence microscopy analysis

For confocal immunofluorescence microscopy analysis, HeLa and C2C12 cells were grown on glass cover slips. Cells were washed twice with PBS before fixation with 3% paraformaldehyde (PFA) for 15 min at room temperature. Mitochondria were stained by incubation of living cells with 50 nM Mitotracker (TMRM, Invitrogen GIBCO) for 20 min. After extensive washing with PBS, cells were fixed with 3% PFA. Cells were permeabilized in PBS containing 0.5% Triton-X-100, washed with PBS, and blocked with 5% NCS (Invitrogen GIBCO) in PBS for 30 min at room temperature. Primary antibodies were diluted in PBS containing 5% NCS and added to the cells for 45 min at room temperature. After three times washing with PBS, cells were incubated with FITC (fluorescein isothiocyanate) or TRITC (tetramethylrhodamine isothiocyanate)-coupled secondary antibodies diluted in PBS containing 5% NSC for 45 min at room temperature under protection from light. After extensively washing with PBS, the cover slips were mounted in Mowiol (Hoechst Pharmaceuticals, Frankfurt, Germany) and cells were examined by sequential excitation at 488 nm for visualization of FITC and at 568 nm for TRITC-signals using a SP2 confocal microscope (Leica, Heerbrugg, Switzerland). The images were processed with the Adobe Photoshop CS2 software (Adobe Systems, San Jose, CA, USA).

4.4.8. Extraction of total RNA

Extraction of total RNA from C2C12 cells was performed with TRIzol (Invitrogen GIBCO). Cells were washed twice with PBS before lysis with TRIzol. Then chloroform was added to the cell lysate, mixed thoroughly for 15 sec and incubated for 3 min at room temperature. After centrifugation for 15 min at 10,000 rpm at 4 °C, the upper RNA-containing aqueous phase was transferred into a new centrifugation tube. RNA was precipited by adding isopropanol and a 10 min incubation at room temperature. The RNA was pelleted by centrifugation for 10 min at 10,000 rpm at 4 °C, washed with 75% ethanol, dried for 10 min at room temperature, and resolved in DEPEC water by incubation for 10 min at 55 °C.

4.4.9. Quantitative Real-Time PCR for quantification of ASK1 knockdown

Quantitative Real-Time PCR was performed in two steps. First, cDNA was synthesized from the extracted total RNA using the Enhanced Avian HS RT-PCR Kit (Sigma) according to the manufacturer's protocol. Briefly, 0.5 µg total RNA were mixed with 1 µl EAMV Reverse Transcriptase, 10x EAMV Reverse Transcriptase Buffer, 1 µl dNTPs, 1 µl Random Nonamers, 2 µl RNase Inhibitor and ddH_2O with a total volume of 20 µl. The reaction mixture was incubated for cDNA synthesis for 15 min at 25 °C followed by 50 min at 48 °C. Quantitative Real-Time PCR was performed in a second step using the Light Cylcer 2.0 (Roche) and the LightCycler-FastStart DNA Master SYBR Green I Kit (Roche). To this end, 5 µl of the synthesized cDNA were mixed with 2.5 mM $MgCl_2$, 0.5 µM Primer1, 0.5 µM Primer2, 2 µl SYBR Green Hot Start Master Mix, and nuclease free ddH_2O in a total volume of 20 µl. The cycling conditions for quantitative Real-Time PCR are shown in Table 1.

The following primers were used: forward 5'-CCATCTTGGAGTGCGAGAAAGC-3' and reverse 5'-CTCGAAGTTAGGCTGCATGAGC-3' for mouse ASK1, and forward 5'-ACAG CTGAGAGGGAAATCGTGCG-3' and reverse 5'-ACTTGCGCTCAGGAGGAGCA ATG-3' for mouse β-Actin, which was used as an internal control (212).

Program:	Pre-incubation			Type:	None	Cycles:	1
Segment Number	**Temperature Target (°C)**	**Hold Time (sec)**	**Slope (C°/sec)**	**2° Target Temp (°C)**	**Step Size (C°)**	**Step Delay (Cycles)**	**Acquisition Mode**
1	95	600	20	0	0	0	None

Program:	Amplification			Type:	Quantification	Cycles:	45
Segment Number	**Temperature Target (°C)**	**Hold Time (sec)**	**Slope (C°/sec)**	**2° Target Temp (°C)**	**Step Size (C°)**	**Step Delay (Cycles)**	**Acquisition Mode**
1	95	10	20	0	0	0	None
2	53	17	20	0	0	0	None
3	72	10	5	0	0	0	Single

Program:	Melting Curve Analysis			Type:	None	Cycles:	1
Segment Number	**Temperature Target (°C)**	**Hold Time (sec)**	**Slope (C°/sec)**	**2° Target Temp (°C)**	**Step Size (C°)**	**Step Delay (Cycles)**	**Acquisition Mode**
1	95	0	20	0	0	0	None
2	63	15	20	0	0	0	None
3	95	0	0.1	0	0	0	Continuous

Program:	Cooling			Type:	None	Cycles:	1
Segment Number	**Temperature Target (°C)**	**Hold Time (sec)**	**Slope (C°/sec)**	**2° Target Temp (°C)**	**Step Size (C°)**	**Step Delay (Cycles)**	**Acquisition Mode**
1	40	30	20	0	0	0	None

Tabel 1: Experimental protocol for quantative Real-Time PCR using the Light Cycler 2.0 (Roche)

4.5. Protein Methods

4.5.1. SDS-gel electrophoresis and immunoblot analysis

Protein lysates were separated by sodiumdodecylsulfate-polyacrylamide gel electrophoresis (SDS-PAGE) using the BioRad Mini Protean II-system (Bio-Rad). The composition of the SDS-polyacrylamide gels was the following (quantities sufficient for 2 gels):

separating gel	7.5%	10%	12.5%	15%	stacking gel
30% Acrylamide	2 ml	2.67 ml	3.33	4 ml	0.64 ml
2% Bisacrylamide	0.8 ml	1.04 ml	1.33	1.6 ml	0.34 ml
1.5 M Tris pH8.8	2 ml	2 ml	2 ml	2 ml	-
1 M Tris pH6.8	-	-	-	-	1.15 ml
ddH_2O	3.76 ml	2.33 ml	1.34 ml	0.4 ml	2.8 ml
10% SDS (w/v)	80 µl	80 µl	80 µl	80 µl	40 µl
TEMED	4 µl	4 µl	4 µl	4 µl	2 µl
10% APS (w/v)	80 µl	80 µl	80 µl	80 µl	40 µl

Gels were run in Laemmli buffer at 120 V for 2 - 3 h, depending on the proteins to be analyzed. Proteins were transferred from the gels to Hybond^{TM}-ECL membranes in transfer

buffer for 2 h at 160 mA. Immunoblot analysis was performed as described previously (213). Briefly, membranes were blocked in Blocking buffer for 1 h before incubation with the primary antibodies over night at 4 °C. Membranes were washed three times in washing buffer and incubated with horseradish peroxidase-coupled (HRP) secondary antibodies for 1 h at room temperature. After three time washing with washing buffer, detection was performed using the ECL detection kit and ECL films (Amersham Pharmacia Biotech) according to the manufacturer's protocol. Quantifications were done using the ImageQuant 5.2 (Molecular Dynamics, Sunnyvale, CA, USA) software.

4.5.2. Determination of protein content (Bradford method)

For determination of the protein content, cell lysates were diluted with ddH_2O in a total volume of 100 µl. Then, 900 µl of a 1:5 dilution of BioRad Bradford solution (Bio-Rad) were added, mixed thoroughly, incubated for 10 min at room temperature, and the OD was measured at 595 nm using an UVIKON spectrophotometer (Flowspek, Basel, Switzerland). A standard series of bovine serum albumine (BSA) was prepared for determination of the protein content.

4.5.3. Preparation of cell lysates and co-immunoprecipitation analysis

Cell lysates were obtained by resuspension in radioimmunoprecipitation buffer (RIPA; 20 mM Tris pH 7.4, 133 mM NaCl, 2 mM EDTA, 0.1% SDS, 1% Triton X-100, 0.5% DOC, 10% glycerol, 1 mM DTT, 10 µm/ml leupeptine, 1% aprotinin/trasylol, 1 mM PMSF, 1 mM sodium orthovanadate, 50 mM NaF, 50 mM β-glycerophosphate). Cells were incubated for 15 min on a spinning wheel at 4 °C. Cell lysates were cleared by centrifugation for 10 min at 13,000 rpm at 4 °C and the supernatant was boiled in sample buffer for 5 min at 95 °C. For immunoprecipitation, cells were lysed in NETN buffer (20 mM Tris pH 7.5, 100 mM NaCl, 1 mM EDTA, 0.5% Nonidet P-40, 1 mM DTT, 1 µg/ml leupeptine, 0.1% aprotinin/trasylol, 1 mM benzamidine, 1 mM PMSF, 1 mM sodium orthovanadate, 40 mM β-glycerophosphate) by incubation for 15 min on a spinning wheel at 4 °C. Lysates were cleared by centrifugation for 10 min at 13,000 rpm at 4 °C before immunoprecipitation of the desired protein with the respective primary antibody for 2 h at 4 °C. The antibody-protein complexes were precipitated by incubation with protein G-Sepharose for 1 h at 4 °C and collected by

centrifugation for 1 min at 13,000 rpm at 4 °C. After four times washing with NETN buffer, immunoprecipitated proteins were eluted in SDS-sample buffer. Direct lysates and immunoprecipitates were separated by SDS-PAGE and analyzed in immunoblots as described above.

4.5.4. Purification of ASK2 GST-fusion proteins

Over night cultures of DH5α cells transformed with pGEX-6P-2 plasmids containing partial sequences of ASK2 (described in chapter 4.3.11) were prepared in LB medium supplemented with ampicillin (amp) in a volume of 20 ml. The next day, 200 ml LB-amp medium were directly inoculated with the over night culture and grown at 28 °C to an OD_{600nm} of 0.5 to 0.6. Expression of the GST-fusion protein was induced by addition of 0.5 mM IPTG (isopropyl-β-D-thiogalactopyranosid, Sigma) and the culture was incubated for 5 h at 28 °C. Cells were harvested by centrifugation for 15 min at 4,000 rpm at 4 °C and resuspended in STE buffer (10 mM Tris pH 8.0, 150 mM NaCl, 2 mM EDTA, supplemented with 1 mM PMSF, 1 mM benzamidine and 1% aprotinin/trasylol). Cells were lysed with 100 μg/ml lysozyme (Sigma) on ice for 20 min before adding 5 mM DTT for 5 min. Then, 1.5% sarcosyl and 2% Triton X-100 were added and cells were sonificated 3 times for 2 min (output control 3, duty cycle 30%) on ice. Cell lysates were cleared by centrifugation for 15 min at 15,000 rpm at 4°C. To precipitate the GST-fusion proteins, the supernatant was mixed with glutathione agarose (Sigma) and incubated on a spinning wheel for 90 min at 4 °C. Precipitated proteins were collected by centrifugation for 15 min at 4,000 rpm at 4 °C and washed twice with PBS containing 0.1% TritonX-100 (supplemented with 1 mM PMSF, 1 mM benzamidine and 1% aprotinin/trasylol). After washing twice with washing buffer (20 mM Tris pH 8.0, 250 mM NaCl, supplemented with 1 mM PMSF, 1 mM benzamidine and 1% aprotinin/trasylol), the GST-fusion proteins were eluted with elution buffer (50 mM Tris pH 8.0, 50 mM NaCl, 10 mM Glutathion, 0.1% TritonX-100, 0.1% β-mercaptoethanol, supplemented with 1 mM PMSF, 1 mM benzamidine and 1% aprotinin/trasylol) for 5 min at room temperature. The eluted proteins were concentrated in a SpeedVac Concentrator (Savant) and stored at -70 °C.

4.5.5. Generation of a rabbit polyconal anti-ASK2 antibody

Rabbit polyclonal anti-ASK2 antibodies were generated against human ASK2. For this, the ASK2 protein fragment containing the amino acids 926-1,288 was fused to glutathione-S-transferase (GST) and used as antigen (GST-ASK2-R3) for immunization of two rabbits (G. Fischer, Institut for Labortierkunde, Zurich, Switzerland). These rabbits were immunized 4 times by injecting 550 μg of GST-ASK2-R3 each time. Rabbits were bled and the obtained immunosera ("CA2" and "324") were purified using a Protein G column affinity chromatography (Amersham Pharmacia BioTech). Briefly, the protein G column was equilibrated with 20 mM HEPES pH 7.3 before running through the immunosera. The column was washed with binding buffer (50 mM NaPhosphate pH 6.0, 500 mM NaCl, 0.05% NaAzide) and the antibodies were eluted with elution buffer (0.1 M glycine pH 3) and finally diluted in 1 M Tris pH 9.0.

4.5.6. Subcellular fractionation

HeLa cells were fractionated using the ProteoExtract™ Subcellular Proteome Extraction Kit (Calbiochem) to obtain extracts from cytoplasm, membrane/organelle, nucleus, and cytoskeleton. Briefly, adherent cells were washed and sequentially incubated with four different extraction buffers yielding the fractions in the supernatant. Fractionation of HeLa cells into cytoplasmic and nuclear extracts was done as described previously by Elzaouk *et al.* (214). Cells were washed twice with PBS and harvested in lysis buffer (10 mM HEPES, pH 7.5, 10 mM NaCl, 1.5 mM $MgCl_2$, 10% glycerol, 1 mM EDTA, 5 mM DTT, 1% NP-40). The cytoplasmic fraction was obtained in the supernatant after centrifugation for 5 min at 4,300 rpm at 4 °C. For nuclear extraction, the pellet was washed twice with washing buffer (10 mM HEPES, pH 7.5, 10 mM NaCl, 1.5 mM $MgCl_2$, 10% glycerol, 1 mM EDTA, 5 mM DTT) and lysed in extraction buffer (25 mM Tris–HCl, pH 8.0, 500 mM NaCl, 1 mM EDTA, 10 mM β-mercaptoethanol, 0.5% Triton X-100). Lysates were incubated on ice for 5 min and the nuclear extract- containing supernatant was prepared by centrifugation for 30 min at 15,000 rpm at 4 °C. Cytoplasmic and mitochondrial fractions of HeLa cells were prepared as described by Zhang *et al*. (134). To obtain the cytoplasmic extract, cells were washed with PBS, pelleted by centrifugation for 3 min at 4,000 g at 4 °C and resuspended in a buffer containing 250 mM sucrose in 70 mM Tris pH 7.0 supplemented with one complete mini

protease inhibitor cocktail tablet (Roche). Cells were lysed by addition of 160 μg/ml digitonin and complete lysis was confirmed by trypan blue staining. The cytosolic fraction was obtained in the supernatant after centrifugation for 2 min at room temperature. Mitochondria were extracted from adherent cells by resuspension of cells in a hypotonic buffer (10 mM NaCl, 1.5 mM $CaCl_2$, 10 mM Tris pH 7.5, supplemented with protease inhibitor tablets) followed by stabilization using MS-buffer [(525 mM mannitol, 175 mM sucrose, 12.5 mM EDTA pH 7.5, 12.5 mM Tris pH 7.5, and supplemented with one complete mini protease inhibitor cocktail tablet (Roche)]. Cells were homogenized using a Dounce homogenizer and nuclei were removed by centrifugation twice for 10 min at 3,000 rpm at 4 °C. The supernatant was centrifuged for 10min at 13,000 rpm at 4 °C and the mitochondria extracts were obtained by lysis of the pellet with a buffer consisting of 50 mM HEPES pH 7.0, 500 mM NaCl, 1% NP-40, supplemented with one complete mini protease inhibitor cocktail tablet (Roche). All obtained fractions were mixed with sample buffer and boiled for 5 min at 95 °C for subsequent immunoblot analysis.

4.5.7. Radioactive *in vitro* phosphorylation assay of ASK2

For a radioactive *in vitro* phosphorylation assay of ASK2 by AKT, 1.5 μg of each GST-fusion protein of ASK2 was mixed separately with 0.1 μg active AKT1 (Upstate), 6 μCi [γ-^{32}P]-ATP (Amersham Pharmacia Biotech), and 1 μM ATP in reaction buffer (100 μl HEPES, 50 mM $MgCl_2$, 50 mM β-glycerophosphate, 25 mM NaF, 10 mM DTT, 5 mM EGTA) in a total volume of 50 μl. This reaction mixture was incubated for 15 min at 30 °C and cooled on ice. Sample buffer was added and the reaction mixture was boiled for 5 min at 95 °C to stop the phosphorylation reaction. Phosphorylation was analyzed by separation of the reaction mixture on a 7.5% SDS-PAGE and blotting on a Hybond™-ECL membrane. Incorporated [γ-^{32}P]-ATP was analyzed using a PhosphoImager (Molecular Dynamics) after exposing the membrane to a PhosphoImager screen.

5. Results

5.1. ASK2 modulates apoptosis

5.1.1. Sequence analysis of ASK2

ASK2 was originally identified as binding partner of ASK1 in a yeast two hybrid screen (91). These two MAPKKK, ASK2 and ASK1, are highly related sharing 45% aa identity and a similar structure with a central kinase domain and a C-terminal coiled-coil sequence. ASK2 is shorter than ASK1 lacking 32 aa in the N-terminal and 54 aa in the C-terminal region (depicted in Figure 12A). We analyzed these aa stretches by a web-based Pfam (Version 21.0) search at the Sanger Institute, which demonstrated that they do not encode any known functional domain. Another protein sequence analysis of ASK2 using the web-based sequence analysis program ScanSite 2.0 was performed to get a hint about a putative biological function of ASK2. This analysis showed that ASK2 contains both serine/threonine and tyrosine kinase activity (Figure 12B). In addition to three domains of unknown function (DUF), four other domains or regions were found. The first domain encodes a sequence that is homologous to the hypertension-related, calcium-regulated gene (HCaRG) protein, which is a nuclear protein that is negatively regulated by extracellular calcium concentrations and potentially involved in cell proliferation. A second domain within the ASK2 N-terminal region shows homology to the Kunitz/Bovine pancreatic trypsin inhibitor domain (Kunitz BPTI). Members of this trypsin inhibitor family negatively regulate endopeptidases of the S1 chymotrypsin family. These peptidases are involved among others in intestinal digestion and IgA-mediated immune response. An aminoglycoside phosphotransferase (APH) domain localized in the kinase domain is the third identified domain and is normally found in the family of phosphotransferase enzymes such as the bacterial antibiotic resistance proteins. This family is related to fructosamine kinase. Finally, a Regional Study of Care for the Dying (RCSD) region was identified that is normally found in proteins involved in muscle M-line assembly, which is a structural component of the sarcomere giving skeletal and cardiac muscle cells their striated appearance. Taken together, the diversity of homologies elucidated by the computational analyses did not allow to draw functional conclusions with respect to ASK2.

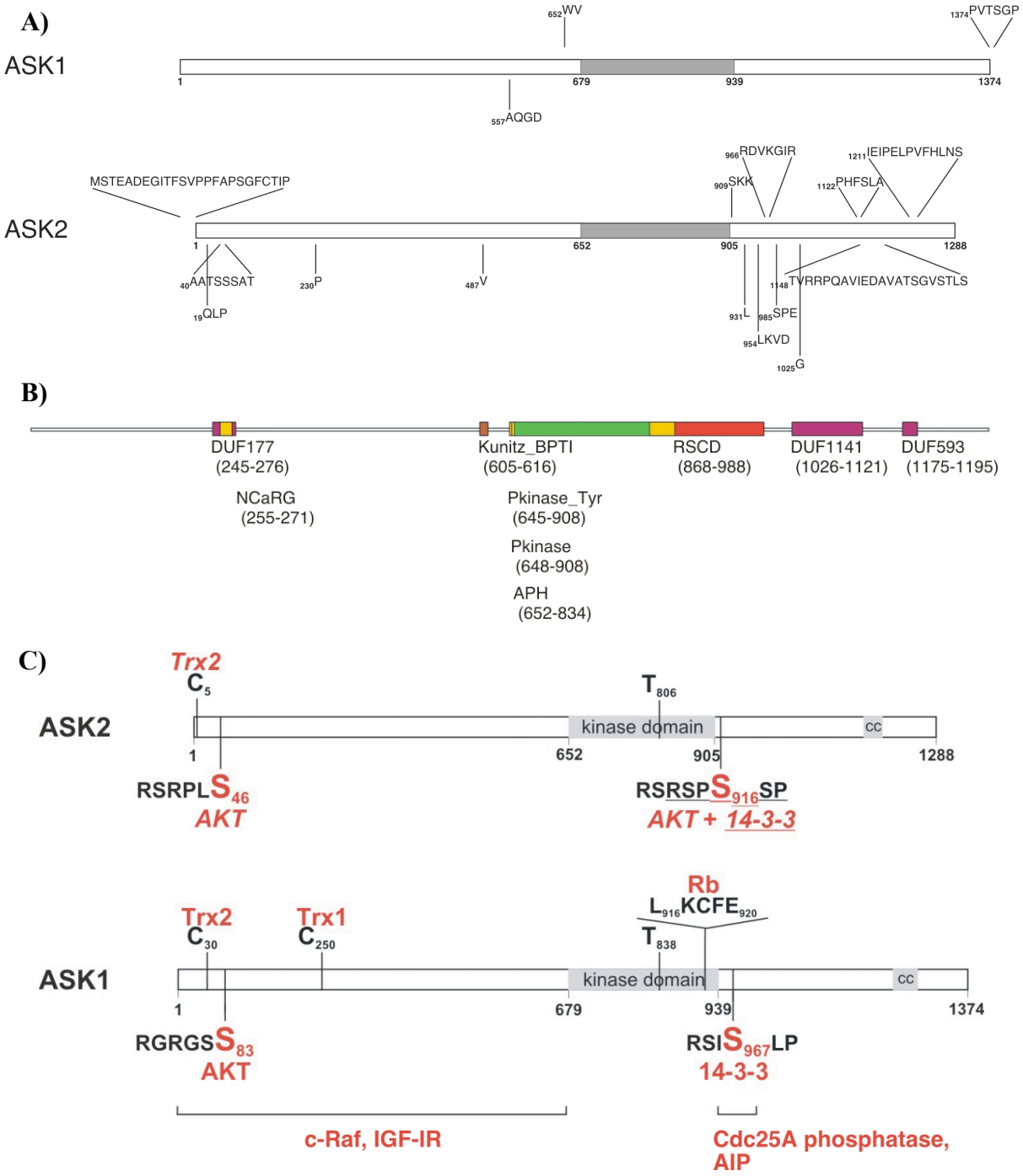

Fig. 12: Sequence comparisons of ASK2 and ASK1. A) ASK2 lacks 32 aa in the N-terminal region and 54 aa in the C-terminal region compared with ASK1. B) Graphical output of a sequence analysis of human ASK2 using the web-based ScanSite 2.0 program. For detailed description of domains see text; DUF: domain of unknown function. C) Sequence comparison of human ASK2 and ASK1 showing binding sites for thioredoxin (Trx) (134,136), retinoblastoma protein (Rb) (156), and 14-3-3 (160,161), an AKT phosphorylation site (146) and interaction regions of other known regulatory proteins (cc: coiled-coil sequence). For ASK2, AKT phosphorylation and 14-3-3 binding sites were determined using the ScanSite program. Binding sites for Trx1 and Trx2 were investigated by standard sequence comparison. Thr806 and Thr838 are the phosphorylation sites for kinase activation of ASK2 and ASK1, respectively (195).

In addition to the domain search, we compared ASK2 with ASK1 at their protein sequences to identify AKT phosphorylation sites and binding sites for interaction partners on ASK2. Figure 12C shows the AKT phosphorylation site and some known regulatoy binding partners of human ASK1, which is discussed in more detail in 3.2.3.1. A basic aa sequence comparison of ASK1 and ASK2 revealed a putative binding site for Trx2 but not for Trx1 on ASK2. Using the ScanSite program two putative AKT phosphorylation sites were found on ASK2 on Ser46 with medium stringency and on Ser916 with high stringency, which overlaps with a 14-3-3 binding site. Similar to ASK1, ASK2 also contains a coiled-coil sequence within the C-terminal region, which mediates protein-protein interactions.

5.1.2. Expression and localization of ASK2

5.1.2.1. Generation of rabbit polyclonal antibodies against human ASK2

To investigate ASK2, we generated rabbit polyclonal antibodies against human ASK2. To this end, two rabbits were immunized with the GST-ASK2-R3 fusion protein, which comprises the whole C-terminal region of human ASK2 (aa 926 to 1288) (see Figure 13A). After the third boost, polyclonal antibodies were purified using G-sepharose filled columns. Both antibodies CA2 and 324 were then tested for specifity by immunoprecipitation of endogenous ASK2 and transiently overexpressed HA-tagged ASK2 (HA-ASK2) from HEK293T cells followed by an immunoblot analysis, which is shown in Figure 13B. The antibodies used for IB were either pre-incubated with the GST-fusion protein that had been used for the immunization in order to compete for binding or were added directly to the immunoprecipitates. Detection of HA-ASK2 with the anti-HA antibody both in the immunoprecipitates and in whole cell lysates served as positive control.

A)

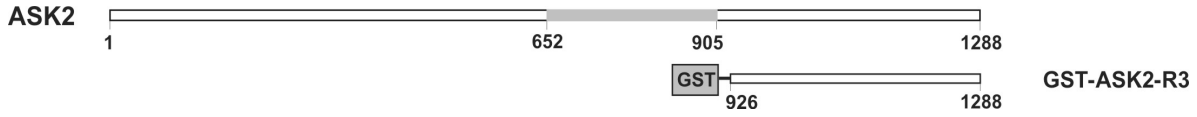

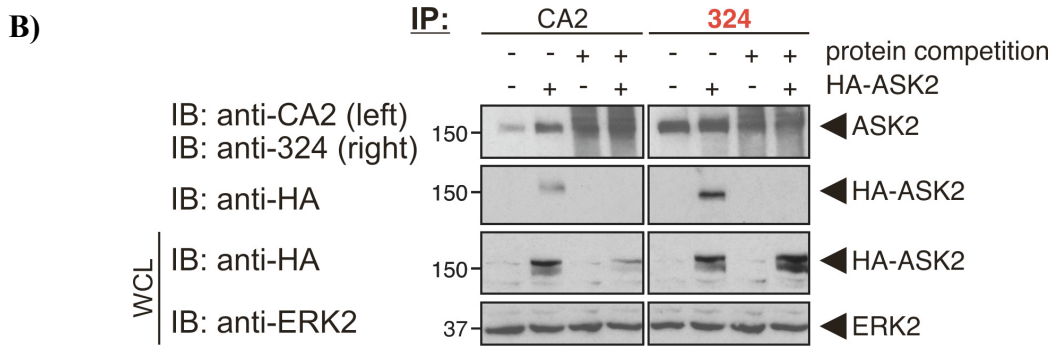

Fig. 13: Generation of rabbit polyclonal antibodies targeted against human ASK2. A) Schematic representation of a GST-fusion protein of human ASK2 encoding the whole C-terminal domain starting from amino acid 926, which was expressed in E.coli, purified and used for immunization of two rabbits, CA2 and 324. B) HEK293T cells were transiently transfected either with an expression vector encoding HA-ASK2 or with empty vector. Endogenous ASK2 and overexpressed HA-ASK2 were immunoprecipitated (IP) with the antibodies CA2 or 324. Antibodies for detection of the immunoprecipitated proteins were used either directly or pre-incubated with GST-ASK2-R3. Expression of HA-ASK2 in whole cell lysates (WCL) and IP of HA-ASK2 were confirmed in immunoblots (IB) with the anti-HA specific antibody. ERK2 expression was analyzed as loading control.

Both ASK2 polyclonal antibodies specifically immunoprecipitated overexpressed as well as endogenous ASK2 detected in immunoblots at the calculated molecular weight of 143 kD. Protein competition did not completely abolish immunoprecipitation of ASK2 but at least led to a marked reduction. Compared with the anti-HA immunoblot, the ASK2 bands were detected at the same molecular weight. Since the antibody 324 (highlighted in red) yielded the better result, it was used for all following experiments and will be named henceforth anti-ASK2.

5.1.2.2. Tissue and cell line distribution of ASK2

After confirming the specificity of the anti-ASK2 antibody, we analyzed the tissue distribution of endogenous ASK2. In a Northern blot analysis of human tissues (91), ASK2 was mainly found in heart and skeletal muscle and to lesser extend in lung, liver, kidney, testis, and spleen. However, ASK2 expression at the protein level has not been investigated yet. Therefore, extracts from mouse tissues were tested for ASK2 distribution in a non-quantitative immunoblot. As can be seen in Figure 14A, ASK2 was detected by the anti-ASK2 antibody in all tissues but in varying quantities, which was partly due to less protein loaded (one fifth) in the case of lung, heart, spleen, and liver. In this tissue blot ASK2

expression was more widely observed than expected from the previously mentioned Northern blot (91), since ASK2 was also found in brain and pancreas. In contrast, only a very weak expression rate was detected in skeletal muscle. However, it has to be taken into account, that the tissue blot comprised mouse tissues instead of human tissues used for the Northern blot analysis. The specificity of the band recognized by the ASK2 antibody was confirmed in a second immunoblot by epitope competition of the antibody with the GST-ASK2-R3 protein, which strongly interfered in the binding.

Next, we examined the expression of ASK2 in immunoblots of several human and mouse cell lines of divers origins (neuronal-, muscle-, adipogenic-, endothelial-, breast-, cervix carcinoma- and embryonic kidney cells), which is shown in Figure 14B. Although equal protein amounts were loaded, this analysis was not quantitative due to different lysis buffers used (R: RIPA, N: NETN, E: Eisenman), but the obtained result was comparable with the previous tissue blot in that ASK2 was detected in all cell lines. These two analyses indicated an ubiquitous expression of ASK2.

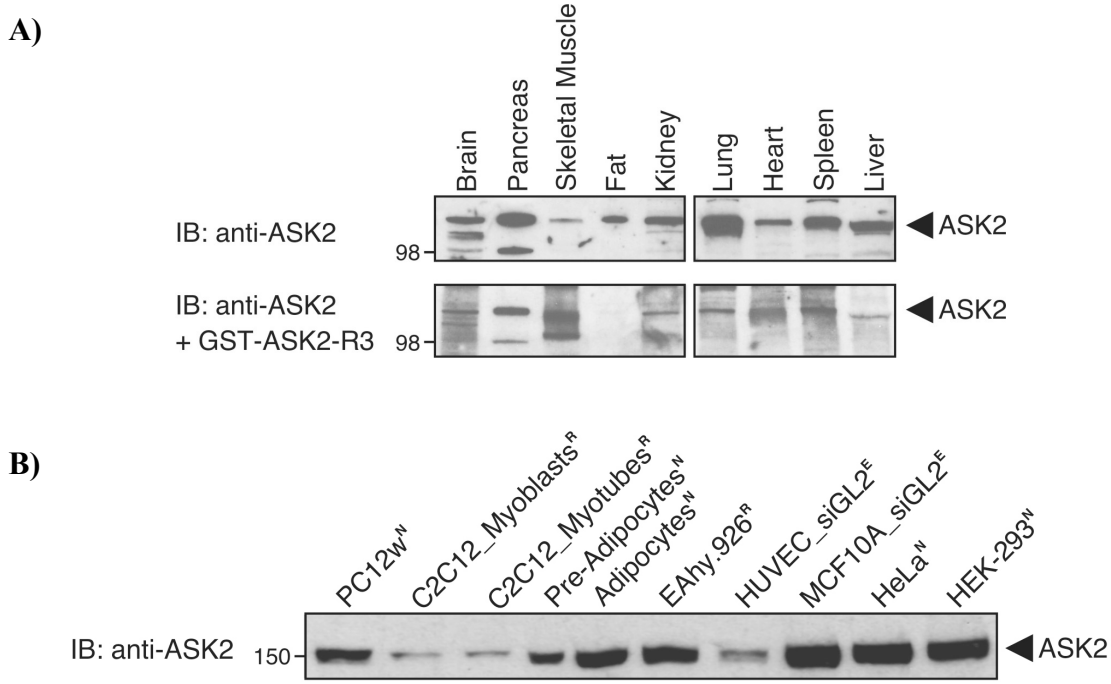

Fig. 14: Expression analyses of ASK2 in mouse tissues and in human and mouse cell lines. A) Endogenous expression of ASK2 was investigated in mouse tissues by immunoblots (IB) using the ASK2 specific antibody. For verification, a second, similarily prepared blot was incubated with the anti-ASK2 antibody pre-incubated with the GST-ASK2-R3 protein. B) Cell lines of human and mouse origin were lysed using different buffers as indicated (R: RIPA, N: NETN, E: Eisenman) and analyzed for ASK2 expression by immunoblots using the anti-ASK2 antibody.

5.1.2.3. Intracellular localization of ASK2

To elucidate the intracellular localization of ASK2, HeLa cells were fractionated using a proteome fractionation kit, which yielded extracts of the following compartments: cytoplasm, membranes and organelles, nuclei, and cytoskeleton. These subcellular fractions were subjected to an immunoblot analysis shown in Figure 15. The anti-ASK2 antibody detected endogenous ASK2 expression in all fractions except for the cytoskeleton. Purity of each fraction was confirmed by the expression of several marker proteins with antibodies against c-Raf for the cytoplasm and membranes and organelles, Trx2 for mitochondria, c-Myc for the nucleus, and cytokeratin 18 for the cytoskeleton. There was a minor contamination of the nuclear fraction with cytoskeletal components as observed by a weak signal of cytokeratin 18.

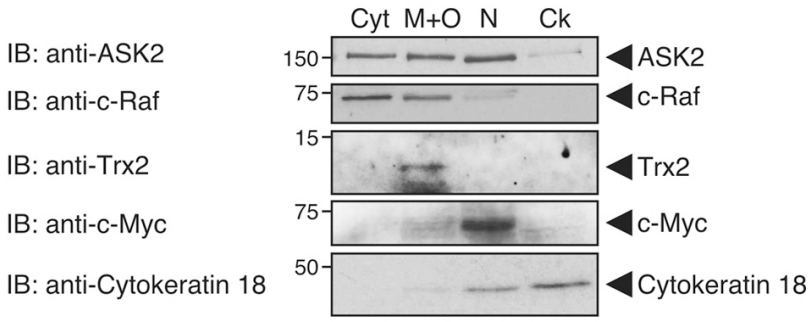

Fig. 15: Fractionation of HeLa cells to determine the localization of endogenous ASK2 using a proteome extraction kit. A) Schematic presentation of the extraction protocol (EB: elution buffer). B) Immunoblot analysis (IB) of the obtained subcellular fractions (Cyt: cytoplasm, M+O: membranes and organelles, N: nucleus, and Ck: cytoskeleton) using the anti-ASK2 antibody to detect endogenous ASK2. Antibodies against marker proteins of individual fractions were used to confirm purity.

The intracellular localization of ASK2 was further verified in immunoblots from either cytoplasmic and nuclear (Figure 16A) or cytoplasmic and mitochondrial fractions (Figure 16B*),* which were obtained from HeLa cells by two different methods. ASK2 was detected using the ASK2 specific antibody and localized in all three cellular compartments, cytoplasm, nucleus and mitochondria, which is in accordance with the previous results. Purity of each fraction was ascertained with antibodies against marker proteins, including Trx1 and c-Raf for the cytoplasm, Lamin A/C and c-Myc for the nuclear fractions, and Trx2 for mitochondria. We interpreted the band shift seen in the case of ASK2 as the result of different salt concentrations used for the lysis buffers.

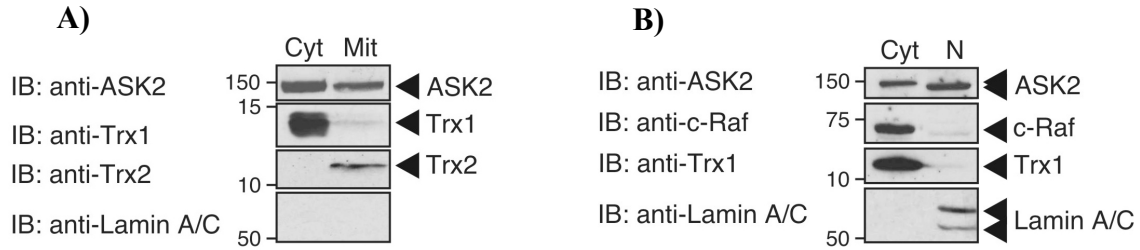

Fig. 16: Subcellular fractionation of HeLa cells for analysis of the intracellular localization of endogenous ASK2. A) Cytoplasmic (Cyt) and mitochondria (Mit) extracts were analyzed in immunoblots (IB) with antibodies against ASK2, Trx1, Trx2, and Lamin A/C. B) Fractions of cytoplasm (Cyt) and nuclei (N) were probed with anti-ASK2, anti-c-Raf, anti-Trx1, and anti-Lamin A/C antibodies.

In addition to the biochemical investigation of ASK2 subcellular localization, confocal immunofluorescence microscopy analysis of HeLa cells was performed to further characterize the intracellular localization of endogenous ASK2 (Figure 17). Live HeLa cells grown under normal growth conditions were incubated with Mitotracker (red) to mark mitochondria. Cells were then fixed and endogenous ASK2 was detected with the anti-ASK2 antibody (green). A cell region indicated with the white square in the very left picture of Figure 17 was enlarged to better visualize ASK2 expression and localization of mitochondria. The merged picture revealed localization of ASK2 in the nucleus, cytoplasm and partial co-localization with mitochondria.

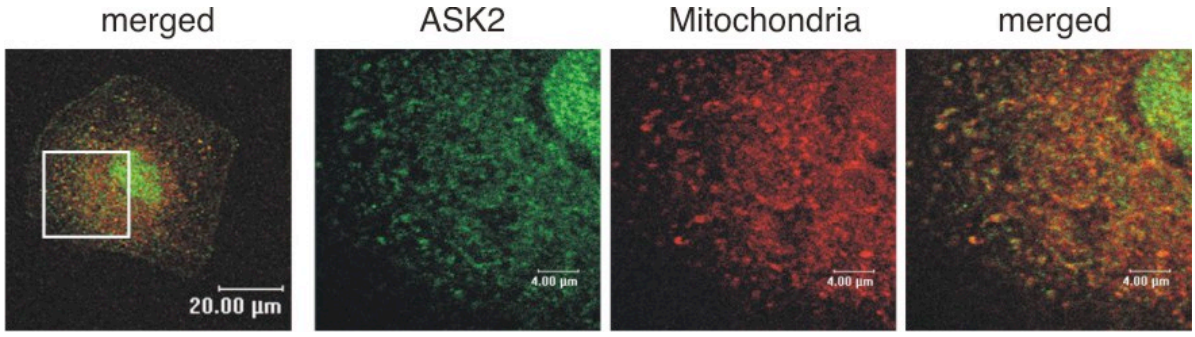

Fig. 17: Confocal immunofluorescence microscopy analysis of HeLa cells for intracellular localization of endogenous ASK2. ASK2 was detected using the ASK2-specific antibody (green) and mitochondria were visualized with MitoTracker (red). The region highlighted by the white square in the left picture was represented enlarged in the following three pictures. A merged picture of the zoomed region was generated to verify partial co-localization of ASK2 with mitochondria (orange).

In conclusion, ASK2 was ubiquitously expressed in tissues and cell lines analyzed. We detected ASK2 localization in cytoplasm, mitochondria and nuclear, which is similar to the localization of ASK1 (134,136,156).

5.1.3. Biological function of ASK2

Although ASK2 and ASK1 are highly related kinases with an aa sequence homology of 45%, ASK2 only weakly promotes phosphorylation and activation of JNK and p38 MAPK (195). To find out whether ASK2 is also involved in the induction of apoptosis as known for ASK1 (89,155), we carried out overexpression and knockdown studies by RNA interference using siRNA. While writing this thesis, a study was published (195) showing that ASK2 forms a heteromeric complex and thereby functions as a MAPKKK. Furthermore, ectopically expressed ASK2 induces phosphorylation of JNK and p38 MAPK and activation of caspase-3 in non-stressed HEK293 cells but only when kinase-inactive ASK1 is co-expressed. However, it has not been examined what impact stress induction has on the kinase activation of ASK2 and if stress induction can lead to apoptosis in ASK2-overexpressing cells.

5.1.3.1. Overexpression of ASK2 induces apoptosis

Since transient overexpression of ASK1 is sufficient to induce apoptosis in several cell lines (89), ectopically expressed ASK2 was investigated for a pro-apoptotic function under similar conditions. N-terminal HA-tagged ASK2 (HA-ASK2) or empty vector were transiently transfected into HeLa and HEK293 cells, which were then subjected to an apoptotic challenge by 24 h serum-starvation. Overexpression of ASK2 induced apoptosis as observed by the activation of caspase-3 and cleavage of its downstream target PARP in immunoblots of cell lysates (Figure 18A).

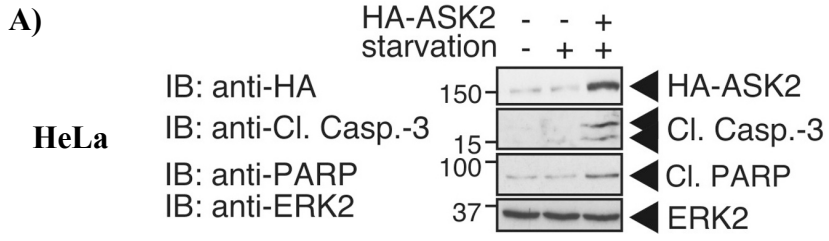

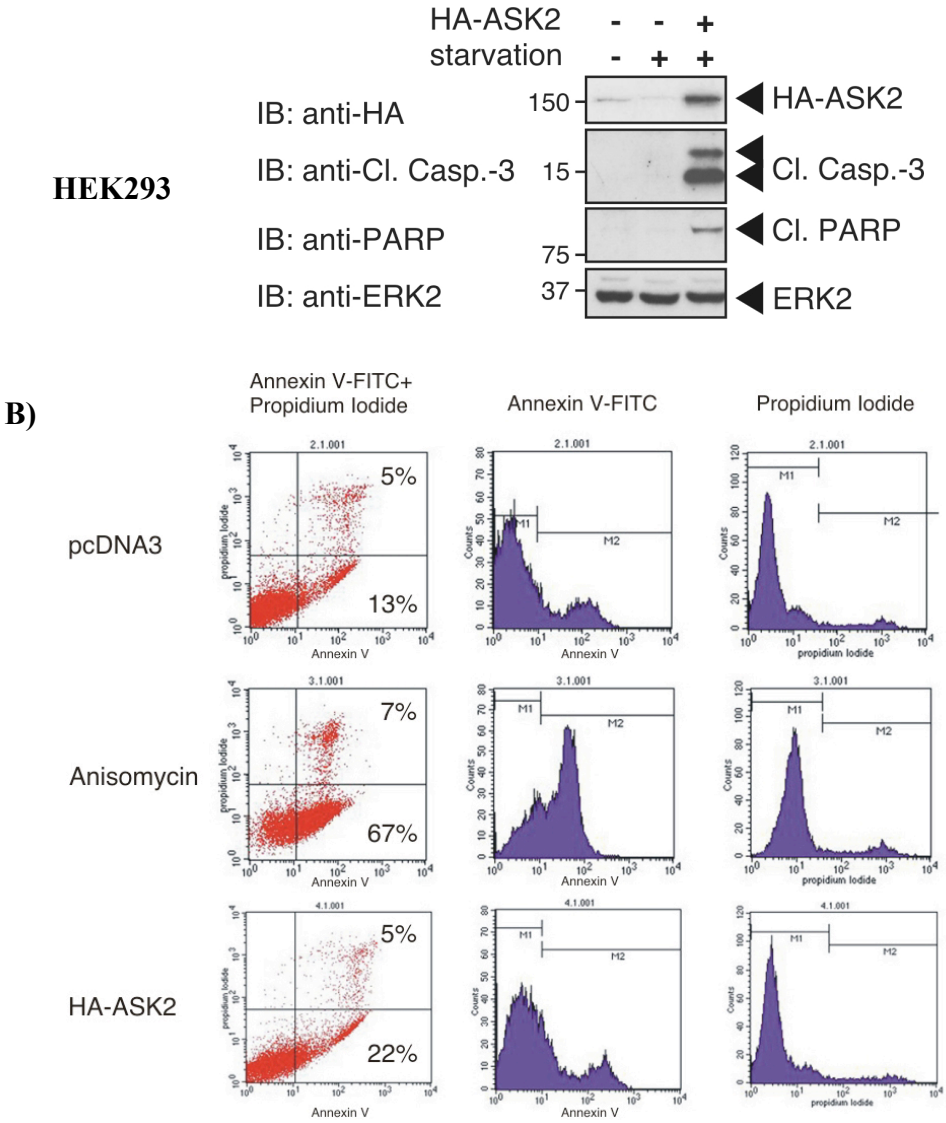

Fig. 18: Overexpression of ASK2 induces apoptosis. A) Immunblot (IB) analyses of HeLa- and HEK293 that were transiently transfected either with an ASK2 expression vector or with empty vector and serum-starved for 24 h. Cell lysates were prepared and analyzed for induction of apoptosis by detecting cleaved caspase-3 (Cl. Casp.-3) and cleaved PARP (Cl. PARP) with the indicated antibodies. HA-ASK2 expression was monitored using anti-HA-antibodies. Equal loading was verified with the anti-ERK2 antibody. B) FACS analysis of HeLa cells for induction of apoptosis. Cells were transiently transfected with HA-ASK2 or with empty vector (pcDNA3), serum-starved for 6 h and analyzed for apoptosis by annexin V-FITC staining. Percentage of apoptotic annexin V-positive) cells is indicated in the lower right squares, percentage of necrotic (annexin V and PI (propidiume iodide)) double-positive cells is indicated in the upper right squares of the dot plots. Histograms represent staining either with annexin V (middle column) or with propidium iodide (right column).

The apoptosis-inducing effect of ASK2 overexpression combined with serum-starvation was confirmed in HeLa cells by annexin-V staining in FACS analysis (Figure 18B). Incubation with anisomycin (5 μg/ml for 5 h) was used as positive control. Serum-starvation for 6 h induced apoptosis in about 13% of empty vector-transfected cells and overexpression of HA-

ASK2 increased apoptosis to 22%, which represents an actual increase of 70%. Summerizing, overexpression of ASK2 caused apoptosis in cells that were stressed by serum-starvation.

5.1.3.2. Knockdown of ASK2 induces apoptosis

The results from the overexpression experiments indicated that ASK2 is an inducer of apoptosis. Therefore, we assumed that downregulation of ASK2 expression should prevent apoptosis. To test this hypothesis, ASK2 expression was downregulated by transient transfection of two different siRNAs directed against human ASK2 (siASK2_5 and siASK2_6) into HeLa cells. Knockdown of ASK2 was confirmed in immunoblots of cell lysates using the anti-ASK2 antibody. By measuring the pixel density of the ASK2 bands with the ImageQuant 5.2 software, a comparable efficiency of both siRNAs was determined (Figure 19A).

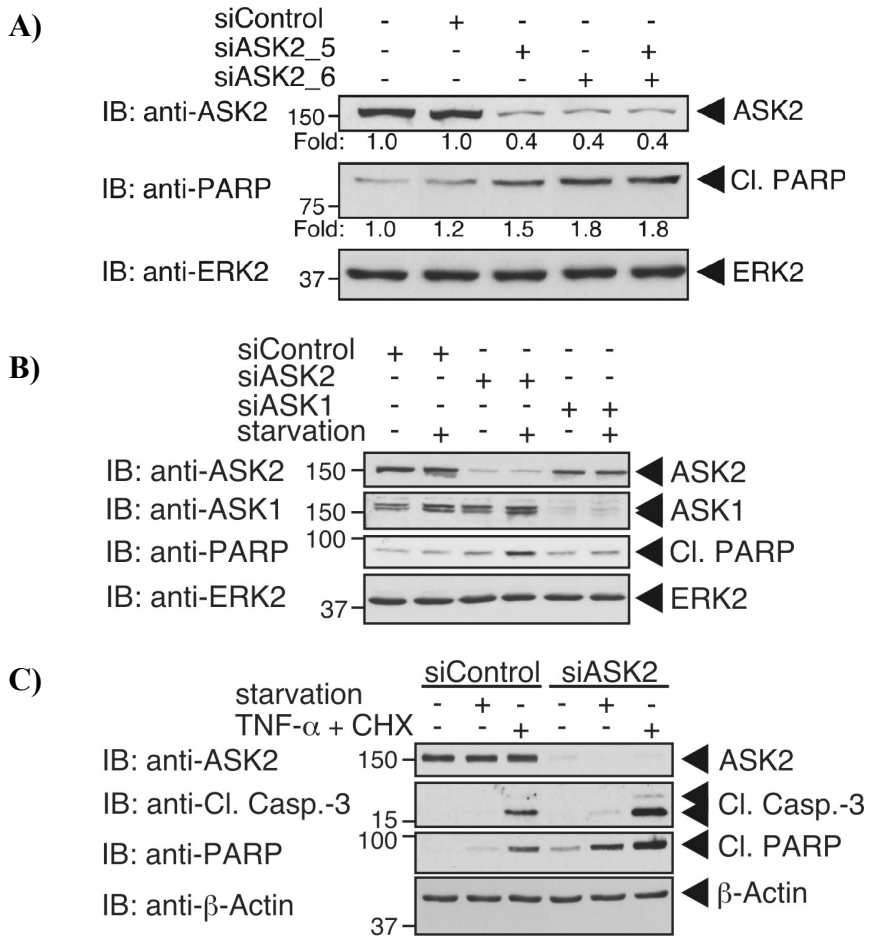

Fig. 19: ASK2 knockdown induces apoptosis in HeLa cells. A) Lysates from cells transiently transfected with two different siRNAs against ASK2 (siASK2_5 and siASK2_6) or with non-specific siControl were immunoblotted (IB) with antibodies as indicated. Pixel density was

quantified with the ImageQuant 5.2. software. B) Cells transiently transfected with siRNAs against ASK2 (siASK2_6) or ASK1 (siASK1) were either left in growth medium or serum-starved for 24 h. Cell lysates were analyzed in immunoblots (IB) with anti-ASK2, anti-ASK1, anti-PARP, or anti-ERK2 antibodies. C) Cells were transiently transfected with siRNAs against ASK2 (siASK2_6) or siControl. After transfection cells were either left in growth medium or serum-starved for 24 h or incubated with 10 ng/ml TNF-α together with 20 μM cycloheximide (CHX) for 2 h prior to cell lysis. Cell lysates were probed with antibodies against ASK2, cleaved caspase-3 (Cl. Casp.-3), PARP, or β-Actin is shown.

Unexpectedly, downregulation of ASK2 also induced apoptosis even in non-stressed cells as demonstrated by the cleavage of PARP. Both ASK2-specific siRNAs induced PARP cleavage therefore an unspecific off-target effect of the siRNA could be excluded. Since ASK1 is necessary for apoptosis and downregulation of ASK1 inhibits stress-induced apoptosis (155,215), ASK2 knockdown was further investigated for its pro-apoptotic effect in comparison with knockdown of ASK1 to rule out any unspecific effect of the experimental set-up regarding the induction of apoptosis. To this end, HeLa cells were transiently transfected with siRNAs either against ASK2 (siASK2_6) or ASK1 (siASK1) or with unspecific siControl. Then cells were either incubated in complete medium or serum-starved for 24 h. As can be seen in immunoblots of cell lysates in Figure 19B, only knockdown of ASK2 but not downregulation of ASK1 induced apoptosis under stress, which was detected by the cleavage of PARP. Transfection of non-targeted control siRNA (siControl) did not markedly increase PARP cleavage after serum-starvation. Downregulation of ASK2 and ASK1 expression were verified using antibodies against ASK2 and ASK1. The antibody generated against human ASK2 did not cross-react with ASK1 confirming its specificity. Interestingly, knockdown of ASK1 weakly decreased ASK2 protein amount and starvation led to a weak increase of ASK1 expression. The observed pro-apoptotic effect was specific for knockdown of ASK2 therefore ASK2 was further investigated for a regulatory function in the extrinsic apoptotic pathway. To clarify this question, ASK2 was transiently downregulated in HeLa cells that were then either incubated in growth medium or stressed by withdrawal of serum for 24 h or treatment with TNF-α together with cycloheximide (CHX). Both apoptotic challenges elevated apoptosis when ASK2 expression was reduced seen by the increased cleavage of caspase-3 and of PARP in immunoblots of cell lysates (Figure 19C).

5.1.3.3. The rate of apoptosis depends on the expression level of ASK2

Based on the observation that both overexpression and knockdown of ASK2 induced apoptosis, we investigated a correlation between the expression level of ASK2 and the rate of apoptosis. Therefore, siRNA specific against ASK2 or HA-ASK2 were titrated into HeLa cells that were subsequently subjected to stress by 24 h serum-starvation. As suspected, higher expression but also stronger downregulation of ASK2 increased apoptosis as visualized by the increase of PARP cleavage in immunblots of cell lysates (Figure 20).

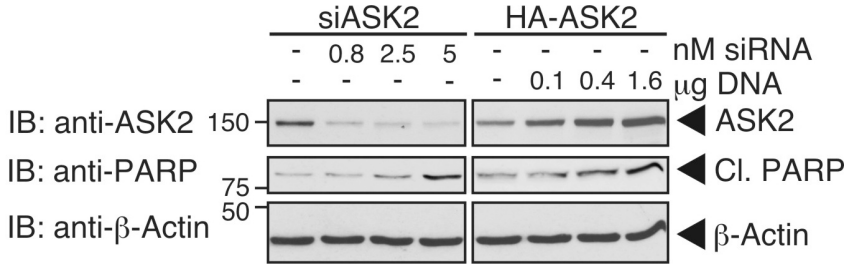

Fig. 20: HeLa cells were transiently transfected either with increasing amounts of siASK2_6 or increasing amounts of pcDNA3-HA-ASK2 (HA-ASK2). Total amounts of transfected siRNA and DNA were equalized with siControl or empty vector, respectively. After 24 h serum-starvation, cell lysates were prepared and analyzed in immunoblots (IB) with anti-ASK2, anti-PARP, and anti-β-Actin antibodies.

5.1.4. ASK2 homo- and hetero-oligomerizes with ASK1

Homo-oligomerization of ASK1 is a prerequisite for kinase activation (158). Therefore, ASK2 was analyzed for homo-oligomerization to assess its activation mechanism. To elucidate whether ASK2 is also able to homo-oligomerize we performed a co-immunoprecipitation analysis. As can be seen in the immunoblots in Figure 21A, immunoprecipitated HA-tagged ASK2 from HEK293 cells co-precipitated Myc-tagged ASK2 and vice versa.

ASK2 and ASK1 can form a hetero-oligomeric complex within which both kinases regulate each other positively (195). However, it is not known whether an apoptotic challenge such as serum-starvation influences ASK2-ASK1 hetero-oligomerization. To investigate hetero-oligomerization of ASK2 and ASK1 under different conditions, endogenous interaction of these two proteins was compared in HeLa cells that were either left in growth medium or serum-starved for 24 h. ASK2 and ASK1 were immunoprecipitated as indicated in Figure 21B, and endogenous ASK2 and ASK1 were found to form hetero-oligomers in non-stressed

cells. Serum-starvation decreased hetero-oligomerization and increased ASK1 immunoprecipitation. In contrast, the amount of precipitated ASK2 was not increased. Consistent with the results in Figure 19B, a weak starvation-induced increase of ASK1 expression was observed in whole cell lysates.

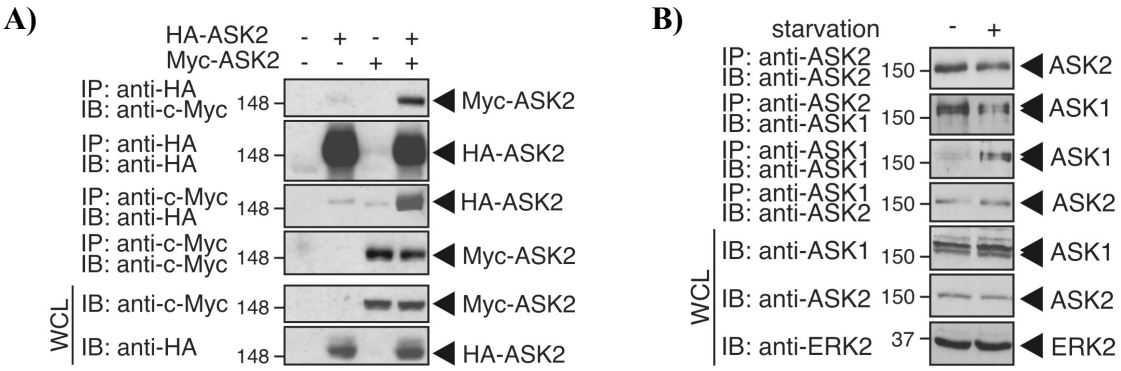

Fig. 21: Homo- and hetero-oligomerization of ASK2 and ASK1. A) HEK293 cells were transiently transfected with HA- or Myc-tagged ASK2 or empty vector. Cell lysates were immunoprecipitated (IP) as indicated. Homo-oligomerization was detected in immunoblots (IB) with the tag-specific antibody that was not used for IP. Expression of both proteins was confirmed in IB of whole cell lysates (WCL). B) HeLa cells were either incubated in growth medium (-) or serum-starved for 24 h (+). Endogenous ASK2 and ASK1 were then immunoprecipitated from whole cell lysates with antibodies against ASK1 or ASK2. The co-precipitated protein was detected in IB with the antibody that was not used for IP. Protein expression and equal loading were confirmed in IB of WCL.

Since changing the physiological amount of ASK2 induced apoptosis and serum-starvation reduced hetero-oligomerization of ASK2 and ASK1, ASK2-ASK1 hetero-oligomers were hypothesized to bear an anti-apoptotic function. To elucidate this, HeLa cells were transfected either with Myc-ASK2 or HA-ASK1 or both together with constant amounts of HA-ASK1 and increasing amounts of Myc-ASK2. Cells were then serum-starved for 24 h to induce apoptosis. The rate of apoptosis was quantified by the amount of cleaved caspase-3 and cleaved PARP (Figure 22A). HA-ASK1 and also Myc-ASK2 caused increased caspase-3 and PARP cleavage when expressed alone. However, co-transfection of Myc-ASK2 and HA-ASK1 reduced cleavage of both caspase-3 and PARP to a level observed in cells transfected with empty vector alone. This indicates that ASK2 and ASK1 have to be expressed at equimolar concentrations to prevent apoptosis.

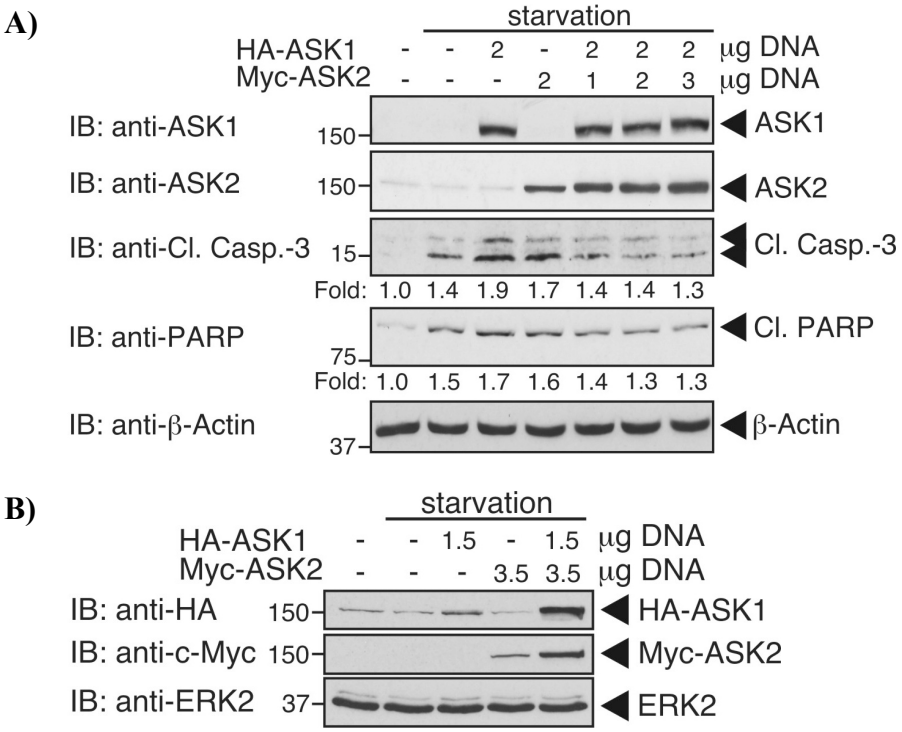

Fig. 22: Anti-apoptotic effect of co-expressed ASK2 and ASK1 in serum-starved HeLa cells. A) Cells were transfected with HA-ASK1 and/or Myc-ASK2 as indicated. Total amount of transfected DNA was equalized with empty vector and transfected cells were serum starved for 24 h. Immunoblot (IB) analysis of whole cell lysates (WCL) was performed using the anti-ASK1, anti-ASK2, anti-cleaved caspase-3 (Cl. Casp.-3), and anti-PARP antibodies. Expression of β-Actin was used as loading control. Pixel density was quantified with the ImageQuant 5.2 software. B) Cells transiently overexpressing HA-ASK1 and/or Myc-ASK2 as indicated were serum-starved for 24 h. WCL were analyzed in IB with anti-HA and anti-Myc antibodies. ERK2 expression was used as loading control.

Interestingly, protein levels of ASK2 and ASK1 increased when both kinases were expressed concomitantly compared to individual expression (Figure 22B). This finding is in agreement with a recent study showing that ASK1 stabilizes ASK2 by a kinase-independent mechanism (195). In the present study, ASK2 in turn also stabilized ASK1, which has not been discussed before.

5.1.5. ASK2 interacts with Trx2 containing the mitochondrial target sequence

To further assess the regulatory function of ASK2 in apoptosis, we investigated ASK2 for interaction with thioredoxins (Trx). ASK1 is regulated negatively by binding of cytoplasmic Trx1 (136) and mitochondrial Trx2 (134) therefore the ASK2 sequence was searched for

putative binding sites for Trx2. A putative Trx2 binding site in ASK2 analogous to ASK1 was found but no Trx1 binding site. Thus, Trx2 binding to ASK2 was studied by co-immunoprecipitation analyses (Figure 23).

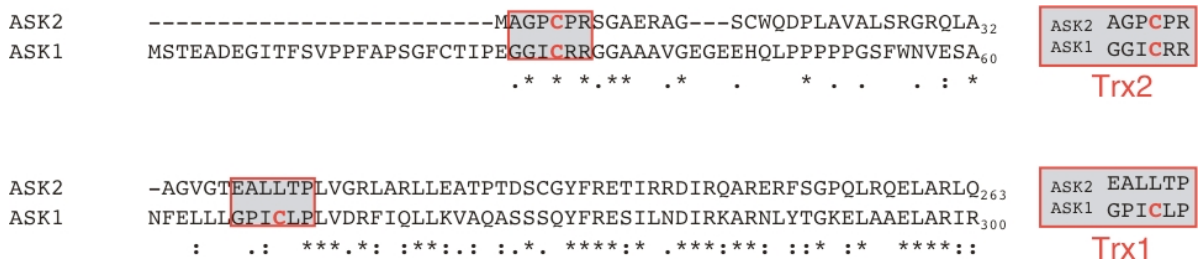

Fig. 23: Sequence alignment of ASK2 and ASK1 with the web-based ClustalW program to identify putative thioredoxin (Trx) binding sites on ASK2. Red boxes highlight Trx1 and Trx2 binding sites on ASK1 and show the respective sequences of ASK2.

Due to the binding of ASK1 with both Trx isoforms (134,136) and also with ASK2 (91,195), we analyzed interactions of overexpressed proteins since a co-immunoprecipitation analysis of endogenous proteins would most likely not exclude binding of thioredoxins to co-precipitated ASK1 in a trimeric complex with ASK2. This could then be misinterpreted as a direct interaction between ASK2 and Trx2. HA-ASK2, HA-ASK1, and Flag-tagged constructs of Trx1 (Flag-Trx1), of Trx2 with a mitochondrial target sequence (Flag-Trx2), or of Trx2 lacking the mitochondrial target sequence (Flag-ΔmtTrx2) were overexpressed in HEK293 cells either alone or in combinations as indicated in the immunoblot analysis in Figure 24A. Immunoprecipitated HA-ASK1 interacted with both Trx1 and Trx2 (upper panel, lanes 9 and 11) whereas only little Flag-Trx2 co-precipitated with HA-ASK2 (upper panel, lane 8). Deletion of the N-terminal mitochondrial target sequence inhibited binding of ΔmtTrx2 to ASK2 (lane 7). To confirm these findings, overexpressed Trx2 or ΔmtTrx2 were immunopreciptated and ASK2 was found to co-precipitate only with Trx2 (Figure 24B). No association was found with the N-terminal truncated cytoplasmic ΔmtTrx2. Therefore, ASK2 differs from ASK1 in binding exclusively to Trx2 containing the N-terminal mitochondrial target sequence suggesting a possible regulatory function of ASK2 in the intrinsic apoptotic pathway.

A)

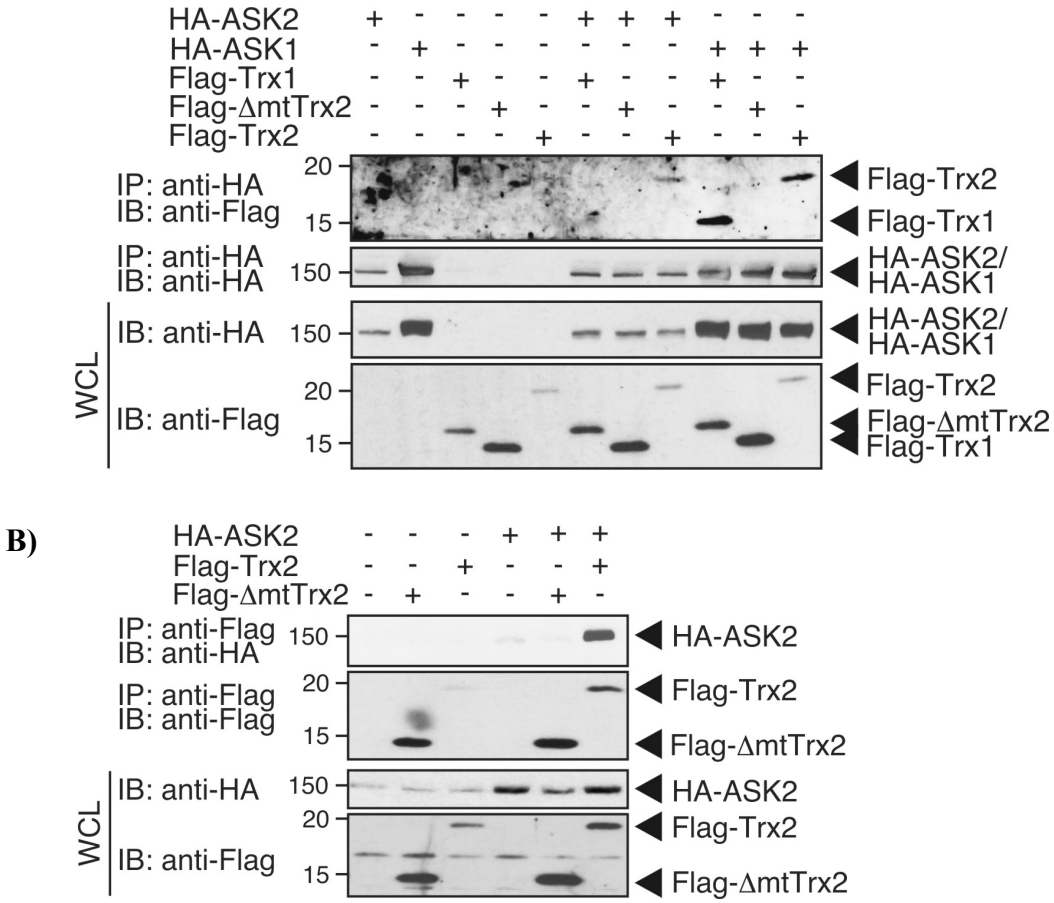

Fig. 24: Exclusive interaction of ASK2 with Trx2 containing the N-terminal mitochondrial target sequence. A) Upper panel: Domain structure of Trx1 and Trx2. Trx2 carries a mitochondrial localization sequence (mt, aa 1 to 22) at its N-terminus (according to a SMART analysis). A processed mitochondrial form of Trx2 lacking the first 60 aa (122) is shown (ΔmtTrx2), which was used as N-terminal deletion construct as described before (134). The glutaredoxin and thioredoxin domains of Trx1 partially overlap (SMART analysis). Lower panel: HEK293 cells were transiently transfected with HA-ASK2, HA-ASK1, Flag-Trx1, Flag-Trx2, Flag-ΔmtTrx2, or empty vector control plasmid as indicated. Cell lysates were immunoprecipitated (IP) using anti-HA antibody. Co-precipitated Flag-Trx constructs were detected by immunoblot (IB) using anti-Flag antibody. Whole cell lysates (WCL) were analyzed for protein expression. B) HA-ASK2, Flag-Trx2, Flag-ΔmtTrx2, or empty vector control plasmid were transfected into HEK293 cells as indicated. The Flag-tagged Trx2 constructs were immunoprecipitated from cell lysates using the anti-Flag antibody and tested for interaction with HA-ASK2 in IB using the anti-HA antibody. WCL were exmined for protein expression.

5.1.6. Regulation of ASK2 by the PI3K-AKT signaling pathway

AKT is an extensively studied pro-survival kinase that regulates numerous signaling pathways involved in proliferation, differentiation, and apoptosis. Several MAPKKKs are known AKT substrates such as c-Raf, which was described to be negatively regulated by

phosphorylation of Ser259, showing an inhibitory crosstalk between the PI3K-AKT pathway and the c-Raf-MEK-ERK pathway (149). The AKT phosphorylation site on Ser259 also serves as binding site for the scaffold protein 14-3-3, which has a second interaction site on c-Raf on Ser621. Phosphorylation-dependent binding of 14-3-3 to Ser621 is essential for c-Raf kinase activity (216). In order to identify new AKT substrates, a radioactive *in vitro* kinase assay was performed using peptides, which contained both the consensus sequence of AKT phosphorylation and an overlapping 14-3-3 binding site (done by Roland Frank and Magnus Bosse). Among others, a peptide encoding a sequence of ASK2 was positively tested with the following sequence: GKRRSRSPS$_{916}$SPRH (data not shown). ASK1 is phosphorylated by AKT in the very N-terminal region on Ser83, which negatively regulates ASK1-induced apoptosis (146). The putative AKT phosphorylation site on ASK2 differs from ASK1 by being located C-terminally to the kinase domain on Ser916. Binding of the scaffold protein 14-3-3 to c-Raf on Ser621 is required for c-Raf-kinase activity (216). Since binding of 14-3-3 is phosphorylation-dependent and Ser621 is located C-terminally to the kinase domain, we speculated that a putative phosphorylation of ASK2 on Ser916 could mediate 14-3-3 binding and thereby lead to kinase activation. A sequence analysis of ASK2 with the ScanSite 2.0 program also identified Ser916 as an AKT phosphorylation and 14-3-3 binding site at high stringency. In addition, a second putative AKT phosphorylation site on ASK2 on Ser46 was found but only at medium stringency, which would be analogous to Ser83 of ASK1. Figure 25A represents a sequence comparison of c-Raf, ASK1, and ASK2 focusing on the AKT phosphorylation and 14-3-3 binding sites. Interestingly, Ser46 is conserved among primates and rodents but Ser916 seems to have an evolutionary importance since it has been mutated from a gylcine among rodents (see multiple sequence alignment in Figure 25B).

A)

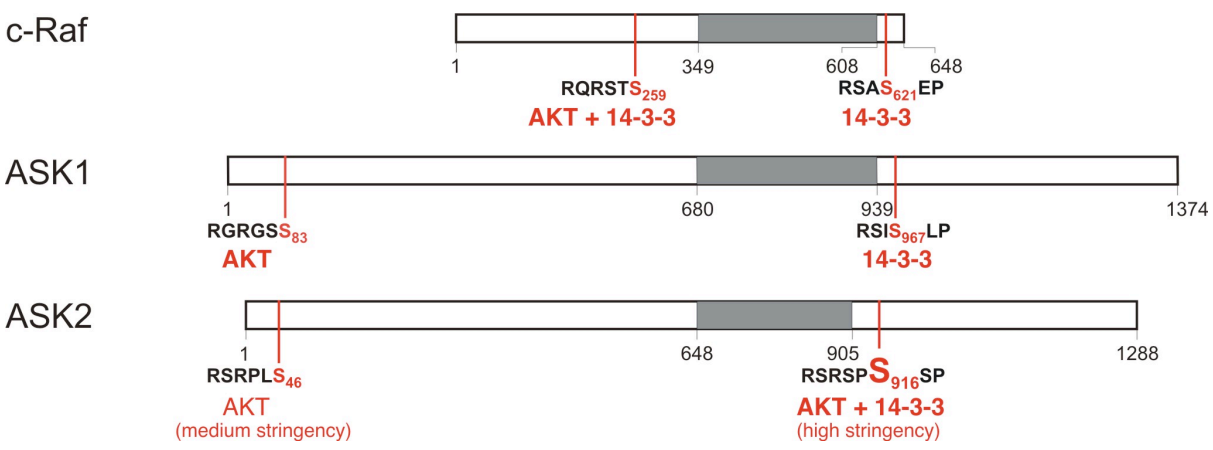

B)

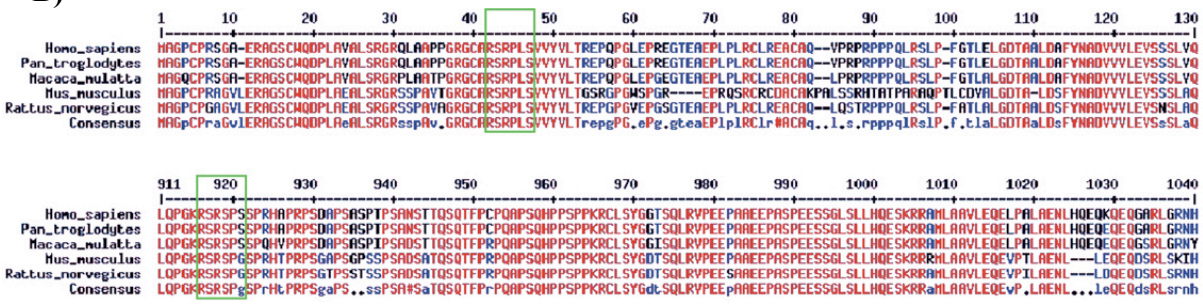

Fig. 25: A) Sequence comparison of c-Raf, ASK1, and ASK2 for AKT phosphorylation and 14-3-3 binding sites (grey bar: kinase domain). ASK2 sequence was analyzed with the ScanSite 2.0 program. B) Multiple sequence alignment (217) of ASK2 proteins from primates and rodents focusing on the 2 speculated AKT phosphorylation sites (green boxes). Colour of capitals indicates concensus values from high in red to low in blue.

AKT phosphorylation of ASK2 was then investigated first by *in vitro* and *in vivo* phosphorylation assays and second for a regulatory mechanism in apoptosis.

5.1.6.1. Investigation of ASK2 for AKT phosphorylation

To analyze phosphorylation of ASK2 by AKT, an *in vitro* phosphorylation assay using [γ-^{32}P]-ATP was performed. Several GST-fusion constructs of ASK2, which are shown in Figure 15A, were expressed in and purified from *E.coli*. Active AKT1 and [γ-^{32}P]-ATP were added to these GST-fusion proteins. After termination of the phosphorylation reaction, all proteins were separated by SDS-PAGE, blotted onto a nitrocellulose membrane and analyzed for [γ-^{32}P]-ATP incorporation by scanning with a phosphoimager. The GST-KA construct (highlighted in red), which contains the previously found AKT phosphorylation site on Ser916, was strongly phosphorylated (Figure 26B, upper panel). The point mutation Ser916^{Ala} (S916A) abolished phosphorylation as observed with the GST-KA-S916A construct. The GST-R1 protein with the second putative AKT phosphorylation site at Ser46 only gave a very weak phosphorylation signal. The band at around 60 kDa resulted from autophosphorylation of the added active AKT1. The scanned membrane was probed immunoblotted with an anti-GST specific antibody to confirm equal amounts of GST-proteins used (Figure 26B, lower panel).

Next, phosphorylation of ASK2 by AKT was investigated *in vivo*. For this purpose, HeLa cells were transiently transfected either with HA-ASK2 wild-type or with HA-ASK2 in

which the two putative AKT phosphorylation sites were mutated individually or collectively. After transfection, cells were either left in growth medium or serum-starved for 24 h to downregulate AKT activity and thereby to prevent a possible phosphorylation by AKT. Then, overexpressed HA-ASK2 constructs were immunoprecipitated from cell lysates using the anti-HA antibody and screened for phosphorylation on serine residues in an immunoblot with an anti-P-Ser specific antibody (Figure 26C). Overexpression of HA-ASK1 was used as a positive control for AKT phosphorylation. Phosphorylation on serine residues could only be detected in the case of HA-ASK1. Serum-starvation led to a downregulation of AKT activity verified by detecting less phosphorylation of AKT on Ser473, which is indicative of the activation status of AKT. Unexpectedly, ASK1 phosphorylation on serine residues was not decreased after serum-starvation. None of the HA-ASK2 constructs showed a phosphorylation on serine residues neither in cells grown under normal growth conditions nor after long-time serum-starvation. Thus, either ASK2 was not phosphorylated by AKT or the anti-P-Ser antibody was not able to detect a possible AKT phosphorylation on serine residues of ASK2. Moreover the question arose whether the serine phosphorylation of ASK1 was mediated by AKT at all because serum-starvation and consequently inhibition of AKT did not prevent this serine phosphorylation. Therefore, another antibody was tested specifically recognizing the AKT consensus sequence only when phosphorylated. This time, serum-starved cells, which overexpressed either HA-ASK2 wild-type, HA-ASK2^{Ser916Ala} or HA-ASK1 as positive control, were incubated individually or collectively with a pharmacological inhibitor of the AKT isoforms 1 and 2 (218) at a concentration of 40 μM for 30 min or with 100 ng/ml IGF-I for 20 min to activate the PI3K-AKT pathway. The immunoblot shown in Figure 26D revealed phosphorylation of HA-ASK2 wild-type, of the Ser916^{Ala} point mutant, and also of HA-ASK1. Serum-starvation did not lead to dephosphorylation neither of HA-ASK2 nor HA-ASK1. However, a residual AKT activity could be detected after serum-starvation. Complete inhibition of AKT activity was achieved by incubation with the AKT inhibitor for 30 min, which caused a reduced phosphorylation of HA-ASK2^{Ser916Ala} but not of HA-ASK1 as expected.

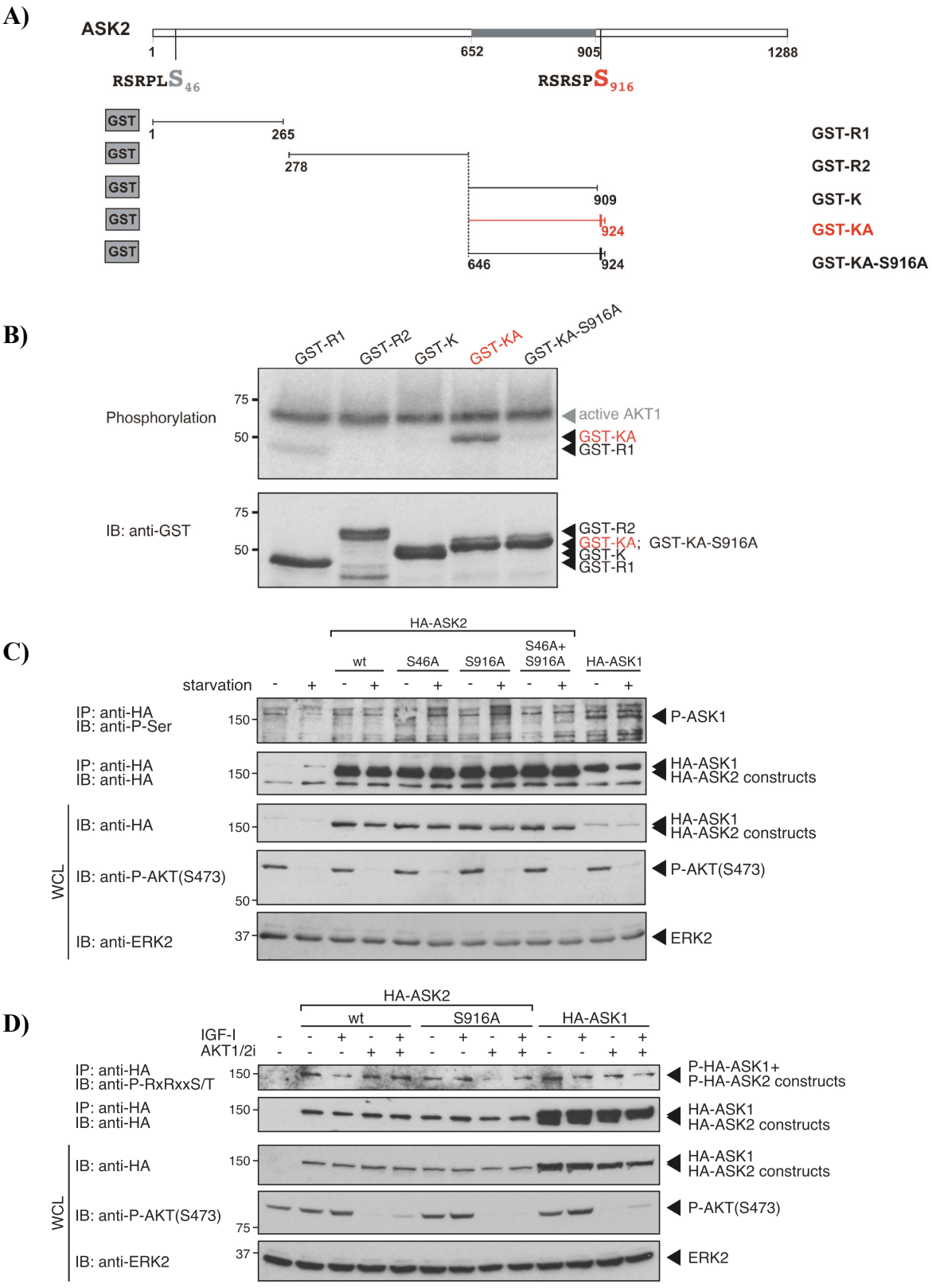

Fig. 26: In vitro and in vivo phosphorylation assay of ASK2. A) GST-fusion constructs of ASK2 that overexpressed in and purified from E.coli for in vitro phosphorylation assay. B) Autoradiogramm of in vitro kinase assay of ASK2. ASK2 kinase reactions using indicated GST-ASK2 constructs as substrates of active AKT1 in the presence of [γ-^{32}P]-ATP were separated by SDS-PAGE and blotted onto a nitrocellulose membrane for scanning with a

phosphoimager. The upper panel shows the obtained phosphoimager picture, the lower panel is an anti-GST immunoblot (IB) of the scanned membrane. C) HeLa cells transiently transfected with the indicated HA-tagged constructs of ASK2 and ASK1, or empty vector (pcDNA3) were either incubated in growth medium (-) or serum-starved for 24 h (+). HA-ASK2 or HA-ASK1 was immunoprecipitated (IP) using an anti-HA antibody and precipitates were analyzed in IB with the anti-P-Ser antibody. Whole cell lysates (WCL) were analyzed with the indicated antibodies. D) Same experimental set-up as described before under C). Immunoprecipitates were probed in IB with the P-RxRxxS/T-specific antibody. Expression of HA-ASK2 and HA-ASK1 constructs was confirmed in WCL with the indicated antibodies.

To further investigate an interaction between ASK2 and AKT, which is a prerequisite for phosphorylation by AKT, Myc-ASK2 overexpressed in HEK293 cells was immunoprecipitated and tested for binding with HA-AKT by immunoblotting for the Myc-tag of overexpressed ASK2 and vice versa. Co-precipitation of ectopically expressed ASK2 and AKT is shown in the immunoblot analysis in Figure 27.

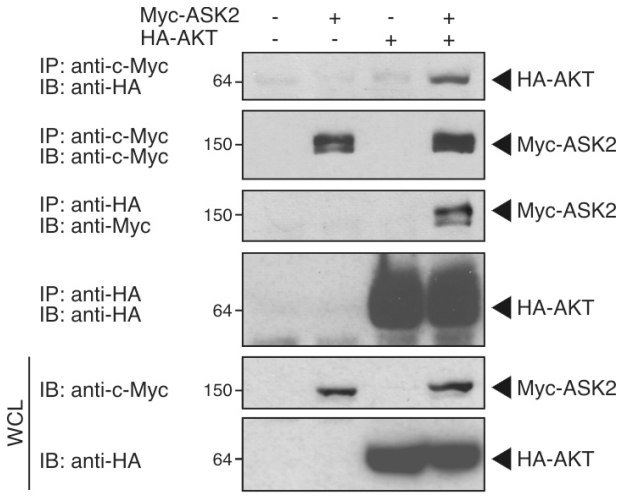

Fig. 27: Interaction of ASK2 and AKT. HEK293 cells were transiently transfected with Myc-ASK2, HA-AKT or empty vector (-) as indicated. Cell lysates were immunoprecipitated (IP) with anti-HA or anti-Myc antibodies. Co-precipitation was detected by immunoblotting (IB) with the anti-tag antibody that was not used for IP (left panel). Whole cell lysates (WCL) were analyzed for protein expression (right panel).

Based on these results, no clear conclusion could be drawn on whether ASK2 is phosphorylated by AKT *in vivo*. However, a GST-fusion construct of ASK2 containing Ser916 was identified *in vitro* as substrate of AKT and a second serine residue at position 46 was also weakly phosphorylated by AKT. Furthermore, interaction of ASK2 and AKT could be confirmed in the co-immunoprecipitation analysis. Therefore, co-expression of AKT wild-type or a kinase-inactive construct, AKT.KD, together with ASK2 was investigated for

regulating apoptosis in HEK293 cells induced by 24 h serum-starvation. Overexpression of HA-AKT together with Myc-ASK2 showed increased cleavage of caspase-3 and of PARP in immunoblots of whole cell lysates (shown in Figure 28A). Unexpectedly, co-expression of HA-AKT.KD had the same inducing effect on cleavage of caspase-3 and PARP. This demonstrated that co-expression of AKT had a pro-apoptotic effect via ASK2, which was independent from AKT kinase activity. This is in contrast to the negative regulatory function of AKT on ASK1 where phosphorylation inhibits ASK1 (146). Since ASK2 was phosphorylated by AKT on Ser916 in the radioactive *in vitro* phosphorylation assay, we examined HA-ASK2 and HA-ASK^{Ser916Ala} for induction of apoptosis when co-expressed with HA-AKT. The immunoblot analysis in Figure 28B revealed that both ASK2 constructs led to comparable activation of caspase-3 and cleavage of PARP. This indicates that ASK2 might not be phosphorylated by AKT on Ser916 and that substitution of Ser916 to alanine does not interefere with the induction of apoptosis caused by serum-starvation.

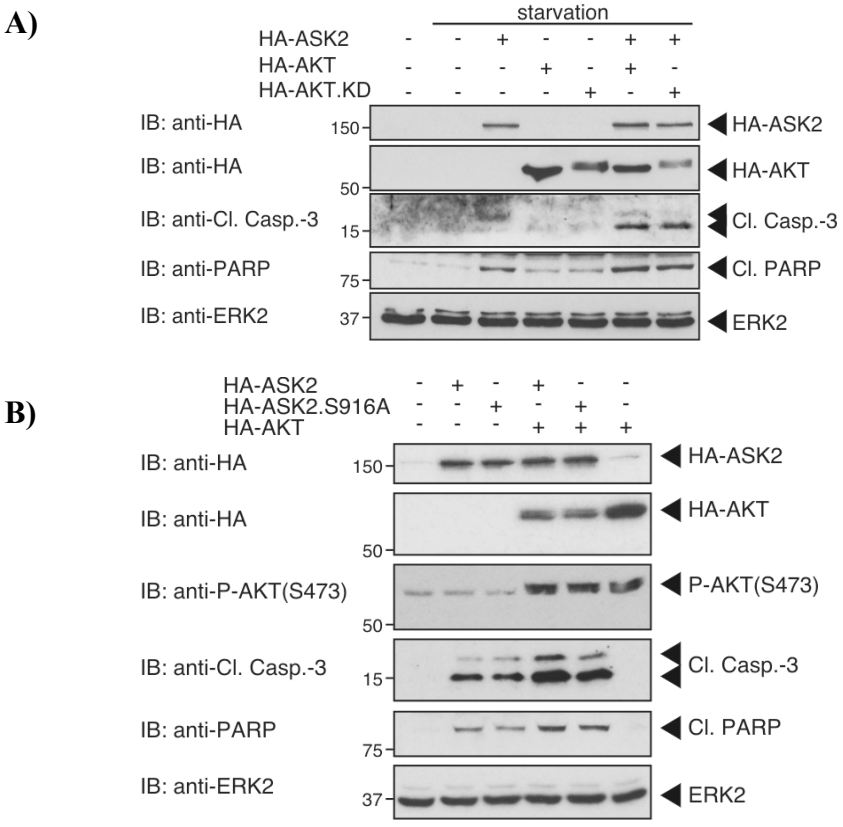

Fig. 28: Influence of AKT on ASK2-induced apoptosis. A) HEK293 cells were transiently transfected with HA-ASK2, HA-AKT, HA-AKT.KD, or empty vector (-) as indicated. After 24 h serum-starvation whole cell lysates were analyzed for apoptosis in immunoblots (IB) using anti-cleaved caspase-3 (Cl. Casp.-3) and anti-PARP antibodies. Protein expression was confirmed with the anti-HA antibody and equal loading was verified by detection of ERK2 with the ERK2-specific antibody. B) Cells transiently transfected with HA-ASK2, HA-

ASK2^{Ser916A} (S916A) or empty vector (-) were serum-starved for 24 h and IB with antibodies against the HA-tag, P-AKT(S473), Cl. Casp.-3, PARP, or ERK2.

5.1.6.2. Negative regulation of ASK2 by a PI3K dependent pathway

Apoptosis induced by overexpression of ASK2 and subsequent serum starvation was increased when AKT was co-expressed. To further investigate a regulation of ASK2 by the PI3K-AKT pathway either endogenous PI3K or AKT were inhibited by the pharmacological inhibitors LY294002 (219) or AKT1/2i (218), respectively. The immunoblot analyses in Figure 29A elucidated that inhibition of PI3K but not of AKT in HA-ASK2 overexpressing and serum-starved HEK293 cells led to an increase of PARP cleavage. The ASK2 point mutation Ser916^{Ala} but not Ser46^{Ala} specifically prevented the pro-apoptotic effect of PI3K inhibition. Efficacy of both inhibitors was confirmed by detecting phosphorylation of AKT on Ser473, which is necessary for AKT kinase activity (218). Next, we studied an influence of PI3K inhibition on ASK2-induced stress signaling via the JNK and p38 MAPK pathway. To this end, HEK293 cells transiently overexpressing either HA-ASK2 or ASK1 or empty vector were serum-starved for 24 h and then incubated with either 100 ng/ml IGF-I for 20 min or 40 μM LY294002 for 30 min or both together. Immunblot analyses of cell lysates shown in Figure 29B elucidated that inhibition of PI3K strongly increased phosphorylation of JNK and p38 MAPK in ASK1 overexpressing cells. HA-ASK2 expression only weakly induced activation of JNK and p38 MAPK after serum-starvation accordingly to the literature (91,195) and incubation with IGF-I reduced JNK and p38 MAPK activity. On the other hand, inhibition of PI3K induced an increase of phosphorylation of JNK and p38 MAPK in serum-starved cells that either overexpressed HA-ASK2 or ASK1. This suggests a similar PI3K-dependent negative regulation mechanism of ASK2 compared with ASK1 regarding the activation of the stress signaling cascades after serum-starvation.

A)

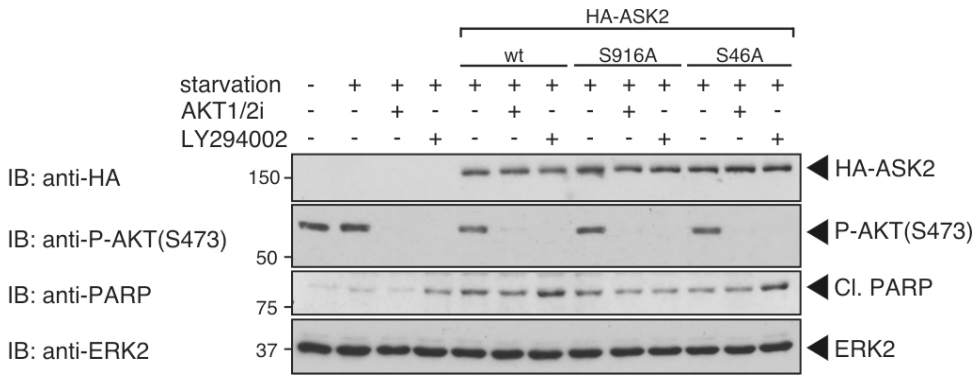

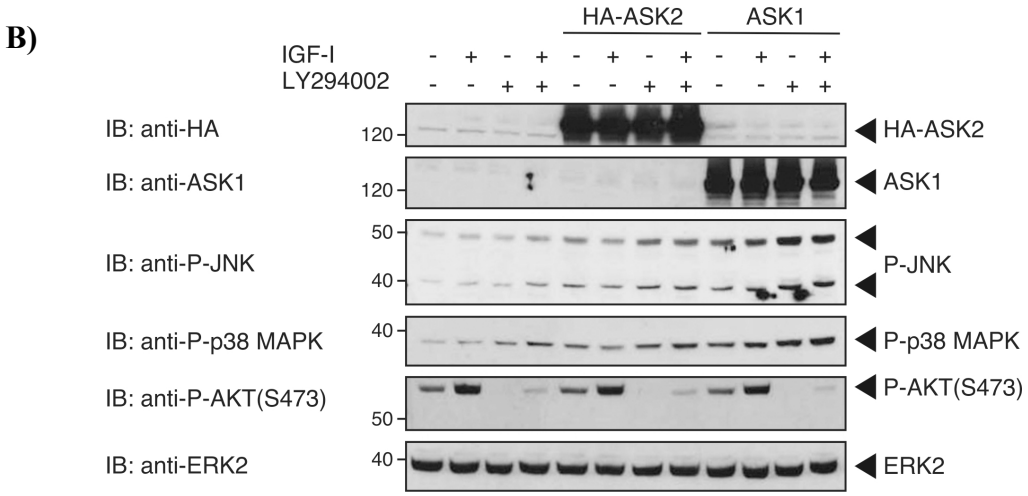

Fig. 29: Regulation of ASK2 and ASK1-induced apoptosis by PI3K. ***A)*** *HEK293 cells were transiently transfected with vectors encoding HA-ASK2, HA-ASK2^{Ser916Ala} (S916A), HA-ASK2^{Ser46Ala} (S46A), or empty vector and serum-starved for 24 h. After serum-starvation, cells were incubated with 40 μM AKT1/2i or 40 μM LY294002 for 30 min. Then, cell lysates were prepared and immunoblotted (IB) with antibodies against the HA-tag, P-AKT(S473), PARP, or ERK2, which was used as loading control. B) HEK293 cells were transiently transfected with HA-ASK2, ASK1 or empty vector (pcDNA3) and serum-starved for 24 h prior to incubation, Then, cells were incubated either with 100 ng/ml IGF-I for 20 min or with 40 μM LY294002 or were pre-incubated with 40 μM LY294002 for 30 min prior to incubation with 100 ng/ml IGF-I for 20 min. Cell lysates were probed in IB with antibodies against the HA-tag, ASK1, P-JNK, P-p38 MAPK, P-AKT(S473), or ERK2, which served as loading control.*

After elucidating that PI3K negatively regulated apoptosis induced by ASK2 overexpression and subsequent serum-starvation in a manner dependent on the serine residue at position 916 of ASK2, we investigated an anti-apoptotic effect of PI3K in cells with downregulated ASK2 expression. The immunoblot analysis in Figure 30 demonstrates that in serum-starved HEK293 cells, knockdown of ASK2 (siASK2_6) induced more cleavage of PARP than in cells transfected with siControl, which we already observed before (5.1.2.2). This ASK2 knockdown-induced PARP cleavage was even higher when PI3K was inhibited by incubation with LY294002. In contrast, inhibition of AKT with AKT1/2i prevented PARP cleavage.

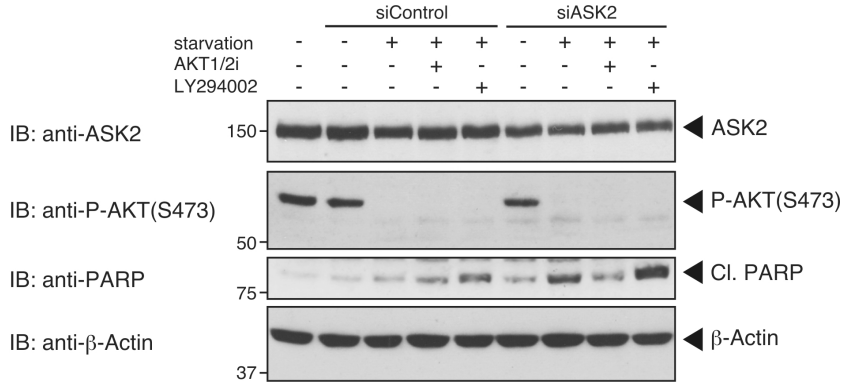

Fig. 30: Regulation of ASK2 knockdown-induced apoptosis by inhibition of PI3K. HEK293 cells were transiently transfected either with ASK2 specific siRNA (siASK2_6) or non-targeted siControl and then serum-starved for 24 h prior to incubation with 40 μM AKT1/2i or with 40 μM LY294002 for 30 min, as indicated. Cell lysates were analyzed by immunoblotting (IB) using antibodies against ASK2, P-AKT(S473), PARP, or β-Actin, which was used as loading control.

Summarizing, both overexpression and downregulation of ASK2 induced apoptosis, which was increased by an additional apoptotic challenge. Endogenous ASK2 and ASK1 were found to hetero-oligomerize in non-stressed cells, which was reduced after serum-starvation. Although ASK2 interacted with AKT and was phosphorylated by AKT *in vitro* on Ser916 and also weakly on Ser46, co-overexpression even of a kinase-inactive AKT construct with ASK2 led to increased apoptosis, which was observed by an elevated PARP cleavage. This indicated a pro-apoptotic function of overexpressed AKT in ASK2 co-expressing cells that were serum-starved and furthermore that this function was mediated in a manner independent from AKT kinase activity. In addition, the ASK2 serine residue at position 916 was required for apoptosis induced by inhibition of PI3K but not of AKT, since a point mutation to alanine abolished PARP cleavage after serum-starvation and subsequent incubation with LY294002. Moreover, activation of JNK and p38 MAPK by overexpression of ASK2 in serum-starved cells was reduced after incubation with IGF-I and increased again when PI3K was inhibited. Finally, the anti-apoptotic effect of PI3K was found to be dependent on the expression of ASK2 since knockdown of ASK2 in serum-starved cells together with PI3K inhibition caused an increase in PARP cleavage compared with cells expressing ASK2 at the endogenous level. In contrast, inhibition of AKT reduced cleavage of PARP indicating a pro-apoptotic function of AKT in serum-starved cells with downregulated ASK2.

5.2. Investigation of a functional role of ASK2 and ASK1 in C2C12 muscle differentiation

5.2.1. Hypothetic model for the regulation of the differentiation process of C2C12 myoblasts

Since ASK2 is mainly expressed in muscle tissues as elucidated in a Northern blot analysis (91), we speculated a functional role of this kinase in the differentiation process of muscle cells. The mouse C2C12 myoblast cell line is a widely used model system for the investigation of regulatory processes during myogenesis. Using this cell line, AKT was identified to negatively regulate the proliferative c-Raf-MEK-ERK pathway during the differentiation process from myoblasts to myotubes (148). During myogenesis, C2C12 cells produce and secrete IGF-II and thereby activate AKT in an autocrine loop (193). During the early differentiation phase, C2C12 myoblasts undergo several morphological changes, which exhibit similarities to apoptosis, including actin fiber dissassembly and reorganization and structural changes of the plasma membrane thereby enabling fusion of myoblasts into multinuclear myotubes. Caspase-3, which is an effector caspase in apoptosis, is essential for C2C12 differentiation since knockout of this caspase completely inhibits myotube formation (42). Activation of caspase-3 occurs in a very early phase after induction of differentiation at about the same time when AKT is activated (42). The upstream activator of caspase-3 in C2C12 myogenesis is not identified yet, however, ASK1 is an already known inducer of caspase-3 and also ASK2 was revealed to be an activator of this caspase. Since ASK2 is more specifically expressed in muscle tissues (91) than the ubiquitously found ASK1 (89), we assumed ASK2 to be the upstream activator of caspase-3 in C2C12 muscle differentiation leading to the following hypothetical model shown in Figure 31. AKT not only negatively regulates proliferation by inhibiting the c-Raf-MEK-ERK pathway (148) but can also concomitantly regulate the pro-apoptotic ASK2 and/or ASK1-induced caspase-3 activation. Partial support for this model comes from the already elucidated requirement of ASK1 for the differentiation of neurons (77) and of keratinocytes (120).

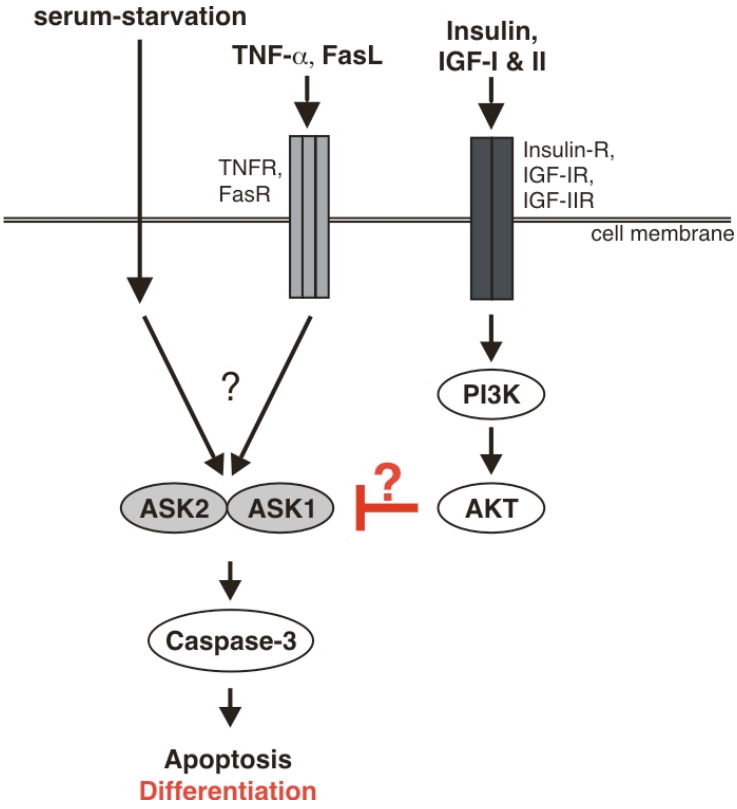

Fig. 31: Hypothetic model for the regulation of C2C12 muscle differentiation. The activation of AKT in a very early phase after induction of differentiation negatively regulates the pro-apoptotic ASK2 and/or ASK1 pathway to inhibit apoptosis but to allow enough caspase-3 activation needed for the differentiation process.

To investigate the putative regulatory function of ASK2 and ASK1 during muscle differentiation, expression of both kinases have to be prevented in C2C12 myoblasts. These myoblasts with downregulated ASK2 or ASK1 or with a double knockdown of both proteins are then subjected to differentiation to examine whether the absence of these kinases influences myogenesis.

5.2.2. The C2C12 myoblast cell line is a model system for muscle differentiation

The C2C12 myoblast cell line is well established and extensively characterized as a standard model system for muscle differentiation (220). Myogenesis is initiated by switching high serum-containing growth medium to 2% horse serum after cells have reached confluency (see Figure 32A). This low-serum differentiation medium is not changed during the next four days of differentiation and formation of multinuclear myotubes to allow for autocrine IGF-II

stimulation (193). As early as one day after switching to differentiation medium, one of the first muscle specific transcription factors, myogenin, is expressed, followed by expression of e.g. myosin heavy chain and in a later phase of troponin (Figure 32B). Formation of myotubes and terminal differentiation are completed after four days. Fully differentiated C2C12 myotubes can be cultivated for two more days before they start to detach from the surface of the cell culture plate and finally undergo apoptosis.

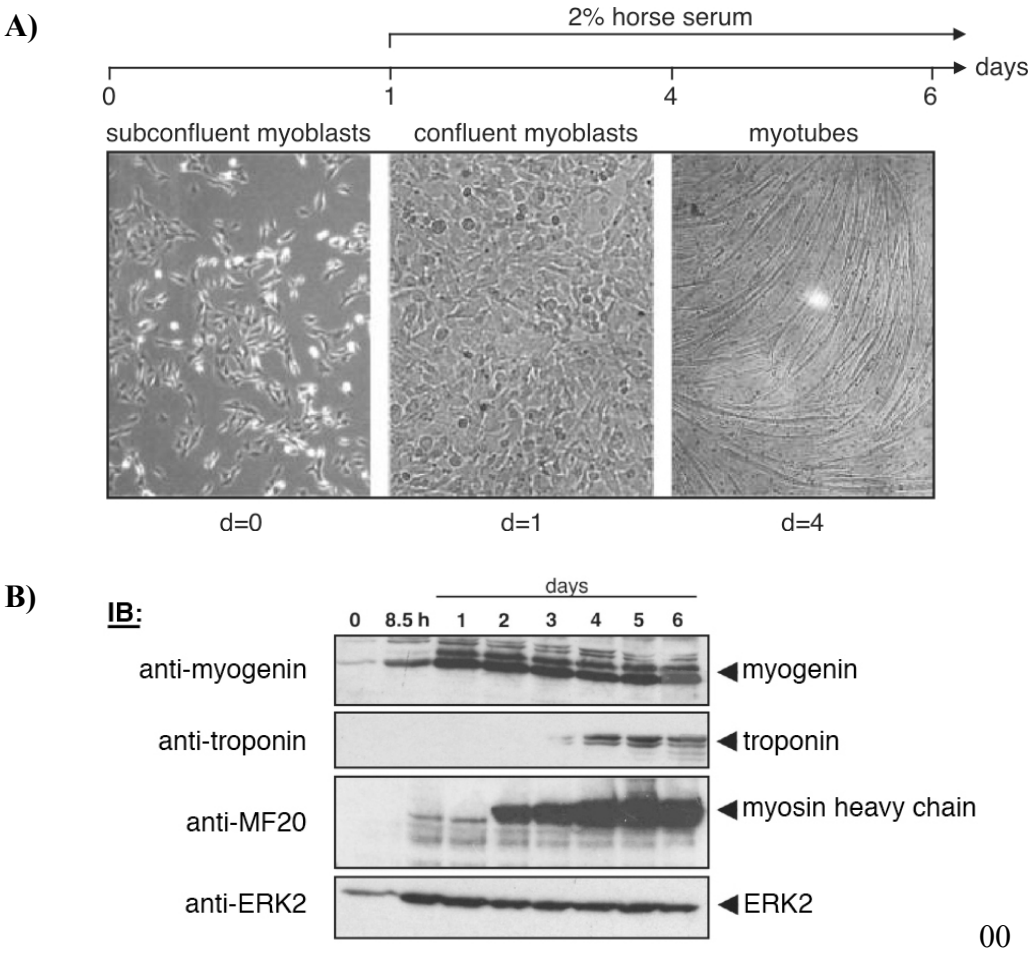

Fig. 32: Differentiation of C2C12 myoblasts into myotubes. A) Differentiation protocol. C2C12 myoblasts are grown subconfluently to prevent spontaneous differentiation (left picture), when cells are confluent (middle picture) medium is switched to 2% horse serum (d: days). Differentiation into multinuclear myotubes is completed after 4 days (right picture). B) Cell lysates of C2C12 were prepared at the indicated time points during the differentiation process and analyzed in immunoblots (IB) for the expression of the following differentiation marker proteins: myogenin, troponin, and myosin heavy chain (anti-MF20). Detection of ERK2 expression with the ERK2-specific antibody was used as loading control.

5.2.3. ASK1 knockdown by shRNA

We designed two shRNAs against ASK2 and ASK1 based on the mRNA structures, which were analyzed by the Mfold program of the Wisconsin GCG package. To ensure sustained expression of all four shRNAs against ASK2 and ASK1 and also of a negative control shRNA against the luciferase gene (siGL2), the shRNAs were cloned into the retroviral vector pMSCV for subsequent transduction of C2C12 myoblasts. The pMSCV vector lacks the 3' LTR and encodes a puromycin resistance gene for selection of transduced cells. After transduction, C2C12 myoblasts were selected with puromycin and finally analyzed for downregulation of ASK2 and ASK1 by quantitative Real-Time PCR. Figure 33A shows the sequences of the two ASK1-targeted shRNAs shA4 and shA5. As can be seen in the evaluation of the quantitative Real-Time PCR in Figure 33B, both shA4 and shA5 reduced the ASK1 mRNA level compared with shGL2 transduced C2C12 cells. shA5 was more efficient and induced a downregulation of ASK1 mRNA of almost 65%. Knockdown of ASK1 was then confirmed by immunoblot analysis (IB) of immunoprecipitated endogenous ASK1 from the stably transduced C2C12 myoblasts, which is shown in Figure 33C. ASK1 expression was not determined in cell lysates because several ASK1-specific antibodies tested detected only overexpressed ASK1.

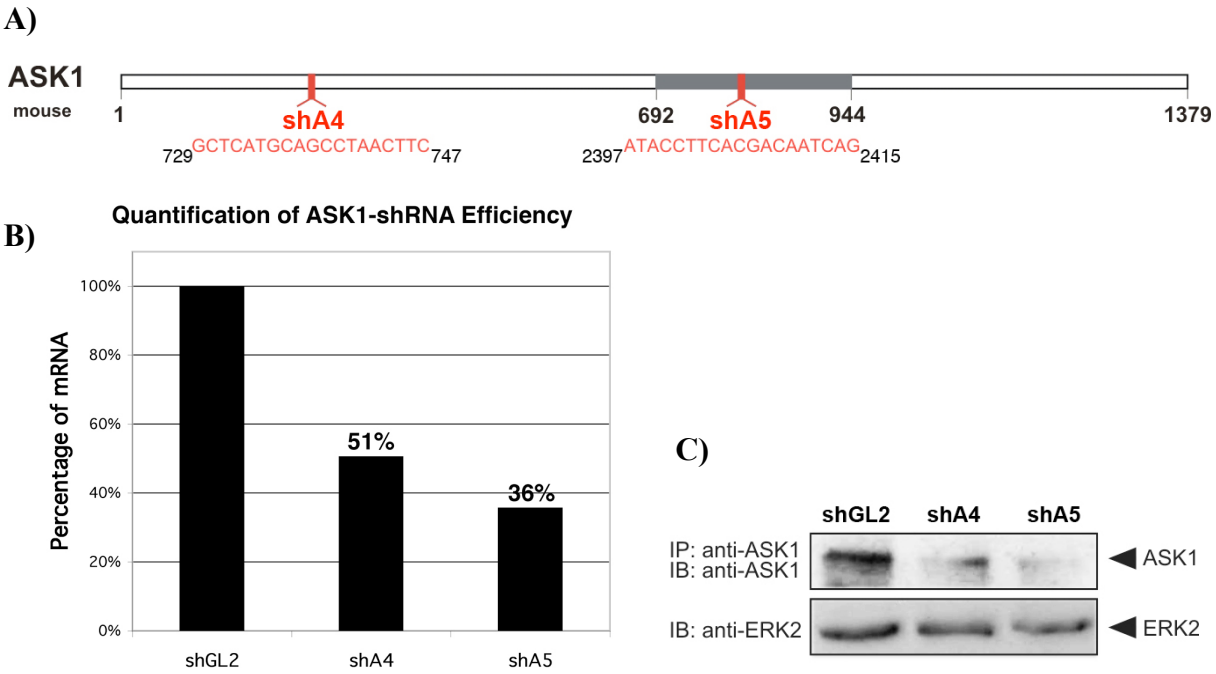

Fig. 33: Knockdown of ASK1 in C2C12 myoblasts. A) Two target sequences, A4 and A5, were chosen for shRNA design against mouse ASK1. B) C2C12 myoblasts were stably transduced with the retroviral vector pMSCV encoding the ASK1-specific shRNAs shA4 or

shA5, or a negative control shRNA targeted against the luciferase gene (shGL2). ASK1 mRNA downregulation was measured by quantitative Real-Time PCR. C) Endogenous ASK1 was immunoprecipitated (IP) from cell lysates of C2C12 myoblast stably expressing the indicated shRNAs and ASK1 expression was detected by immunoblot (IB) analysis with the ASK1 specific antibody. ERK2 expression was used as loading control.

Since a better downregulation of ASK1 expression was found in shA5 stably transduced C2C12 cells, this cell line was used for the following studies and called siASK1.
ShRNAs against ASK2 did not work or insufficiently reduced ASK2 mRNA, therefore we investigated only ASK1 for its role during C2C12 muscle differentiation.

5.2.4. Influence of ASK1 knockdown on C2C12 muscle cell differentiation

The stably transduced C2C12-shGL2 and -shASK1 myoblasts, which were analyzed for ASK1 downregulation by quantitative Real-Time PCR, were used only at low passage number for investigation of an influence of reduced ASK1 expression on C2C12 myogenesis. A light microscopy analysis was performed of C2C12 wild-type (wt), -shGL2 or -shASK1, which were subjected to myogenic differentiation for three days (shown in Figure 34A). C2C12-wt and negative control shGL2 expressing myoblasts already formed myotubes within two days after induction of differentiation by switching to low-serum medium. In contrast, C2C12 cells with downregulated ASK1 revealed a delayed differentiation and started to form multinuclear myotubes after three days. This slowed differentiation caused by ASK1 knockdown was verified by immunoblot analyses for expression of muscle-specific marker proteins in whole cell lysates prepared from C2C12 cells after two days of differentiation. (Figure 34B). Knockdown of ASK1 delayed the expression of myogenin and myosin heavy chain. Interestingly, caspase-3 cleavage was decreased.
Next, a confocal immunofluorescence microscopy analysis was performed shown in Figure 34C and confirmed the reduced myosin heavy chain expression in ASK1 knockdown cells after two days of differentiation (upper row). A more detailed analysis of differentiating cells (lower row) revealed decreased myosin heavy chain expression. Additionally, a hypertophic phenotype (white arrow heads) was observed, which is characterized by the increase in myotube diameter (221) and was visualized by the expression of cytoplasmic myosin heavy chain (red) and nuclear myogenin (green). The morphological difference of C2C12 cells with downregulated ASK1 expression was further evaluated by measuring the percentage of

multinucleated cells (blue), the number of nuclei per multinucleated cell (red), and by the number of hypertrophic cells (green). For this, eight different confocal immunofluorescence pictures from each C2C12 cell line (shown in Figure 34C) were counted and quantified with respect to the percentage of multinucleated cells, the number of nuclei per cell, and the percentage of hypertrophic cells (Figure 34D). The expression of negative control shGL2 already influenced C2C12 myogenesis in the percentage of hypertrophic cells by doubling their amount compared with C2C12-wt. Downregulation of ASK1 increased the number of hypertrophic cells and more than half of all myotubes appeared to have a hypertrophic phenotype. The percentage of multinucleated cells and the number of nuclei per multinucleated cell were comparable for all three cell lines.

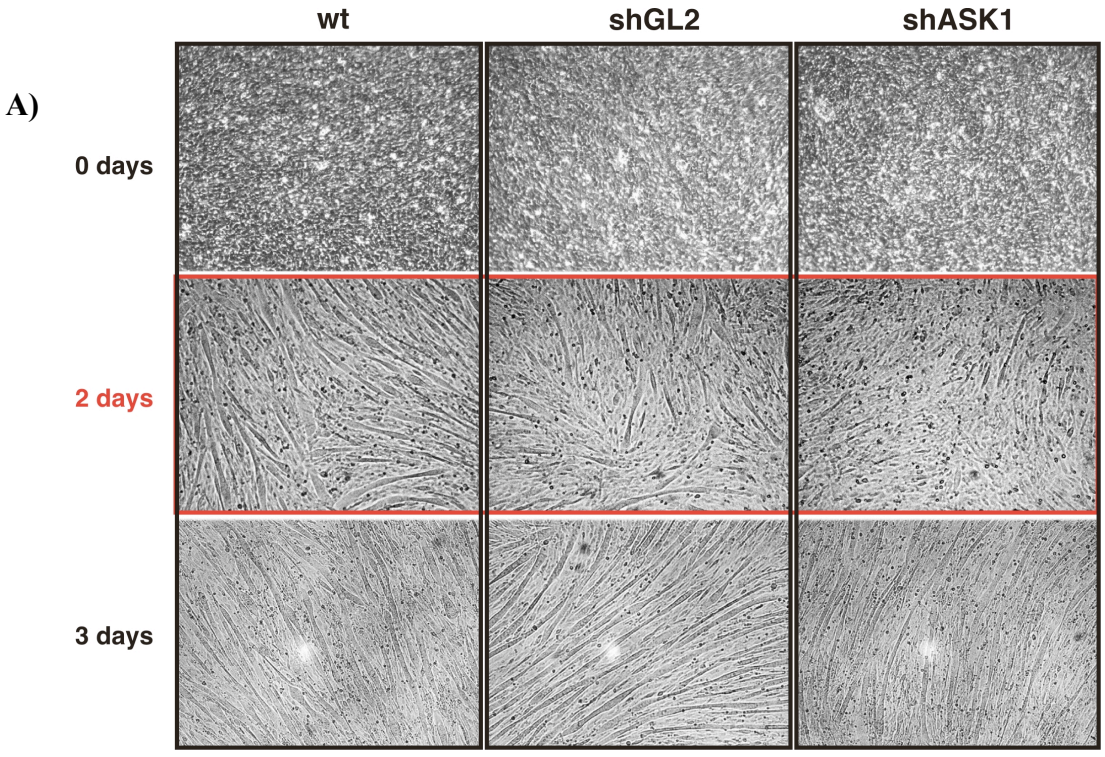

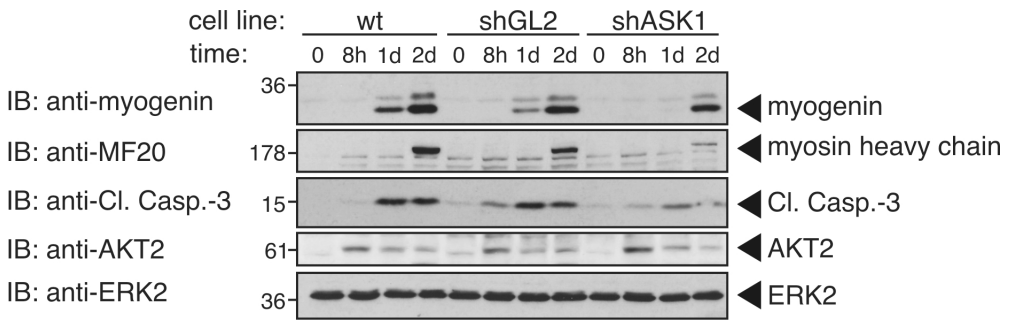

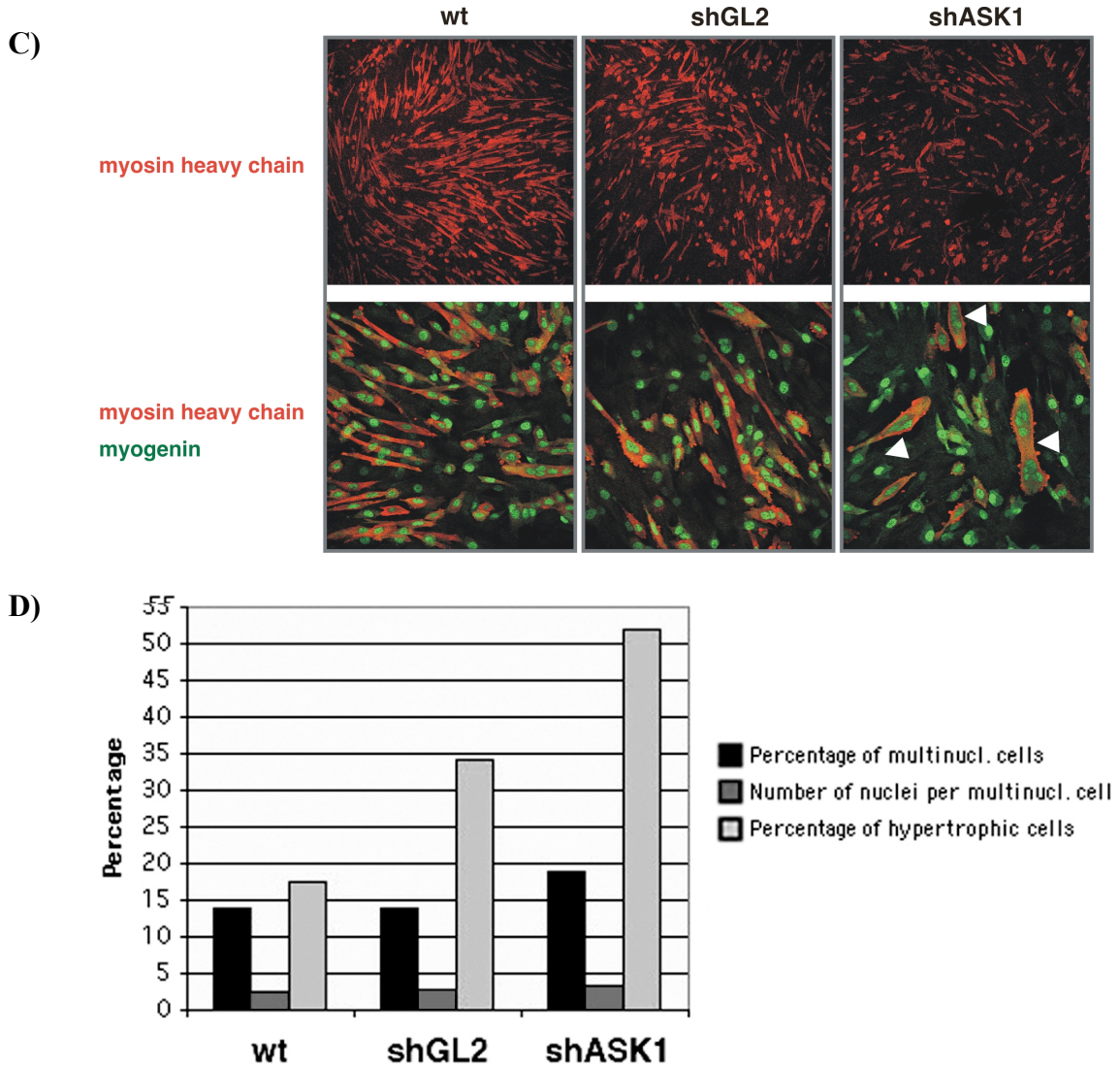

Fig. 34: Knockdown of ASK1 influences C2C12 muscle differentiation. A) C2C12 wild-type (wt) myoblasts or cells stably expressing shRNAs targeted against the luciferase gene (shGL2) or ASK1 (shASK1) were subjected to differentiation and morphologically compared by light microscopy during the first 3 days of differentiation. B) Cell lysates prepared from differentiated C2C12-wt, shGL2, or shASK1 stably expressing cells at day 2 after induction of differentiation were analyzed for musle differentiation in immunoblots (IB) with the indicated antibodies. C) C2C12-wt, shGL2- or shASK1 stably expressing cells were analyzed in confocal immunofluorescence microscopy for the expression of myosin heavy chain (red) and myogenin (green) after 2 days of differentiation. D) C2C12-wt, shGL2 or shASK1 stably expressing cells from the previous immunofluorescence analysis (C) were compared by quantifying the percentage of multinucleated cells (black), the number of nuclei per multinucleated cell (dark grey), and by the number of hypertrophic cells (light grey) from eight different pictures (as shown under C)) of each cell line.

Taken together these findings, downregulated ASK1 expression caused a delay in the C2C12 muscle differentiation process confirmed by two morphological assays and biochemical studies of the expression of muscle specific proteins (Figure 34). This effect was only

observed when cells with low-passage number after transduction were used and was completely lost at high-passage number.

To confirm the requirement of ASK1 for appropriate C2C12 myogenesis, the transduction was repeated and also the empty retroviral vector pMSCV was transduced. Thereby, puromycin-selected empty vector-transduced cells and C2C12-wt cells could be compared to rule out a possible effect of puromycin selection on C2C12 myogenesis and on the expression of ASK1. This time, myoblasts expressing shGL2 and cells transduced only with the empty vector pMSCV already showed a reduced ASK1 expression as evaluated in quantitative Real-Time PCR (Figure 35). This indicated that the transduction process per se and/or the subsequent selection with puromycin negatively regulated ASK1 expression. In addition, we could observe a slowed myogenesis of all cell lines that underwent transduction and selection (data not shown). One explanation for this delay in muscle differentiation might be the downregulated ASK1 expression that was detected in all transduced cells compared with C2C12-wt cells.

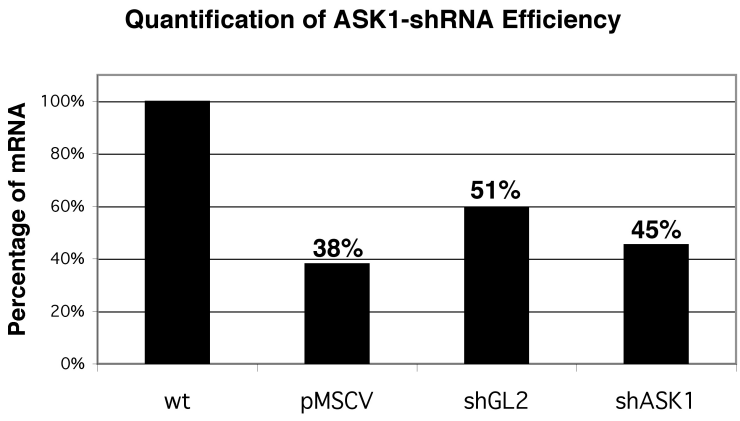

Fig. 35: Analysis of ASK1 downregulation by quantitative Real-Time PCR. C2C12 myoblasts were transduced either with empty vector pMSCV or vector encoding shRNAs against the luciferase gene (shGL2) or ASK1 (shASK1). After transduction cells were selected with puromycin cells and finally analyzed for ASK1 mRNA expression by quantitative Real-Time PCR. ASK1-mRNA level of each cell line was compared with C2C12 wild type (wt) cells.

To rule out an unspecific effect of the puromycin selection on the ASK1 expression, C2C12 myoblasts were transduced with the lentiviral vector c-FUGW (210). This vector integrates also in non-dividing cells thereby ensuring a high transduction efficiency, which makes a further selection step dispensable. Moreover, the c-FUGW vector carries the GFP gene therbey transduced cells can be directly quantified by the GFP expression in a FACS

analysis. The shGL2 and shASK1-encoding c-FUGW and empty vector transduced C2C12 myoblasts exhibited a general transduction efficiency of about 90% (data not shown). However, there was no downregulation of ASK1 mRNA detectable by quantitative Real-Time PCR indicating that the shRNA against ASK1 did not work and also none of the transduced cell lines exhibited reduced ASK1 expression. Accordingly, neither the shASK1 nor the shGL2 expressing cells showed the previously observed delay in the muscle differentiation process when subjected to myogenic differentiation immediately after transduction (data not shown).

In conclusion, a reduced ASK1 expression, seen in the first retroviral transduction experiment, was correlated with a partial impairment of the C2C12 myoblast differentiation into myotubes. However, the retroviral transduction procedure with subsequent puromycin-selection already negatively regulated the expression of ASK1. This unspecific effect of puromycin was evaluated by changing the transduction procedure using lentiviral vectors that made an additional selection step unnecessary. Thus, to further study a requirement of ASK1 for the differentiation process, a more efficient shRNA targeted against ASK1 has to be used for lentiviral stable transduction of C2C12 myoblasts.

6. Discussion

Apoptosis is a highly regulated suicide program of cells and is involved in the development and homeostasis of multicellular organisms, host defence and elimination of damaged cells (2,222,223). This genetically encoded cell death program is induced either by the death receptor-mediated extrinsic pathway or the mitochondrial intrinsic pathway (reviewed in (9) and (7)). Serum-starvation can activate the mitochondrial intrinsic pathway by elevation of cellular ROS levels (224-226) and overlaps with the extrinsic pathway by induction of ceramide production. Ceramide production converges partially with the intrinsic pathway by inducing mitochondrial cytochrome c release (227-229). Both apoptotic pathways result in the activation of the executioner caspases-3, -6 and -7, which cleave numerous substrates including poly (ADP-ribose) polymerase (PARP), resulting in the self-destruction of the cell (9,16,228,229).

ASK2 was initially identified as interaction partner of the apoptosis-inducing kinase ASK1 both belonging to the family of MAPKKK (91), which is involved in multifunctional signaling networks, regulating cell survival, proliferation, differentiation, and apoptosis (53-55,138). Although ASK2 and ASK1 are closely related, the role of ASK2 in apoptosis has been unclear. Therefore in the first part of the present study, ASK2 was investigated for its function in the regulation of apoptosis induced by serum-starvation. As expected from its sequence homology to ASK1, ASK2 overexpression combined with stress-induction by serum-starvation caused cell death as demonstrated by the cleavage of caspase-3 and PARP, and by annexin V-staining. Surprisingly, knockdown of ASK2 by siRNA also induced apoptosis, which was analyzed by caspase-3 activation and cleavage of PARP, and was increased by serum-starvation. Interestingly, ASK2 knockdown leads to a decrease in JNK-phosphorylation (195) indicating that downregulated ASK2 expression induces caspase-3 activation and PARP cleavage in a JNK-independent manner. It is conceivable that in the absence of ASK2, serum-starvation may induce this JNK-independent apoptosis via the mitochondria-located ASK1 within the intrinsic pathway as already described for TNF-α induced apoptosis (134). Such a dose-dependence for the induction of apoptosis has not been shown for ASK1, which is essential for extrinsic TNF-α stress-induced and intrinsic oxidative stress-induced apoptosis (155). We further characterized an anti-apoptotic function of ASK2 by its capability to form a heteromeric complex with ASK1. Stress-induction by

serum-starvation decreased the formation of ASK2-ASK1 heteromers and increased protein levels of ASK1. Consistently, concomitant overexpression of ASK2 and ASK1 reduced apoptosis induced by serum-starvation compared to overexpression of only one of the two proteins. Larger amounts of both proteins were also observed, confirming the mutually stabilizing effect described recently (195).

Summarizing these data, we propose the following functional model of ASK2 shown in Figure 36. At physiological levels, ASK2 and ASK1 reside as heteromeric complexes in non-stressed cells. This restricts the pro-apoptotic function of ASK1, which in the homo-oligomeric form induces apoptosis (158). ASK2 overexpression and downregulation together with serum-starvation disturbs the balance between ASK2 and ASK1 thereby leads to cell death. Overexpressed ASK2 only weakly induces activation of JNK and p38 MAPK (91,195) therefore the main function of ASK2 may be to prevent apoptosis induced by ASK1 homo-oligomers (158). Consistently, overexpression but not downregulation of ASK1 leads to stress-induced cell death (89,155). Overexpression of ASK2 might lead to homo-oligomerization of ASK2 and ASK1 and simultanously to the formation of ASK2-ASK1 hetero-oligomers.

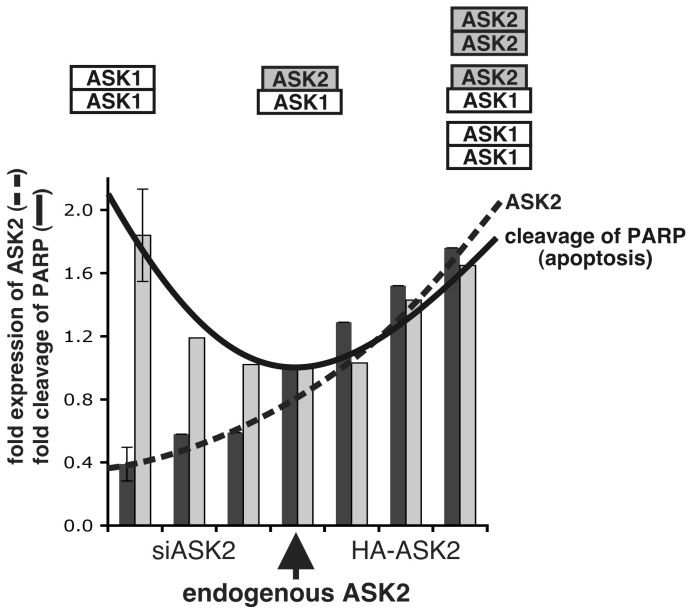

Fig. 36: Model for the regulatory function of ASK2 in apoptosis. Hetero-oligomers of ASK2 and ASK1 inhibit apoptosis. A change of ASK2 expression (grey bars) either by downregulation (left) or overexpression (right) leads to increased serum-starvation-induced apoptosis (black bars), PARP cleavage was used to quantify apoptosis (quantifications are obtained from Figure 20; standard deviation is calculated from Figures 19B, 19C, and 20;

the arrow indicates endogenous expression of ASK2). Serum-starvation was accompanied by decreased hetero-oligomerization of endogenous ASK2 and ASK1.

Phosphorylation of ASK2 and ASK1 within the activation loop on Thr806 or Thr838 (shown in chapter 5: Figure 12C), respectively, indicates kinase activation (91,195). It remains to be clarified why in non-stressed cells, overexpressed ASK2 is not phosphorylated on Thr806 but co-expression of kinase-inactive ASK1 induces this phosphorylation, which is increased by H_2O_2 treatment for stress activation. Furthermore, the stress signaling kinases JNK and p38 MAPK, and caspase-3 are only activated in non-stressed cells when kinase-inactive ASK1 is co-expressed with ASK2 (195). This suggests that hetero-oligomerization of ASK2 and ASK1 is needed for ASK2 kinase-activity. However, it remains to be determined whether in non-stressed versus serum-starved cells the threonine phosphorylation within the activation loop is changed, which would elucidate the activation status of these two kinases under different growth conditions. Additionally, it has to be examined, which role ASK2 kinase activity plays in the regulation of apoptosis and heteromeric complex formation with ASK1. Homo-oligomerization is essential for ASK1 kinase activation (158) therefore, the starvation-induced decrease in ASK2-ASK1 heteromeric complexes may result in homo-oligomerization of both kinases and thereby to phosphorylation on their threonine residues. It is conceivable that ASK2 more likely functions similarly to c-Raf by negatively regulating ASK1 in a kinase-independent manner (167) rather than acting as an apoptosis-inducing kinase. Therefore, in serum-starved cells, apoptosis may be mainly mediated by ASK1 homo-oligomers. This hypothesis is strengthened by the fact that ASK2 only weakly activates the stress signaling kinases JNK and p38 MAPK and caspase-3 compared to ASK1 (91,195). It might be also possible that the scaffold protein 14-3-3 mediates the association of ASK2 and ASK1. ASK2 encodes a putative 14-3-3 binding site, Arg-Ser-Pro-Ser_{916}-Ser-Pro, which correlates with the subtype 1 of 14-3-3 consensus binding sites (230). ASK1 is negatively regulated by binding of 14-3-3 to Ser967 (160,161), therefore dimerized 14-3-3 could bring together ASK2 and ASK1. Such a bridging function of 14-3-3 is already described in the heterodimerization process of c-Raf with B-Raf (231). Thus, overexpressed ASK2 may titrate out 14-3-3, which could cause increased homo-oligomerization of ASK1 and ASK2 and consequently caspase-3 activation and cleavage of PARP. Thr807 phosphorylation of ASK2 induced by co-expression of kinase-inactive ASK1 in the absence of stress may also be explained by the disturbance of the endogenous balance between ASK2 and ASK1. The coiled-coil sequences of ASK2 and ASK1 differ in amino acid composition and also in their

length, which most likely results in different structural configurations. Therefore, overexpressed kinase-inactive ASK1 may preferentially bind to endogenous ASK1 thereby inducing a dissociation of the ASK2-ASK1 hetero-oligomer, which we observed in non-stressed cells. Simultaneously, ASK2 would form homomeric complexes leading to phosphorylation on Thr807 as shown for homo-oligomerized ASK1 (158).

Since both the cytosolic and nuclear Trx1 and the mitochondrial Trx2 negatively regulate apoptosis by binding to the N-terminal regulatory domain of ASK1 (134,136), we investigated a possible regulatory contribution of Trx-binding to ASK2. Trx2 differs from Trx1 by a 60 aa extension at the N-terminus containing a mitochondrial-translocation sequence (122), which we identified to be encoded within the first 22 aa by SMART analysis. Treatment with H_2O_2 or tumor necrosis factor-α (TNF-α) causes dissociation of cytoplasmic Trx1 from ASK1 and additionally, TNF-α induces JNK-independent apoptosis by releasing mitochondrial ASK1 from the inhibitory binding to Trx2 (134,152,158,159). In the present study, we elucidated an exclusive binding of ASK2 to full-length Trx2 and not to ΔmtTrx2, which is predicted to be identical to the processed mitochondrial Trx2 (122,232). ASK1 associated with Trx1 and full-length Trx2 but not with ΔmtTrx2. This suggests that ASK2 and ASK1 bind to Trx2 in a region between the mitochondrial-target sequence and the thioredoxin domain or that another protein mediates this interaction. Binding of Trx2 to ASK2 could be characterized in more detail by GST-pull down assay and co-immunoprecipitation analysis of overexpressed ASK2 and Trx2 only from the mitochondrial fraction. Since Trx2 is an enzyme located in mitochondria and ASK2 is mainly expressed in tissues containing large amounts of mitochondria (91), ASK2 may carry out its pro- and anti-apoptotic regulatory function mainly in the intrinsic mitochondria-mediated cell death pathway. ASK2 could negatively regulate induction of apoptosis by mitochondrial ASK1 through heteromeric complex formation and on the other hand may also weakly induce intrinsic apoptosis in a JNK-independent manner as described for mitochondrial ASK1 (134). This regulation of apoptosis may be dependent on the stress stimulus. Induction of the mitochondrial apoptosis pathway by serum-starvation and also by treatment with TNF-α could lead to caspase-3 activation by ASK1 and ASK2 homo-oligomers through dissociation of their inhibitor Trx2 (Figure 37). At the same time, cytoplasmic ASK1 may be still inhibited by binding to ASK2 mediated by other unknown regulatory mechanisms. Dissociation of cytoplasmic ASK2-ASK1 heteromeric complexes might mainly induce

apoptosis via ASK1 homo-oligomers, since ASK1 is a stronger activator of the JNK and p38 MAPK stress signaling pathways compared to ASK2 (91,195).

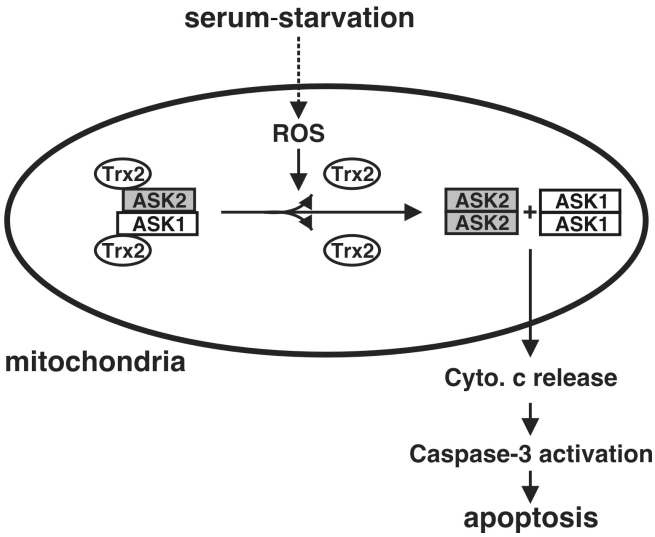

Fig. 37: Apoptosis-regulatory function of ASK2 in mitochondria. ASK2 and ASK1 form hetero-oligomers and both interact with Trx2. ASK2 may now inhibit apoptosis by interaction with ASK1 and by preventing ASK1 homo-oligomers in mitochondria. Serum-starvation induces generation of mitochondrial ROS, which might release ASK2 and ASK1 from the inhibitory binding to Trx2 and lead to homo-oligomerization of both kinases and finally to apoptosis.

We hypothesized that ASK2 not only regulates apoptosis by interaction with ASK1 but like ASK1 is also regulated by AKT phosphorylation. Crosstalks between the PI3K-AKT pathway and MAPK pathways have already been described. Zimmermann and Moelling demonstrated that phosphorylation of c-Raf on Ser259 by AKT negatively regulates the c-Raf-MEK-ERK pathway (149). This phosphorylation of c-Raf by AKT mediates binding to 14-3-3 and inhibits c-Raf (233). Another substrate of AKT is ASK1, which is phosphorylated on Ser83. This phosphorylation leads to reduced ASK1-induced stress signaling via JNK and p38 MAPK resulting in decreased apoptosis (146). To identify additional MAPK signaling cascades that are regulated by AKT phosphorylation, we tested several peptides encoding the consensus sequences for AKT phosphorylation and 14-3-3 binding in a radioactive *in vitro* screen for AKT phosphorylation. One peptide among others that was tested positively contained a sequence surrounding Ser916 of ASK2. Phosphorylation-dependent binding of 14-3-3 to Ser621 is essential for c-Raf kinase activity. Analogously, phosphorylation on Ser916 by AKT could positively regulate ASK2, since the AKT phosphorylation and the 14-3-3 binding sites exhibit a similar localization in the C-terminal regulatory domain of both c-

Raf and ASK2. On the other hand, AKT phosphorylation on Ser916 of ASK2 could be inhibitory similar to the negative regulation of ASK1 by AKT phosphorylation on Ser83. Sequence analyses with the ScanSite program revealed a second medium stringency putative AKT phosphorylation site on ASK2 on Ser46, comparable to the AKT phosphorylation site on Ser83 of ASK1. An additional multiple sequence alignment elucidated that the ASK2 serine residue at position 46 is conserved from rodents to primates. In contrast, Ser916 in primates has emerged later in the evolution substituting a glycine residue in rodents. Thus, Ser916 might have played a role, not further elucidated, in the evolutionary process from rodents to primates.

In a radioactive *in vitro* phosphorylation assay using several GST-fusion proteins of ASK2 as substrates of active AKT only a fusion protein containing Ser916 was phosphorylated. AKT phosphorylation in this fusion protein was completely inhibited when Ser916 was substituted with alanine. A second very weak phosphorylation was observed in a GST-protein comprising a sequence with the N-terminal Ser46. This weak phosphorylation of Ser46 could be due to high amounts of protein used in the experimental set-up, which could positively influence an AKT phosphorylation caused by an excess of an artificial substrate. However, Ser46 might be the endogenous *in vivo* AKT phosphorylation site because of its similarity to the AKT phosphorylation site of ASK1 on Ser83. In this case, incorrect folding of the Ser46-containing GST-fusion protein could prevent proper AKT phosphorylation. Interestingly, overexpressed AKT and ASK2 were found to interact in a co-immunoprecipitation analysis. Direct interaction of AKT with its substrate molecule is a prerequisite for carrying out the phosphorylation step. Since, A co-immunoprecipitation experiment might clarify the possible interaction between ASK2 and AKT. However, one has to bear in mind that ASK2 and ASK1 form hetero-oligomers (own data and (91,195)) and that ASK1, ASK2 and AKT could form a trimeric complex.

In immunoblots using an antibody, which specifically recognizes phosphorylated serines, immunoprecipitated ASK1 exhibited serine phosphorylation independent of whether it was overexpressed in cells that were serum-starved or stimulated with IGF-I to activate endogenous AKT. Unexpectedly, no serine-phosphorylation was detected for ASK2 suggesting that ASK2 is either no AKT substrate, which is contradictory to the previous *in vitro* data, or that the anti-phospho-serine antibody might not recognize phosphorylated serine residues on ASK2. An antibody specifically binding to the phosphorylated AKT consensus sequence revealed phosphorylation of both ASK2 wild-type and the ASK2-

Ser916^{Ala} point mutant. Based on these observations, we assumed that Ser46 of ASK2 is more likely the *in vivo* target site for AKT phosphorylation. To avoid specificity problems of the antibody or the potential misfolding of the GST-fusion protein tested as AKT substrates, a radioactive *in vivo* phosphorylation assay should be considered to clarify the AKT phosphorylation site on ASK2. Alternatively, additional kinases might be involved in ASK2 phosphorylation. Consistently, we observed that ASK1 was phosphorylated in serum-starved cells where AKT was detected to be inactive. Hence, more detailed analysis of the *in vivo* regulation of ASK2 by phosphorylation will be required to unravel the mechanism of ASK2 regulation.

Since ASK1-induced apoptosis is negatively regulated by AKT phosphorylation (146), we studied whether apoptosis induced by overexpressed ASK2 in serum-starved cells is also negatively regulated by AKT. AKT is an anti-apoptotic kinase, therefore we expected that co-expression of ASK2 and AKT would prevent cell death rather than positively regulate ASK2-induced apoptosis. According to the literature, overexpression of AKT alone in serum-starved cells did not induce caspase-3 activation whereas overexpression of ASK2 activated caspase-3 under similar conditions. Unexpectedly, co-expression not only of wild-type but also kinase-inactive AKT caused increased cleavage of caspase-3 and PARP. Increased cleavage of caspase-3 and PARP was not dependent on Ser916 of ASK2. These results are difficult to interpret, since AKT is an established anti-apoptotic kinase whereas we here found that co-expression of AKT increased cleavage of caspase-3 and PARP, suggesting a pro-apoptotic function. An explanation for this contradiction could be that overexpression of ASK2 induced apoptosis while overexpression of AKT counteracted the apoptotic signaling and activation of caspase-3 by ASK2 thereby inhibiting final cell death. To clarify this possibility, DNA fragmentation or nuclear condensation assays should be used to assess the percentage of cells undergoing apoptosis. However, also kinase-inactive AKT increased caspase-3 cleavage indicating that AKT mediated this caspase-3 activating effect in a kinase-independent manner. It remains to be investigated whether AKT directly effects ASK2 signaling in those assays or whether another signaling pathway or molecule links the AKT and ASK2 pathways. We observed no influence of Ser916 in ASK2 on the induction of apoptosis in cells overexpressing AKT. Therefore, ASK2 might differ from ASK1 and not be regulated by AKT phosphorylation. Alternatively, the sequence comprising Ser46 and not Ser916 may constitute the AKT target site. However, the hypothesis that ASK2 might not be directly regulated by AKT phosphorylation was strengthened by our finding that inhibition of

endogenous PI3K but not of AKT led to an increase in PARP cleavage by ASK2 in serum-starved cells. The serine residue of ASK2 at position 916 but not at 46 was essential for apoptosis since the point mutation of $Ser916^{Ala}$ reversed the pro-apoptotic effect of PI3K inhibition. This would indicate that ASK2 is controlled by PI3K but through a pathway that is independent of AKT activity.

Taken together, we propose the following model. Activation of caspase-3 and cleavage of PARP induced by overexpression or knockdown of ASK2 in serum-starved cells is increased in an AKT-dependent manner (see Figure 38A). On the other hand, in ASK2-overexpressing cells PI3-kinase activity is required for inhibition of apoptosis and acts either directly on ASK2 or via another unknown protein (see Figure 38B). In serum-starved cells, inhibition of PI3K increased the cleavage of PARP when ASK2 was downregulated suggesting an anti-apoptotic function of ASK2, probably by acting on ASK1 as discussed earlier in this chapter. Alternatively, PI3K might not act directly on ASK2 and only inhibit ASK1 through activation of AKT (146).

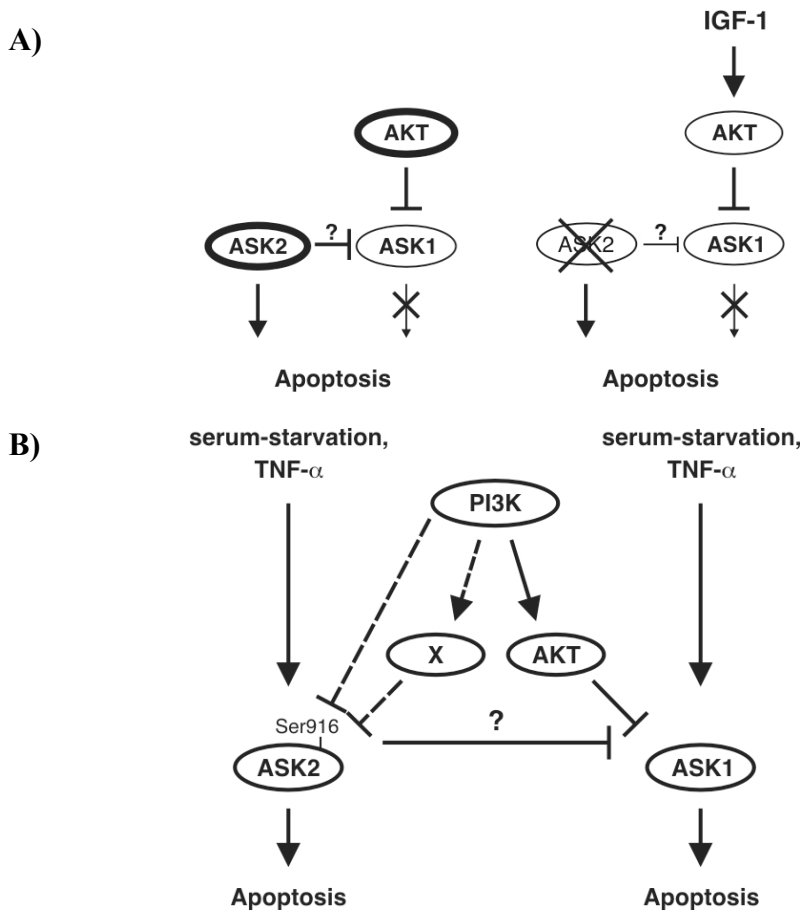

Fig. 38: Model for the regulation of ASK2 in apoptosis. (A) left panel: overexpression of AKT together with ASK2 induces apoptosis in serum-starved cells (overexpression shown in bold

lines). right panel: in serum-starved cells, IGF-I activates AKT, which negatively regulates ASK1, but simultaneous knockdown of ASK2 induces apoptosis (knockdown shown cross). (B) Induction of apoptosis by ASK2 overexpression is negatively regulated dependent on the ASK2 serine residue at position 916 either directly by PI3K or through an unknown protein (X). Concomitantly, the PI3K-AKT pathway inhibits ASK1-induced apoptosis.

Based on these findings, it would be interesting to determine whether the PI3K-AKT pathway is involved in the regulation of homo- and hetero-oligomerization of endogenous ASK2 and ASK1. AKT phosphorylation of ASK1 inhibits the activation of the stress signaling kinases JNK and p38 MAPK and apoptosis in a yet not further characterized manner (146). One possible scenario is that AKT phosphorylation of ASK1 supports the interaction of ASK2 and ASK1. This would increase the rate of ASK2-ASK1 heteromeric complexes and consequently inhibit apoptosis.

Lastly, a tissue immunoblot demonstrated an ubiquitous expression of ASK2, which is in contrast to the specific mRNA expression in muscle tissues observed in a human tissue Northern blot (91). A species difference may account for the difference between human and mouse and expression of mRNA may not be equivalent to protein expression. As the mouse tissue blot was non-quantitative, the expression rate of ASK2 may vary and be highest in heart and skeletal muscle tissue as could be expected from the Northern blot. Since we observed ASK2 localization not only in mitochondria but also in the cytoplasm and nucleus similar to ASK1 (134,156), heteromeric complex formation of ASK2 and ASK1 may be regulated by different interacting proteins dependent on the cellular compartment. ASK1 is negatively regulated by binding to several proteins including c-Raf (167), 14-3-3 (161), and retinoblastoma protein (Rb) (134,156). In the cytoplasm c-Raf inhibits ASK1 in a kinase-independent manner by binding to the N-terminal regulatory domain of ASK1 (167). However, c-Raf can also negatively regulate ASK1 in mitochondria shown by bFGF (basic fibroblast growth factor) treatment of endothelial cell, which leads to mitochondrial-translocation of c-Raf (234,235). Additionally, incubation with both insulin and IGF-I recruits c-Raf to the cytoplasmic membrane, which is the first activation step of c-Raf (149,236). ASK1 is also inhibited by binding to the IGF-I receptor in a manner independent from PI3K (170). Therefore, it is conceivable that ASK1 is not only negatively regulated by association with the IGF-I receptor but also inhibited within the cytoplasm by hetero-oligomerization with other interaction partners such as Trx1 (136), Hsp72 (166) or ASK2 as discussed previously. ASK2 could then take over the inhibitory function of the cytoplasmic membrane-recruited c-Raf. Concluding, the composition of the protein complexes containing

ASK2 and/or ASK1 may be regulated dependent on the cellular compartment and on the cytokine stimulation or apoptotic challenge of the cell.

Several aspects of apoptosis are also required for differentiation processes. Final differentiation of erythrocytes (44), keratinocytes (43), and lens fibers (237) shares similarities with programmed cell death regarding structural changes in the nucleus that finally lead to enucleation. Activation of caspases, which is essential for the above mentioned differentiation processes, may cause among others the cleavage of Lamin B (238). This intermediate filament supports the integrity of the nuclear membrane and degradation of this cytoskeletal protein leads to nuclear membrane disintegration. In skeletal muscle differentiation, activation of the executioner caspase-3 is indispensable since knockout of caspase-3 in myoblasts inhibits formation of multinuclear myotubes and muscle cell differentiation (42). This differentiation process is accompanied by structural changes of the plasma membrane, which again resembles apoptotic features, to allow fusion of the differentiating myoblasts. Caspase-3 activity has to be tightly regulated to prevent apoptosis during C2C12 muscle differentiation (239). However, it is not elucidated until now, which pathway finally leads to the regulated activation of caspase-3 in skeletal muscle differentiation.

ASK1 induces caspase-3 activation after stress-induction (153) and is required for the differentiation of neurons (77,172) and keratinocytes (120). We also identified ASK2 as an activator of caspase-3 after serum-starvation. Therefore, we investigated whether ASK1 and ASK2 are the upstream kinases responsible for caspase-3 activation during C2C12 muscle differentiation using an RNAi-mediated knockdown approach to downregulate expression of both kinases. Since C2C12 myoblasts are rapidly replicating and the differentiation process takes at least 4 days, we chose stable transduction of shRNAs instead of transient transfection of siRNAs. Due to often occurring off-target effects of siRNAs, more than one siRNA is normally used. Analogously, we designed two different shRNAs against ASK1 and ASK2 based on mathematical structural analyses of the mRNA secondary structure. Predicted stem loop structures were chosen as target sites because of an estimated higher accessibility for the shRNA. One of the two shRNAs, shA5, could downregulate ASK1 mRNA to 36% expression rate compared with non-transduced wild-type C2C12 myoblasts. However, the shRNA against luciferase (shGL2) also reduced ASK1 expression down to 51% indicating that the transduction process and or the puromycin selection permanently decreased the

expression of ASK1. Both shRNAs against ASK2 did not work, although some cells survived the puromycin selection. These surviving cells were most likely transduced successfully but presumably the shRNA target sequences were inaccessible because they were chosen by a quite inaccurate mathematical structural analysis. Since no ASK2 antibody was commercially available at that time and the polyclonal anti-ASK2 antibody had not been produced then, no further shRNAs were tested against ASK2. Analyses of the ASK1 knockdown myoblasts based on morphology and biochemical studies revealed a delay in myogenesis around day 2 after induction of differentiation. Although these effects could be demonstrated reproducibly, they were only observed in low-passage myoblasts and were lost with the increase of passage number. A second transduction experiment revealed that not only the shRNA against ASK1 but also the empty retrovirus and shGL2 caused a reduction of ASK1 transcription. A morphological comparison of the differentiation kinetics of all transduced cell lines with non-transduced wild-type C2C12 cells by light microscopy demonstrated a general delay in myogenesis probably as a consequence of the transduction and/or puromycin selection. To rule out an unspecific effect of puromycin on ASK1 expression and to confirm the efficacy of the ASK1-targeted shRNA, the transduction was repeated using the lentiviral vector cFUGW without subsequent puromycin selection. Although the transduction efficiency was above 90%, ASK1 was not downregulated. Generally, the transduction procedure did not reduce ASK1 expression. Moreover, neither of the transduced cell lines (shASK1, shGL2 or empty virus) exhibited a delay in muscle differentiation demonstrating that the selection process with puromycin caused the detected decrease in ASK1 expression. Puromycin is an antibiotic that inhibits translation by binding to the premature tRNA chain at the A-site within ribosomes thereby preventing further chain elongation. A second feature of puromycin is the inhibition of protein import into mitochondria. Thus, puromycin might inhibit translation of a protein that is needed for ASK1 mRNA transcription and thereby causes reduced ASK1 expression in all puromycin-selected cells.

Summarizing, the ASK1 expression level played a role in the differentiation process of C2C12 myoblasts to myotubes. Less ASK1 expression caused either by shRNA-mediated knockdown or by puromycin selection resulted in decelerated myogenesis. It remains to be elucidated whether downregulation of ASK1 influences the expression of ASK2. A recent report demonstrated that knockout of ASK1 upregulates ASK2 mRNA transcription but ASK2 is then degraded through the ubiquitin-proteasome system (195). We previously observed an activation of caspase-3 by overexpression of ASK2 in serum-starved cells,

therefore ASK2 could promote the cleavage of caspase-3 in differentiating myoblasts with downregulated ASK1 expression. Thus, it would be interesting whether in myoblasts with a complete knockdown of ASK1, ASK2 could substitute the ASK1 function in muscle cell differentiation. We would speculate that knockdown of ASK1 results in protein degradation. If ASK2 does not substitute the function of ASK1 it would indicate that ASK1 alone is responsible for the essential caspase-3 activation and that the delay of muscle differentiation observed in myoblasts with an ASK1 knockdown is caught up by the slow accumulation of ASK1 protein and not mediated by ASK2. We demonstrated that hetero-oligomerization of ASK2 and ASK1 was reduced after serum-starvation. We further showed in serum-starved cells that concomitant overexpression of both proteins decreased caspase-3 and PARP cleavage caused by overexpression of each one of these proteins. Therefore, it would be interesting to examine whether ASK2 and ASK1 also hetero-oligomerize in proliferating C2C12 myoblasts and whether a reduction of these heteromeric complexes can be observed after induction of differentiation by low-serum conditions.

Early steps in myogenesis are accompanied not only by activation of caspase-3 (42) and AKT (240) and by production of IGF-II. IGF-II leads to an autocrine stimulation of the PI3K-AKT pathway in differentiating myoblast (241,242), which inhibits the pro-proliferative c-Raf-MEK-ERK pathway by AKT phosphorylation of c-Raf on Ser259 (149). This crosstalk between the two signaling pathways occurs stage-specifically only in differentiated myotubes but not in proliferating myoblasts (148). We speculate that AKT negatively regulates ASK1 during early-phase C2C12 myogenesis. Differentiation of C2C12 myoblasts is induced by incubation in low-serum and this stress induction by serum-starvation activates ASK1 signaling as discussed before. This potential negative, anti-apoptotic crosstalk between AKT and ASK1 during myogenesis could be tested by reconstitution of completely downregulated ASK1. Reconstitution with wild-type ASK1 should enable muscle differentiation prevented by ASK1 knockdown. A point mutant of ASK1 preventing phosphorylation by AKT will most likely lead to increased caspase-3 activation and thus to more increased apoptosis. In contrast, expression of kinase-inactive ASK1 would probably impair caspase-3 activation and thus delay myogenesis.

In addition to IGF-II, TNF-α is necessary and sufficient for myogenesis (243). TNF-α stimulates the production of mitochondrial ROS and leads to the activation of caspase-3 and p38 MAPK. This is indispensable for muscle differentiation and is mediated via an autocrine loop already occuring in early differentiating myoblast (42,243-246). p38 MAPK signaling is

part of the ASK1-induced stress signaling cascade and therefore has to be tightly regulated during myogenesis to prevent cell death (247,248). We hypothesize that during C2C12 muscle differentiation, cytoplasmic ASK1 is not only negatively regulated by AKT phosphorylation but also by binding to c-Raf in a c-Raf kinase-independent manner (167). This would limit the cytoplasmic p38 MAPK activation required for C2C12 muscle differentiation. Furthermore, ASK1 and ASK2 differ in their binding to the anti-apoptotic thioredoxins with ASK1 interacting with Trx1 and Trx2 whereas ASK2 only associates with full-length Trx2. Therefore, it is conceivable that during C2C12 myogenesis mitochondrial ROS production induced by autocrine activation by TNF-α- leads to a dissociation of Trx2 from both ASK1 and ASK2. Consequently, homo-oligomerization of both kinases will be enabled resulting in the activation of caspase-3. On the other hand, cytosolic Trx1 may still bind to ASK1 forming an inactive complex with ASK2 and/or c-Raf. Thus, TNF-α may activate caspase-3 via the intrinsic mitochondrial pathway and binding of ASK1 to ASK2 and/or c-Raf may limit ASK1-induced activation of p38 MAPK.

Figure 39 summarizes a model for the regulation of an ASK1-induced activation of caspase-3 during the C2C12 muscle differentiation process. Downregulation of ASK1 expression leads to a deceleration of C2C12 myogenesis. Presumably, AKT phosphorylation limits caspase-3 activation occurring during the early phase of the differentiation process. In proliferating myoblasts growing in high serum-containing medium, c-Raf (148,149) and also ASK2 may inhibit ASK1 by forming heteromeric complexes.

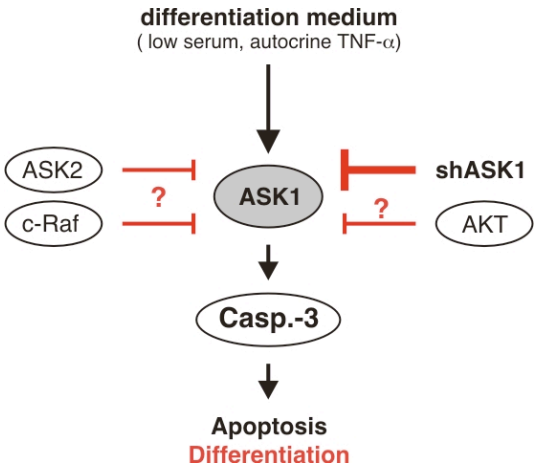

Fig. 39: Regulation of ASK1 during C2C12 muscle differentiation. After induction of C2C12 myogenesis with low serum-containing medium, differentiating myoblasts start producing TNF-α. This serum-starvation together with TNF-α then leads to an autocrine stimulation of ASK1, which induces caspase-3 (Casp.-3) activation. Downregulation of ASK1 by shRNA slows down myogenesis (shASK1 indicates knockdown of ASK1 by shRNA). AKT (146) and c-

Raf (148,149) are both negative regulators of ASK1 and are suggested to limit ASK1-induced caspase-3 activation to prevent apoptosis. ASK2 might also restrict activation of caspase-3 by hetero-oligomerization of ASK1 in proliferating myoblasts.

It remains to be clarified how apoptosis is regulated in proliferating and differentiating myoblasts and also in differentiated myotubes. Since ASK1 and ASK2 differ in the binding to thioredoxins as discussed previously, it is conceivable that a differential dissociation of Trx1 or Trx2 is regulated by e.g. TNF-α or ROS in a dose-dependent manner either leading to differentiation or apoptosis. Interestingly, TNF-α leads faster to oxidation of mitochondrial Trx2 than of cytoplasmic Trx1 (246). Furthermore, in diseased muscle high levels of Bax are expressed while only low levels of the anti-apoptotic proteins Bcl-2 and Bcl-XL are synthesized. In addition to the altered expression of Bcl-2 family members, localized changes Ca^{2+} changes in the cytoplasm can lead to an excess of Ca^{2+} taken up by mitochondria and thereby to cytochrome c release and apoptosis (249). Mechanical stretch-induced Ca^{2+} signaling induces NO (nitric oxide) synthesis, which leads to inducible NO synthase (iNOS) expression (250). Finally, G-protein-coupled receptor agonists (GPCR) such as angitotensin II, endothelin-1, and phenylephrine are implicated in causing hypertrophic effects in cardiomyocytes. Binding of these vasoactive peptides to GPCR increases intracellular Ca^{2+} and ROS. ROS activates ASK1, which then induces p38 MAPK signaling leading to activation of the redox-sensitive transcription factor NFκB (251,252). Interestingly, in HL-5 cardiomyocytes serum withdrawal alone is not sufficient to induce apoptosis and additional ROS triggers cell death (253). In addition, increased apoptosis observed in early differentiating myoblasts might be the consequence of the negative regulation of the proliferative c-Raf-MEK-ERK pathway. This negative regulation could be mediated by the anti-proliferative AKT-Raf crosstalk, which is already described in differentiated myotubes (148) or by downregulation of c-Raf expression with a concomitant upregulation of the dominant-negative c-Raf splice variant DA-Raf1 (254). Caspase-3 cleaves and thereby inactivates AKT1 and AKT2 (255) thus caspase-3 activated during early myogenesis might also promote apoptosis.

Concluding, since several apoptotic features and caspase-3 activity are essential for skeletal muscle differentiation, ASK1 and ASK2 must be tightly regulated to prevent cell death during the differentiation process. Additional pathways including the vasoactive GPCR agonists and intracellular levels of Ca^{2+} and ROS are important mediators of skeletal muscle apoptosis apoptosis.

7. References

1. Vaux, D. L., and Korsmeyer, S. J. (1999) *Cell* **96**(2), 245-254
2. Danial, N. N., and Korsmeyer, S. J. (2004) *Cell* **116**(2), 205-219
3. Kerr, J. F., Wyllie, A. H., and Currie, A. R. (1972) *Br J Cancer* **26**(4), 239-257
4. Wyllie, A. H., Kerr, J. F., and Currie, A. R. (1980) *Int Rev Cytol* **68**, 251-306
5. Frisch, S. M., Vuori, K., Kelaita, D., and Sicks, S. (1996) *J Cell Biol* **135**(5), 1377-1382
6. Ruoslahti, E., and Reed, J. C. (1994) *Cell* **77**(4), 477-478
7. Lavrik, I., Golks, A., and Krammer, P. H. (2005) *J Cell Sci* **118**(Pt 2), 265-267
8. Shiraishi, H., Okamoto, H., Yoshimura, A., and Yoshida, H. (2006) *J Cell Sci*
9. Hengartner, M. O. (2000) *Nature* **407**(6805), 770-776
10. Jimbo, A., Fujita, E., Kouroku, Y., Ohnishi, J., Inohara, N., Kuida, K., Sakamaki, K., Yonehara, S., and Momoi, T. (2003) *Exp Cell Res* **283**(2), 156-166
11. Leist, M., and Jaattela, M. (2001) *Nat Rev Mol Cell Biol* **2**(8), 589-598
12. Ashkenazi, A., and Dixit, V. M. (1998) *Science* **281**(5381), 1305-1308
13. Nagata, S. (1997) *Cell* **88**(3), 355-365
14. Green, D. R. (2005) *Cell* **121**(5), 671-674
15. Czerski, L., and Nunez, G. (2004) *J Mol Cell Cardiol* **37**(3), 643-652
16. Chang, H. Y., and Yang, X. (2000) *Microbiol Mol Biol Rev* **64**(4), 821-846
17. Tschopp, J. M. (2003) *Schweiz Rundsch Med Prax* **92**(34), 1397-1402
18. Wajant, H. (2003) *Essays Biochem* **39**, 53-71
19. Peter, M. E., and Krammer, P. H. (2003) *Cell Death Differ* **10**(1), 26-35
20. Chang, D. W., Xing, Z., Capacio, V. L., Peter, M. E., and Yang, X. (2003) *Embo J* **22**(16), 4132-4142
21. Micheau, O., Thome, M., Schneider, P., Holler, N., Tschopp, J., Nicholson, D. W., Briand, C., and Grutter, M. G. (2002) *J Biol Chem* **277**(47), 45162-45171
22. Yang, X., Khosravi-Far, R., Chang, H. Y., and Baltimore, D. (1997) *Cell* **89**(7), 1067-1076
23. Micheau, O., and Tschopp, J. (2003) *Cell* **114**(2), 181-190
24. Jin, Z., and El-Deiry, W. S. (2006) *Mol Cell Biol*
25. Bhardwaj, A., and Aggarwal, B. B. (2003) *J Clin Immunol* **23**(5), 317-332
26. Karin, M., and Lin, A. (2002) *Nat Immunol* **3**(3), 221-227
27. Gross, A., McDonnell, J. M., and Korsmeyer, S. J. (1999) *Genes Dev* **13**(15), 1899-1911
28. Garrido, C., Galluzzi, L., Brunet, M., Puig, P. E., Didelot, C., and Kroemer, G. (2006) *Cell Death Differ* **13**(9), 1423-1433
29. Li, H., Zhu, H., Xu, C. J., and Yuan, J. (1998) *Cell* **94**(4), 491-501
30. Luo, X., Budihardjo, I., Zou, H., Slaughter, C., and Wang, X. (1998) *Cell* **94**(4), 481-490
31. Ellis, H. M., and Horvitz, H. R. (1986) *Cell* **44**(6), 817-829
32. Cain, K., Bratton, S. B., Langlais, C., Walker, G., Brown, D. G., Sun, X. M., and Cohen, G. M. (2000) *J Biol Chem* **275**(9), 6067-6070
33. Conradt, B., and Horvitz, H. R. (1998) *Cell* **93**(4), 519-529
34. del Peso, L., Gonzalez, V. M., and Nunez, G. (1998) *J Biol Chem* **273**(50), 33495-33500
35. Zou, H., Henzel, W. J., Liu, X., Lutschg, A., and Wang, X. (1997) *Cell* **90**(3), 405-413
36. Yuan, J., Shaham, S., Ledoux, S., Ellis, H. M., and Horvitz, H. R. (1993) *Cell* **75**(4), 641-652
37. Cerretti, D. P., Kozlosky, C. J., Mosley, B., Nelson, N., Van Ness, K., Greenstreet, T. A., March, C. J., Kronheim, S. R., Druck, T., Cannizzaro, L. A., and et al. (1992) *Science* **256**(5053), 97-100
38. Green, D. R. (1998) *Cell* **94**(6), 695-698
39. Strasser, A., O'Connor, L., and Dixit, V. M. (2000) *Annu Rev Biochem* **69**, 217-245
40. Deveraux, Q. L., Takahashi, R., Salvesen, G. S., and Reed, J. C. (1997) *Nature* **388**(6639), 300-304
41. Du, C., Fang, M., Li, Y., Li, L., and Wang, X. (2000) *Cell* **102**(1), 33-42

42. Fernando, P., Kelly, J. F., Balazsi, K., Slack, R. S., and Megeney, L. A. (2002) *Proc Natl Acad Sci U S A* **99**(17), 11025-11030
43. Weil, M., Raff, M. C., and Braga, V. M. (1999) *Curr Biol* **9**(7), 361-364
44. Zermati, Y., Garrido, C., Amsellem, S., Fishelson, S., Bouscary, D., Valensi, F., Varet, B., Solary, E., and Hermine, O. (2001) *J Exp Med* **193**(2), 247-254
45. Kuwana, T., and Newmeyer, D. D. (2003) *Curr Opin Cell Biol* **15**(6), 691-699
46. Zamzami, N., Larochette, N., and Kroemer, G. (2005) *Cell Death Differ* **12 Suppl 2**, 1478-1480
47. Chipuk, J. E., Bouchier-Hayes, L., and Green, D. R. (2006) *Cell Death Differ* **13**(8), 1396-1402
48. Blume-Jensen, P., Janknecht, R., and Hunter, T. (1998) *Curr Biol* **8**(13), 779-782
49. Datta, S. R., Dudek, H., Tao, X., Masters, S., Fu, H., Gotoh, Y., and Greenberg, M. E. (1997) *Cell* **91**(2), 231-241
50. del Peso, L., Gonzalez-Garcia, M., Page, C., Herrera, R., and Nunez, G. (1997) *Science* **278**(5338), 687-689
51. Harada, H., Becknell, B., Wilm, M., Mann, M., Huang, L. J., Taylor, S. S., Scott, J. D., and Korsmeyer, S. J. (1999) *Mol Cell* **3**(4), 413-422
52. Haupt, S., Berger, M., Goldberg, Z., and Haupt, Y. (2003) *J Cell Sci* **116**(Pt 20), 4077-4085
53. Schaeffer, H. J., and Weber, M. J. (1999) *Mol Cell Biol* **19**(4), 2435-2444
54. Widmann, C., Gibson, S., Jarpe, M. B., and Johnson, G. L. (1999) *Physiol Rev* **79**(1), 143-180
55. Kyriakis, J. M., and Avruch, J. (1996) *J Biol Chem* **271**(40), 24313-24316
56. Waskiewicz, A. J., and Cooper, J. A. (1995) *Curr Opin Cell Biol* **7**(6), 798-805
57. Ichijo, H. (1999) *Oncogene* **18**(45), 6087-6093
58. Woodgett, J. R., Avruch, J., and Kyriakis, J. (1996) *Cancer Surv* **27**, 127-138
59. Gupta, S., Barrett, T., Whitmarsh, A. J., Cavanagh, J., Sluss, H. K., Derijard, B., and Davis, R. J. (1996) *Embo J* **15**(11), 2760-2770
60. Fuchs, S. Y., Adler, V., Buschmann, T., Yin, Z., Wu, X., Jones, S. N., and Ronai, Z. (1998) *Genes Dev* **12**(17), 2658-2663
61. Fuchs, S. Y., Adler, V., Pincus, M. R., and Ronai, Z. (1998) *Proc Natl Acad Sci U S A* **95**(18), 10541-10546
62. Cao, J., Semenova, M. M., Solovyan, V. T., Han, J., Coffey, E. T., and Courtney, M. J. (2004) *J Biol Chem* **279**(34), 35903-35913
63. Finkel, T. (2000) *FEBS Lett* **476**(1-2), 52-54
64. Rahaus, M., Desloges, N., and Wolff, M. H. (2004) *J Gen Virol* **85**(Pt 12), 3529-3540
65. Kagan, V. E., Borisenko, G. G., Tyurina, Y. Y., Tyurin, V. A., Jiang, J., Potapovich, A. I., Kini, V., Amoscato, A. A., and Fujii, Y. (2004) *Free Radic Biol Med* **37**(12), 1963-1985
66. Kharbanda, S., Saxena, S., Yoshida, K., Pandey, P., Kaneki, M., Wang, Q., Cheng, K., Chen, Y. N., Campbell, A., Sudha, T., Yuan, Z. M., Narula, J., Weichselbaum, R., Nalin, C., and Kufe, D. (2000) *J Biol Chem* **275**(1), 322-327
67. Davis, R. J. (2000) *Cell* **103**(2), 239-252
68. Whitmarsh, A. J., Cavanagh, J., Tournier, C., Yasuda, J., and Davis, R. J. (1998) *Science* **281**(5383), 1671-1674
69. Yasuda, J., Whitmarsh, A. J., Cavanagh, J., Sharma, M., and Davis, R. J. (1999) *Mol Cell Biol* **19**(10), 7245-7254
70. Kelkar, N., Gupta, S., Dickens, M., and Davis, R. J. (2000) *Mol Cell Biol* **20**(3), 1030-1043
71. Le-Niculescu, H., Bonfoco, E., Kasuya, Y., Claret, F. X., Green, D. R., and Karin, M. (1999) *Mol Cell Biol* **19**(1), 751-763
72. Xia, Z., Dickens, M., Raingeaud, J., Davis, R. J., and Greenberg, M. E. (1995) *Science* **270**(5240), 1326-1331
73. Sakata, N., Patel, H. R., Terada, N., Aruffo, A., Johnson, G. L., and Gelfand, E. W. (1995) *J Biol Chem* **270**(51), 30823-30828
74. Amura, C. R., Marek, L., Winn, R. A., and Heasley, L. E. (2005) *Mol Cell Biol* **25**(24), 10791-10802

75. Zhang, S., Liu, H., Liu, J., Tse, C. A., Dragunow, M., and Cooper, G. J. (2006) *Febs J* **273**(16), 3779-3791
76. Sarker, K. P., Biswas, K. K., Yamakuchi, M., Lee, K. Y., Hahiguchi, T., Kracht, M., Kitajima, I., and Maruyama, I. (2003) *J Neurochem* **85**(1), 50-61
77. Takeda, K., Hatai, T., Hamazaki, T. S., Nishitoh, H., Saitoh, M., and Ichijo, H. (2000) *J Biol Chem* **275**(13), 9805-9813
78. Soh, J. W., Mao, Y., Liu, L., Thompson, W. J., Pamukcu, R., and Weinstein, I. B. (2001) *J Biol Chem* **276**(19), 16406-16410
79. Yan, M., Dai, T., Deak, J. C., Kyriakis, J. M., Zon, L. I., Woodgett, J. R., and Templeton, D. J. (1994) *Nature* **372**(6508), 798-800
80. Guan, Z., Buckman, S. Y., Pentland, A. P., Templeton, D. J., and Morrison, A. R. (1998) *J Biol Chem* **273**(21), 12901-12908
81. Lange-Carter, C. A., Pleiman, C. M., Gardner, A. M., Blumer, K. J., and Johnson, G. L. (1993) *Science* **260**(5106), 315-319
82. Deacon, K., and Blank, J. L. (1997) *J Biol Chem* **272**(22), 14489-14496
83. Blank, J. L., Gerwins, P., Elliott, E. M., Sather, S., and Johnson, G. L. (1996) *J Biol Chem* **271**(10), 5361-5368
84. Deacon, K., and Blank, J. L. (1999) *J Biol Chem* **274**(23), 16604-16610
85. Gerwins, P., Blank, J. L., and Johnson, G. L. (1997) *J Biol Chem* **272**(13), 8288-8295
86. Takekawa, M., and Saito, H. (1998) *Cell* **95**(4), 521-530
87. Chi, H., Lu, B., Takekawa, M., Davis, R. J., and Flavell, R. A. (2004) *Embo J* **23**(7), 1576-1586
88. Chi, H., Sarkisian, M. R., Rakic, P., and Flavell, R. A. (2005) *Proc Natl Acad Sci U S A* **102**(10), 3846-3851
89. Ichijo, H., Nishida, E., Irie, K., ten Dijke, P., Saitoh, M., Moriguchi, T., Takagi, M., Matsumoto, K., Miyazono, K., and Gotoh, Y. (1997) *Science* **275**(5296), 90-94
90. Wang, X. S., Diener, K., Jannuzzi, D., Trollinger, D., Tan, T. H., Lichenstein, H., Zukowski, M., and Yao, Z. (1996) *J Biol Chem* **271**(49), 31607-31611
91. Wang, X. S., Diener, K., Tan, T. H., and Yao, Z. (1998) *Biochem Biophys Res Commun* **253**(1), 33-37
92. Yamaguchi, K., Shirakabe, K., Shibuya, H., Irie, K., Oishi, I., Ueno, N., Taniguchi, T., Nishida, E., and Matsumoto, K. (1995) *Science* **270**(5244), 2008-2011
93. Shirakabe, K., Yamaguchi, K., Shibuya, H., Irie, K., Matsuda, S., Moriguchi, T., Gotoh, Y., Matsumoto, K., and Nishida, E. (1997) *J Biol Chem* **272**(13), 8141-8144
94. Moriguchi, T., Kuroyanagi, N., Yamaguchi, K., Gotoh, Y., Irie, K., Kano, T., Shirakabe, K., Muro, Y., Shibuya, H., Matsumoto, K., Nishida, E., and Hagiwara, M. (1996) *J Biol Chem* **271**(23), 13675-13679
95. Aoki, M., Akiyama, T., Miyoshi, J., and Toyoshima, K. (1991) *Oncogene* **6**(9), 1515-1519
96. Salmeron, A., Ahmad, T. B., Carlile, G. W., Pappin, D., Narsimhan, R. P., and Ley, S. C. (1996) *Embo J* **15**(4), 817-826
97. Hagemann, D., Troppmair, J., and Rapp, U. R. (1999) *Oncogene* **18**(7), 1391-1400
98. Chiariello, M., Marinissen, M. J., and Gutkind, J. S. (2000) *Mol Cell Biol* **20**(5), 1747-1758
99. Patriotis, C., Makris, A., Chernoff, J., and Tsichlis, P. N. (1994) *Proc Natl Acad Sci U S A* **91**(21), 9755-9759
100. Dorow, D. S., Devereux, L., Dietzsch, E., and De Kretser, T. (1993) *Eur J Biochem* **213**(2), 701-710
101. Hirai, S., Katoh, M., Terada, M., Kyriakis, J. M., Zon, L. I., Rana, A., Avruch, J., and Ohno, S. (1997) *J Biol Chem* **272**(24), 15167-15173
102. Nagata, K., Puls, A., Futter, C., Aspenstrom, P., Schaefer, E., Nakata, T., Hirokawa, N., and Hall, A. (1998) *Embo J* **17**(1), 149-158
103. Ing, Y. L., Leung, I. W., Heng, H. H., Tsui, L. C., and Lassam, N. J. (1994) *Oncogene* **9**(6), 1745-1750
104. Gallo, K. A., Mark, M. R., Scadden, D. T., Wang, Z., Gu, Q., and Godowski, P. J. (1994) *J Biol Chem* **269**(21), 15092-15100

105. Rana, A., Gallo, K., Godowski, P., Hirai, S., Ohno, S., Zon, L., Kyriakis, J. M., and Avruch, J. (1996) *J Biol Chem* **271**(32), 19025-19028
106. Kim, K. Y., Kim, B. C., Xu, Z., and Kim, S. J. (2004) *J Biol Chem* **279**(28), 29478-29484
107. Fan, G., Merritt, S. E., Kortenjann, M., Shaw, P. E., and Holzman, L. B. (1996) *J Biol Chem* **271**(40), 24788-24793
108. Hirai, S., Kawaguchi, A., Suenaga, J., Ono, M., Cui, D. F., and Ohno, S. (2005) *Gene Expr Patterns* **5**(4), 517-523
109. Holzman, L. B., Merritt, S. E., and Fan, G. (1994) *J Biol Chem* **269**(49), 30808-30817
110. Reddy, U. R., and Pleasure, D. (1994) *Biochem Biophys Res Commun* **202**(1), 613-620
111. Ikeda, A., Hasegawa, K., Masaki, M., Moriguchi, T., Nishida, E., Kozutsumi, Y., Oka, S., and Kawasaki, T. (2001) *J Biochem (Tokyo)* **130**(6), 773-781
112. Ikeda, A., Masaki, M., Kozutsumi, Y., Oka, S., and Kawasaki, T. (2001) *FEBS Lett* **488**(3), 190-195
113. Sakuma, H., Ikeda, A., Oka, S., Kozutsumi, Y., Zanetta, J. P., and Kawasaki, T. (1997) *J Biol Chem* **272**(45), 28622-28629
114. Bloem, L. J., Pickard, T. R., Acton, S., Donoghue, M., Beavis, R. C., Knierman, M. D., and Wang, X. (2001) *J Mol Cell Cardiol* **33**(9), 1739-1750
115. Gotoh, I., Adachi, M., and Nishida, E. (2001) *J Biol Chem* **276**(6), 4276-4286
116. Gross, E. A., Callow, M. G., Waldbaum, L., Thomas, S., and Ruggieri, R. (2002) *J Biol Chem* **277**(16), 13873-13882
117. Chen, Y., Cai, J., Murphy, T. J., and Jones, D. P. (2002) *J Biol Chem* **277**(36), 33242-33248
118. Powis, G., Mustacich, D., and Coon, A. (2000) *Free Radic Biol Med* **29**(3-4), 312-322
119. Liu, Y., Yin, G., Surapisitchat, J., Berk, B. C., and Min, W. (2001) *J Clin Invest* **107**(7), 917-923
120. Sayama, K., Hanakawa, Y., Shirakata, Y., Yamasaki, K., Sawada, Y., Sun, L., Yamanishi, K., Ichijo, H., and Hashimoto, K. (2001) *J Biol Chem* **276**(2), 999-1004
121. Patenaude, A., Ven Murthy, M. R., and Mirault, M. E. (2004) *J Biol Chem* **279**(26), 27302-27314
122. Spyrou, G., Enmark, E., Miranda-Vizuete, A., and Gustafsson, J. (1997) *J Biol Chem* **272**(5), 2936-2941
123. Holmgren, A. (1985) *Annu Rev Biochem* **54**, 237-271
124. Holmgren, A. (1989) *J Biol Chem* **264**(24), 13963-13966
125. Gendron, M. C., Schrantz, N., Metivier, D., Kroemer, G., Maciorowska, Z., Sureau, F., Koester, S., and Petit, P. X. (2001) *Biochem J* **353**(Pt 2), 357-367
126. Macho, A., Hirsch, T., Marzo, I., Marchetti, P., Dallaporta, B., Susin, S. A., Zamzami, N., and Kroemer, G. (1997) *J Immunol* **158**(10), 4612-4619
127. Nieminen, A. L., Byrne, A. M., Herman, B., and Lemasters, J. J. (1997) *Am J Physiol* **272**(4 Pt 1), C1286-1294
128. Zamzami, N., Marchetti, P., Castedo, M., Decaudin, D., Macho, A., Hirsch, T., Susin, S. A., Petit, P. X., Mignotte, B., and Kroemer, G. (1995) *J Exp Med* **182**(2), 367-377
129. Tanaka, T., Hosoi, F., Yamaguchi-Iwai, Y., Nakamura, H., Masutani, H., Ueda, S., Nishiyama, A., Takeda, S., Wada, H., Spyrou, G., and Yodoi, J. (2002) *Embo J* **21**(7), 1695-1703
130. Bannister, A. J., Cook, A., and Kouzarides, T. (1991) *Oncogene* **6**(7), 1243-1250
131. Cromlish, J. A., and Roeder, R. G. (1989) *J Biol Chem* **264**(30), 18100-18109
132. Lundstrom, J., and Holmgren, A. (1990) *J Biol Chem* **265**(16), 9114-9120
133. Thelander, L., and Reichard, P. (1979) *Annu Rev Biochem* **48**, 133-158
134. Zhang, R., Al-Lamki, R., Bai, L., Streb, J. W., Miano, J. M., Bradley, J., and Min, W. (2004) *Circ Res* **94**(11), 1483-1491
135. Liu, Y., and Min, W. (2002) *Circ Res* **90**(12), 1259-1266
136. Saitoh, M., Nishitoh, H., Fujii, M., Takeda, K., Tobiume, K., Sawada, Y., Kawabata, M., Miyazono, K., and Ichijo, H. (1998) *Embo J* **17**(9), 2596-2606
137. Kyriakis, J. M., and Avruch, J. (2001) *Physiol Rev* **81**(2), 807-869
138. Qi, M., and Elion, E. A. (2005) *J Cell Sci* **118**(Pt 16), 3569-3572

139. Burack, W. R., and Shaw, A. S. (2000) *Curr Opin Cell Biol* **12**(2), 211-216
140. Yao, Z., Zhou, G., Wang, X. S., Brown, A., Diener, K., Gan, H., and Tan, T. H. (1999) *J Biol Chem* **274**(4), 2118-2125
141. Hanada, M., Feng, J., and Hemmings, B. A. (2004) *Biochim Biophys Acta* **1697**(1-2), 3-16
142. Jacinto, E., Facchinetti, V., Liu, D., Soto, N., Wei, S., Jung, S. Y., Huang, Q., Qin, J., and Su, B. (2006) *Cell* **127**(1), 125-137
143. Lawlor, M. A., and Alessi, D. R. (2001) *J Cell Sci* **114**(Pt 16), 2903-2910
144. Kandel, E. S., and Hay, N. (1999) *Exp Cell Res* **253**(1), 210-229
145. Barthwal, M. K., Sathyanarayana, P., Kundu, C. N., Rana, B., Pradeep, A., Sharma, C., Woodgett, J. R., and Rana, A. (2003) *J Biol Chem* **278**(6), 3897-3902
146. Kim, A. H., Khursigara, G., Sun, X., Franke, T. F., and Chao, M. V. (2001) *Mol Cell Biol* **21**(3), 893-901
147. Gratton, J. P., Morales-Ruiz, M., Kureishi, Y., Fulton, D., Walsh, K., and Sessa, W. C. (2001) *J Biol Chem* **276**(32), 30359-30365
148. Rommel, C., Clarke, B. A., Zimmermann, S., Nunez, L., Rossman, R., Reid, K., Moelling, K., Yancopoulos, G. D., and Glass, D. J. (1999) *Science* **286**(5445), 1738-1741
149. Zimmermann, S., and Moelling, K. (1999) *Science* **286**(5445), 1741-1744
150. Guan, K. L., Figueroa, C., Brtva, T. R., Zhu, T., Taylor, J., Barber, T. D., and Vojtek, A. B. (2000) *J Biol Chem* **275**(35), 27354-27359
151. Kane, L. P., Mollenauer, M. N., Xu, Z., Turck, C. W., and Weiss, A. (2002) *Mol Cell Biol* **22**(16), 5962-5974
152. Gotoh, Y., and Cooper, J. A. (1998) *J Biol Chem* **273**(28), 17477-17482
153. Hatai, T., Matsuzawa, A., Inoshita, S., Mochida, Y., Kuroda, T., Sakamaki, K., Kuida, K., Yonehara, S., Ichijo, H., and Takeda, K. (2000) *J Biol Chem* **275**(34), 26576-26581
154. Sumbayev, V. V., and Yasinska, I. M. (2005) *Arch Biochem Biophys* **436**(2), 406-412
155. Tobiume, K., Matsuzawa, A., Takahashi, T., Nishitoh, H., Morita, K., Takeda, K., Minowa, O., Miyazono, K., Noda, T., and Ichijo, H. (2001) *EMBO Rep* **2**(3), 222-228
156. Dasgupta, P., Betts, V., Rastogi, S., Joshi, B., Morris, M., Brennan, B., Ordonez-Ercan, D., and Chellappan, S. (2004) *J Biol Chem* **279**(37), 38762-38769
157. Charette, S. J., Lambert, H., and Landry, J. (2001) *J Biol Chem* **276**(39), 36071-36074
158. Tobiume, K., Saitoh, M., and Ichijo, H. (2002) *J Cell Physiol* **191**(1), 95-104
159. Noguchi, T., Takeda, K., Matsuzawa, A., Saegusa, K., Nakano, H., Gohda, J., Inoue, J., and Ichijo, H. (2005) *J Biol Chem* **280**(44), 37033-37040
160. Goldman, E. H., Chen, L., and Fu, H. (2004) *J Biol Chem* **279**(11), 10442-10449
161. Zhang, L., Chen, J., and Fu, H. (1999) *Proc Natl Acad Sci U S A* **96**(15), 8511-8515
162. Morita, K., Saitoh, M., Tobiume, K., Matsuura, H., Enomoto, S., Nishitoh, H., and Ichijo, H. (2001) *Embo J* **20**(21), 6028-6036
163. Huang, S., Shu, L., Easton, J., Harwood, F. C., Germain, G. S., Ichijo, H., and Houghton, P. J. (2004) *J Biol Chem* **279**(35), 36490-36496
164. Song, J. J., Rhee, J. G., Suntharalingam, M., Walsh, S. A., Spitz, D. R., and Lee, Y. J. (2002) *J Biol Chem* **277**(48), 46566-46575
165. Song, J. J., and Lee, Y. J. (2003) *Biochem J* **373**(Pt 3), 845-853
166. Park, H. S., Cho, S. G., Kim, C. K., Hwang, H. S., Noh, K. T., Kim, M. S., Huh, S. H., Kim, M. J., Ryoo, K., Kim, E. K., Kang, W. J., Lee, J. S., Seo, J. S., Ko, Y. G., Kim, S., and Choi, E. J. (2002) *Mol Cell Biol* **22**(22), 7721-7730
167. Chen, J., Fujii, K., Zhang, L., Roberts, T., and Fu, H. (2001) *Proc Natl Acad Sci U S A* **98**(14), 7783-7788
168. Zou, X., Tsutsui, T., Ray, D., Blomquist, J. F., Ichijo, H., Ucker, D. S., and Kiyokawa, H. (2001) *Mol Cell Biol* **21**(14), 4818-4828
169. Nevins, J. R. (2001) *Hum Mol Genet* **10**(7), 699-703
170. Galvan, V., Logvinova, A., Sperandio, S., Ichijo, H., and Bredesen, D. E. (2003) *J Biol Chem* **278**(15), 13325-13332
171. Zhang, R., He, X., Liu, W., Lu, M., Hsieh, J. T., and Min, W. (2003) *J Clin Invest* **111**(12), 1933-1943

172. Faigle, R., Brederlau, A., Elmi, M., Arvidsson, Y., Hamazaki, T. S., Uramoto, H., and Funa, K. (2004) *Mol Cell Biol* **24**(1), 280-293
173. Rubiolo, C., Piazzolla, D., Meissl, K., Beug, H., Huber, J. C., Kolbus, A., and Baccarini, M. (2006) *Blood* **108**(1), 152-159
174. Wellbrock, C., Karasarides, M., and Marais, R. (2004) *Nat Rev Mol Cell Biol* **5**(11), 875-885
175. Storm, S. M., Cleveland, J. L., and Rapp, U. R. (1990) *Oncogene* **5**(3), 345-351
176. Garnett, M. J., and Marais, R. (2004) *Cancer Cell* **6**(4), 313-319
177. Tzivion, G., Luo, Z., and Avruch, J. (1998) *Nature* **394**(6688), 88-92
178. Kubicek, M., Pacher, M., Abraham, D., Podar, K., Eulitz, M., and Baccarini, M. (2002) *J Biol Chem* **277**(10), 7913-7919
179. O'Neill, E., and Kolch, W. (2004) *Br J Cancer* **90**(2), 283-288
180. Marais, R., Light, Y., Paterson, H. F., Mason, C. S., and Marshall, C. J. (1997) *J Biol Chem* **272**(7), 4378-4383
181. Mason, C. S., Springer, C. J., Cooper, R. G., Superti-Furga, G., Marshall, C. J., and Marais, R. (1999) *Embo J* **18**(8), 2137-2148
182. York, R. D., Yao, H., Dillon, T., Ellig, C. L., Eckert, S. P., McCleskey, E. W., and Stork, P. J. (1998) *Nature* **392**(6676), 622-626
183. Dumaz, N., and Marais, R. (2003) *J Biol Chem* **278**(32), 29819-29823
184. Schramm, K., Niehof, M., Radziwill, G., Rommel, C., and Moelling, K. (1994) *Biochem Biophys Res Commun* **201**(2), 740-747
185. O'Neill, E., Rushworth, L., Baccarini, M., and Kolch, W. (2004) *Science* **306**(5705), 2267-2270
186. Ehrenreiter, K., Piazzolla, D., Velamoor, V., Sobczak, I., Small, J. V., Takeda, J., Leung, T., and Baccarini, M. (2005) *J Cell Biol* **168**(6), 955-964
187. Molkentin, J. D., and Olson, E. N. (1996) *Curr Opin Genet Dev* **6**(4), 445-453
188. Yun, K., and Wold, B. (1996) *Curr Opin Cell Biol* **8**(6), 877-889
189. Borycki, A. G., and Emerson, C. P. (1997) *Curr Biol* **7**(10), R620-623
190. Sabourin, L. A., and Rudnicki, M. A. (2000) *Clin Genet* **57**(1), 16-25
191. Blau, H. M., Pavlath, G. K., Hardeman, E. C., Chiu, C. P., Silberstein, L., Webster, S. G., Miller, S. C., and Webster, C. (1985) *Science* **230**(4727), 758-766
192. Florini, J. R., Ewton, D. Z., and Roof, S. L. (1991) *Mol Endocrinol* **5**(5), 718-724
193. Florini, J. R., Magri, K. A., Ewton, D. Z., James, P. L., Grindstaff, K., and Rotwein, P. S. (1991) *J Biol Chem* **266**(24), 15917-15923
194. Virkamaki, A., Ueki, K., and Kahn, C. R. (1999) *J Clin Invest* **103**(7), 931-943
195. Takeda, K., Shimozono, R., Noguchi, T., Umeda, T., Morimoto, Y., Naguro, I., Tobiume, K., Saitoh, M., Matsuzawa, A., and Ichijo, H. (2007) *J Biol Chem* **282**(10), 7522-7531
196. Fire, A., Xu, S., Montgomery, M. K., Kostas, S. A., Driver, S. E., and Mello, C. C. (1998) *Nature* **391**(6669), 806-811
197. Meister, G., and Tuschl, T. (2004) *Nature* **431**(7006), 343-349
198. Moffat, J., and Sabatini, D. M. (2006) *Nat Rev Mol Cell Biol* **7**(3), 177-187
199. Fritz, J. H., Girardin, S. E., and Philpott, D. J. (2006) *Sci STKE* **2006**(339), pe27
200. Hannon, G. J. (2002) *Nature* **418**(6894), 244-251
201. He, L., and Hannon, G. J. (2004) *Nat Rev Genet* **5**(7), 522-531
202. Filipowicz, W. (2005) *Cell* **122**(1), 17-20
203. Matzke, M. A., and Birchler, J. A. (2005) *Nat Rev Genet* **6**(1), 24-35
204. Shi, Y. (2003) *Trends Genet* **19**(1), 9-12
205. Bogenhagen, D. F., Sakonju, S., and Brown, D. D. (1980) *Cell* **19**(1), 27-35
206. Pasquinelli, A. E., and Ruvkun, G. (2002) *Annu Rev Cell Dev Biol* **18**, 495-513
207. Jakymiw, A., Pauley, K. M., Li, S., Ikeda, K., Lian, S., Eystathioy, T., Satoh, M., Fritzler, M. J., and Chan, E. K. (2007) *J Cell Sci* **120**(Pt 8), 1317-1323
208. Berghammer, H., and Auer, B. (1993) *Biotechniques* **14**(4), 524, 528
209. Gschwind, A., Hart, S., Fischer, O. M., and Ullrich, A. (2003) *Embo J* **22**(10), 2411-2421
210. Lois, C., Hong, E. J., Pease, S., Brown, E. J., and Baltimore, D. (2002) *Science* **295**(5556), 868-872

211. Naldini, L., Blomer, U., Gallay, P., Ory, D., Mulligan, R., Gage, F. H., Verma, I. M., and Trono, D. (1996) *Science* **272**(5259), 263-267
212. Tokunaga, K., Taniguchi, H., Yoda, K., Shimizu, M., and Sakiyama, S. (1986) *Nucleic Acids Res* **14**(6), 2829
213. Radziwill, G., Erdmann, R. A., Margelisch, U., and Moelling, K. (2003) *Mol Cell Biol* **23**(13), 4663-4672
214. Elzaouk, L., Laufs, S., Heerklotz, D., Leimbacher, W., Blau, N., Resibois, A., and Thony, B. (2004) *Biochim Biophys Acta* **1670**(1), 56-68
215. Ouyang, M., and Shen, X. (2006) *J Neurochem* **97**(1), 234-244
216. Light, Y., Paterson, H., and Marais, R. (2002) *Mol Cell Biol* **22**(14), 4984-4996
217. Corpet, F. (1988) *Nucleic Acids Res* **16**(22), 10881-10890
218. Barnett, S. F., Defeo-Jones, D., Fu, S., Hancock, P. J., Haskell, K. M., Jones, R. E., Kahana, J. A., Kral, A. M., Leander, K., Lee, L. L., Malinowski, J., McAvoy, E. M., Nahas, D. D., Robinson, R. G., and Huber, H. E. (2005) *Biochem J* **385**(Pt 2), 399-408
219. Vlahos, C. J., Matter, W. F., Hui, K. Y., and Brown, R. F. (1994) *J Biol Chem* **269**(7), 5241-5248
220. Yaffe, D., and Saxel, O. (1977) *Differentiation* **7**(3), 159-166
221. Park, I. H., Erbay, E., Nuzzi, P., and Chen, J. (2005) *Exp Cell Res* **309**(1), 211-219
222. Jacobson, M. D., Weil, M., and Raff, M. C. (1997) *Cell* **88**(3), 347-354
223. Rich, T., Watson, C. J., and Wyllie, A. (1999) *Nat Cell Biol* **1**(3), E69-71
224. Lee, S. B., Cho, E. S., Yang, H. S., Kim, H., and Um, H. D. (2005) *Cell Signal* **17**(2), 197-204
225. Satoh, T., Sakai, N., Enokido, Y., Uchiyama, Y., and Hatanaka, H. (1996) *Brain Res* **733**(1), 9-14
226. Lee, S. B., Bae, I. H., Bae, Y. S., and Um, H. D. (2006) *J Biol Chem* **281**(47), 36228-36235
227. Caricchio, R., D'Adamio, L., and Cohen, P. L. (2002) *Cell Death Differ* **9**(5), 574-580
228. Hannun, Y. A. (1996) *Science* **274**(5294), 1855-1859
229. Mathias, S., Pena, L. A., and Kolesnick, R. N. (1998) *Biochem J* **335 (Pt 3)**, 465-480
230. Aitken, A. (2006) *Semin Cancer Biol* **16**(3), 162-172
231. Rushworth, L. K., Hindley, A. D., O'Neill, E., and Kolch, W. (2006) *Mol Cell Biol* **26**(6), 2262-2272
232. Powis, G., and Montfort, W. R. (2001) *Annu Rev Biophys Biomol Struct* **30**, 421-455
233. Jaumot, M., and Hancock, J. F. (2001) *Oncogene* **20**(30), 3949-3958
234. Alavi, A., Hood, J. D., Frausto, R., Stupack, D. G., and Cheresh, D. A. (2003) *Science* **301**(5629), 94-96
235. Alavi, A. S., Acevedo, L., Min, W., and Cheresh, D. A. (2007) *Cancer Res* **67**(6), 2766-2772
236. Goetz, C. A., O'Neil, J. J., and Farrar, M. A. (2003) *J Biol Chem* **278**(51), 51184-51189
237. Ishizaki, Y., Jacobson, M. D., and Raff, M. C. (1998) *J Cell Biol* **140**(1), 153-158
238. Buendia, B., Santa-Maria, A., and Courvalin, J. C. (1999) *J Cell Sci* **112 (Pt 11)**, 1743-1753
239. Nakanishi, K., Sudo, T., and Morishima, N. (2005) *J Cell Biol* **169**(4), 555-560
240. Fujio, Y., Guo, K., Mano, T., Mitsuuchi, Y., Testa, J. R., and Walsh, K. (1999) *Mol Cell Biol* **19**(7), 5073-5082
241. Rosen, K. M., Wentworth, B. M., Rosenthal, N., and Villa-Komaroff, L. (1993) *Endocrinology* **133**(2), 474-481
242. Stewart, C. E., and Rotwein, P. (1996) *J Biol Chem* **271**(19), 11330-11338
243. Chen, S. E., Jin, B., and Li, Y. P. (2006) *Am J Physiol Cell Physiol*
244. Keren, A., Tamir, Y., and Bengal, E. (2006) *Mol Cell Endocrinol* **252**(1-2), 224-230
245. Li, Y. P., and Schwartz, R. J. (2001) *Faseb J* **15**(8), 1413-1415
246. Hansen, J. M., Zhang, H., and Jones, D. P. (2006) *Toxicol Sci* **91**(2), 643-650
247. Cuenda, A., and Cohen, P. (1999) *J Biol Chem* **274**(7), 4341-4346
248. Lechner, C., Zahalka, M. A., Giot, J. F., Moller, N. P., and Ullrich, A. (1996) *Proc Natl Acad Sci U S A* **93**(9), 4355-4359
249. Sandri, M. (2002) *Curr Opin Clin Nutr Metab Care* **5**(3), 249-253

250. Liao, X., Liu, J. M., Du, L., Tang, A., Shang, Y., Wang, S. Q., Chen, L. Y., and Chen, Q. (2006) *Faseb J* **20**(11), 1883-1885
251. Force, T., Haq, S., Kilter, H., and Michael, A. (2002) *Circulation* **105**(4), 402-404
252. Hirotani, S., Otsu, K., Nishida, K., Higuchi, Y., Morita, T., Nakayama, H., Yamaguchi, O., Mano, T., Matsumura, Y., Ueno, H., Tada, M., and Hori, M. (2002) *Circulation* **105**(4), 509-515
253. Cicconi, S., Ventura, N., Pastore, D., Bonini, P., Di Nardo, P., Lauro, R., and Marlier, L. N. (2003) *J Cell Physiol* **195**(1), 27-37
254. Yokoyama, T., Takano, K., Yoshida, A., Katada, F., Sun, P., Takenawa, T., Andoh, T., and Endo, T. (2007) *J Cell Biol* **177**(5), 781-793
255. Jahani-Asl, A., Basak, A., and Tsang, B. K. (2007) *FEBS Lett*

8. Appendix

8.1. Abbreviations

AGC	PKA, PKB and PKC related kinase family
AIP	ASK1-interacting protein
AKT	AKR mouse transforming retrovirus
AP-1	Activator protein-1
Apaf-1	Apoptosis protease-activating factor-1
ASK1/2	Apoptosis signal-regulating kinase 1/2
BAD	Bcl-2/Bcl-X antagonist
Bak	Bcl-2 antagonist killer
Bax	Bcl-2 associated X-protein
Bcl-2	B-cell leukemia 2
Bcl-XL	Bcl-2 related protein long isoform
Bid	BH3 interacting death domain
BH	Bcl-2 homology domain
bHLH	Basic helix-loop-helix transcription factor
cAMP	Cyclic adenosine monophosphate
CARD	Caspase activating and recruiting domain
CED	Cell death deffective
CHX	Cycloheximide
CNK	Connector enhancer of KSR
CR	Conserved region
CRD	Cysteine rich domain
DED	Death effector domain
DISC	Death-inducing signaling complex
DLK	Dual-leucine zipper-bearing kinase
DR	Death receptor
dsRBD	Double-stranded RNA-binding domain
DUF	Domain of unknown function
EGF	Epidermal growth factor
ER	Endoplasmic reticulum
ERK	Extracellular signal-regulated kinase
FADD	Fas-associated death domain containing protein
FasL	Fas ligand
FLIP	FLICE inhibitory protein
GPCR	G-protein-coupled receptor agonists
GRX	Glutharedoxin
GST	Gluthation-S-transferase
HEK293	Human embryonic kidney cells 293
HM	Hydrophobic motif
Hsp	Heat shock protein
IAP	Inhibitor of apoptosis
ICE	Interleukin-1β converting enzyme
IGF-I	Insulin-like growth factor-I

IGF-IR	IGF-I receptor
JNK	c-Jun NH2-terminal Kinase
MAPK	Mitogen-activated protein kinase
MAPKKK	Mitogen-activated protein kinase kinase kinase
MEF2	Myocyte enhancer factor 2
MEK	Mitogen/extracellular signal-regulated kinase
miRNA	micro RNA
MLK	Mixed lineage kinase
MnSOD	Manganese superoxide dismutase
MOMP	Mitochondrial outer membrane permeabilization
mPT	Mitochondrial permeability transition pore
mTOR	mammalian target of rapamycin
MRF	muscle regulatorx factors
MST	Mammalian sterile 20-like kinase
NADPH	Nicotinamide adenine dinucleotide phosphate hydrogen
NFkB	Nuclear factor kappa B
NGF	Nerve growth factor
NO	Nitric oxide
PAK	p21-activated kinase
PCD	Programmed cell death
PDGF	Platelet-derived growth factor
PDK	Phosphoinositide-dependend kinase
PH	Pleckstrin homology domain
PI3K	Phosphatidylinositol-3'-kinase
PIP_2	Phosphatidyl inositol-4,5-bisphosphate
PIP_3	Phosphatidyl inositol-3,4,5-trisphosphate
PKA	cAMP-dependent protein kinase
PKB	Protein kinase B (= AKT)
PKC	Protein kinase C
PP5	Protein phosphatase 5
PARP	Poly (ADP-ribose) polymerase
Raf	Rapid fibrosarcoma
Ras	Rat sarcoma virus oncogene 1
RIP	Receptor-interacting protein
RISC	RNA-induced silencing complex
RBD	Ras binding domain
RNAi	RNA interference
ROS	Reactive oxygen species
SAPK	Stress-activated protein kinase
SDS-PAGE	Sodiumdodecylsulfate-polyacrylamide gel electrophoresis
siRNA	small interfering RNA
shRNA	Short hairpin RNA
TNF-a	Tumor necrosis factor-α
TNFR	TNF-α receptor
TRADD	TNFR-associated death domain containing protein
TRAF2	TNFR-associated Factor 2
Trx1/2	Thioredoxin1/2
Trx2R	Trx2 reductase
TRAIL	TNF-related apoptosis-inducing ligand

8.2. Acknowledgment

First of all, I want to thank Prof. Dr. Karin Moelling, Head of the Institute of Medical Virology, University of Zurich, for giving me the opportunity to conduct my PhD thesis at her institute and the excellent working possibilities and stimulating scientific environment. I would furthermore like to thank her for her continuous support and motivating discussions during all phases of this thesis.

I want to express my gratitude to Prof. Dr. Urs Greber for co-supervising me as external PhD student.

I am greatly indebted to Dr. Martin Baumgartner and Dr. Gerald Radziwill for critically reading this thesis. Special thanks are going to my colleagues at the Institute of Medical Virology, who always supported me, for their encouraging discussions, for helpful technical advice and for their solidarity and motivating ambience. I want to pronounce my warmest thanks especially to (in alphabetical order) Renata Bernasconi, Dr. Magnus Bosse, Dr. Thorsten Fritzius, Dr. Mihaela Lorger, Dr. Andreas Weiss, Dr. Lina Wittmer, and Monika Wiget for their constant help. My acknowledgments also go to Dr. Jochen Heinrich for his supervision and support in the first half of my thesis.

My special and most profound thanks are going to my parents, who stood behind me and supported me throughout the years of my study and my thesis. Without their loving support, their encouragement and understanding, I would not have accomplished this very important phase in my life.

8.3. Curriculum vitae

Personal data:

First name:	Elisabeth
Last name:	Ortner
Present Address:	Mainaustrasse 31 CH-8008 Zurich Phone: ++41-43-499 91 19 E-mail: eortner@immv.unizh.ch
Date and Place of Birth:	1.10.1976, Vienna, Austria
Citizenship:	Austrian
Marital Status:	Single

Education:

1984 - 1995	Elementary and High school in Vienna, Austria
1995 – 2001	Study of Microbiology at the University of Vienna, Austria
1998/1999	Erasmus student-exchange program: one-year intercalating course of microbiology (BSc.MedSci) at the Institute of Biomedical and Life Sciences at the University of Glasgow, Scotland
1999 - 2001	Diploma thesis at the Institute of Medical Biochemistry, University of Vienna, Austria, under the supervision of Prof. Dr. Ernst Kuechler. Thesis: "*The N-Terminal Deletion of Cytokeratin 8 During Rhinoviral Infection and Its Effects on the Cytoskeleton"*
2002 - 2007	Ph. D. degree at the Institute of Medical Virology, University of Zurich, Switzerland, under ther supervision of Prof. Dr. Karin Moelling and Prof. Dr. Urs Greber

Poster Presentations:

July 2003	Special FEBS Meeting in Brussels, Belgium
February 2004	USGEB 36th Annual Meeting in Fribourg, Switzerland
December 2006	Conference "Targeting the Kinome" in Basel, Switzerland
March 2007	USGEB 39th Annual Meeting in Basel, Switzerland

Publication:

Ortner, E. and Moelling, K. (2007) "Heteromeric complex formation of ASK2 and ASK1 regulates stress-induced signaling". Biochem Biophys Res Commun 362(2): 454-9